

Response to Reviewer #1's Comments

Anonymous Referee #1:

This manuscript presents a year of continuous measurements of atmospheric Hg species at a suburban site in eastern China, which is an important anthropogenic Hg source region in China. This study combines the analysis of speciated Hg concentrations, local meteorology, receptor-based modelling, PMF and specific event, showing the sources and transformations of atmospheric Hg.

Major comments:

The authors discussed the impact of local emissions and long-range transport of Hg on observed atmospheric Hg. The analysis, however, do not generate a conclusion that which of these two processes were the dominant sources of the observations, and some of the conclusions from the analysis are contradictory to each other at times. The analysis of using PSCF model neglect the local meteorology. For example, when there is a shallow boundary layer formed at the sampling site, an analysis of long range transport could be not suitable because local to regional are more important in this case. This manuscript seems not have a clear motivating hypothesis. The authors made a brief introduction of Hg emissions in East Asia, but have not summarized the findings of many previous studies conducted in this region or in East Asia. They also have not addressed the scientific gaps existing after many previous studies in this region. Therefor, it is not clear to what extent that this study could contribute to the science. The descriptions of the materials and methods section are not clear. The collection of GOM and PBM at 2-hour interval indicates a GOM or PBM concentration could be obtained every 3 hours (1 hour thermal desorption and detection is needed after collection). This does not match the backward trajectories simulated every two hours. The operations of the speciated Tekran system did not followed the standard method very well. For example, a replacement of filter at a monthly interval is too longer under heavily PM pollution conditions. The calculation of backward trajectory is not clear. What is the arrival height used for the calculation of backward trajectories? What is the threshold concentrations of speciated atmospheric Hg and the reasons of the selection of the thresholds.

We sincerely thank for the reviewer's in-depth comments and helpful suggestions on this manuscript. Based on the specific comments, we have responded to all the comments point-by-point and made corresponding changes in the manuscript as highlighted in red color. The reviewer has raised a number of issues and we quite agree. We feel the substantial revisions based on the reviewer's comments have greatly improved the quality of this manuscript. Please check the detailed responses to all the comments as below.

Specific comments:

1. Line 26-27: a conclusion of impact of the long-range transport and local emissions on observations is meaningless. All observations could be impacted by local and long-range sources.

Response: We agree with the reviewer that this sentence is redundant. This statement has been revised as “An application of the GOM/PBM tracer method and trajectory-based source region identification distinguished the relative importance of long-range transport from northern China and quasi-local emission sources on the magnitudes of Hg species.” in the revision.

2. Line 46 and 48: the citations of references are not correct. Please check the similar errors throughout the manuscript.

Response: Thanks for pointing out this. The references have been checked throughout the manuscript.

3. Line 53: as for the anthropogenic mercury?

Response: The sentence has been revised as “As for the anthropogenic emission sources of mercury, coal combustion, non-ferrous smelters, cement production, waste incineration, and mining are considered to be the main sources.” in the revision.

4. Line 71-72: are you sure that atmospheric transformations such as redox reactions could not impact atmospheric GEM. There are many evidences that transformations including oxidation of GEM and foliar uptake of GEM could significantly affect GEM observations.

Response: We agree with the reviewer that the redox reactions can indeed significantly affect GEM observations and our statement was not appropriate. we have revised the original sentence as “Generally, the levels of GEM could be affected by various emission sources, redox reactions, and foliar uptake, while the GOM species from the GEM oxidation and subsequent formation of PBM by adsorption on the particulate matters can significantly affect their ambient concentrations, especially in regions with high GEM levels.” in the revision.

5. Line 75-85: a detailed introduction of previous studies in eastern China should be added here. You should also introduce the progress of atmospheric Hg observations and point out the remaining questions regarding sources and transformation in this region.

Response: Thanks for the suggestion. A detailed introduction of previous studies has been added in the revision. “Early field measurements in urban Shanghai found that the sources of TGM were most likely derived from coal fired power plants, smelters and industrial activities (Friedli et al., 2011). One study in urban Nanjing indicated that natural sources were important while most sharp peaks of TGM were caused by anthropogenic sources (Zhu et al., 2012). Modeling of atmospheric mercury in eastern China simulated by the CMAQ-Hg model showed that natural emissions with a contribution of 36.6% were the most important source for GEM in eastern China (Zhu et al., 2015). One study at Chongming (an island belonging to Shanghai) observed a downward trend for GEM concentrations from 2014 to 2016 due to the reduction of

domestic emissions (Wang et al., 2016). Studies conducted in Changbai Mountain (Wan et al., 2009) and Xiamen (Xu et al., 2015) used Principal Components Analysis (PCA) to identify potential sources of atmospheric mercury, but the specific contributions of each source couldn't be quantified due to the limitation of the PCA method. Overall, studies with respect to the specific sources and their quantified contributions to atmospheric mercury in the suburbs of East China and the formation and transformation processes among Hg species in the atmosphere are still lacking.”

6. Section 2.1: the authors declare that there is no large point sources within 20 km of the sampling site. This seems not correct. From the Chinese inventory and global inventory, I can calculate the total GEM emission reaches more than 10 tons within $0.4^\circ \times 0.4^\circ$ grid of the site (corresponding to a 20 Km cycle around the site). For such a strong local emission, is it suitable to use PSCF modelling to study the long-range transport. How could you separate the local emissions from long-range transport signals?

Response: Thank for the reviewer's carefully check on the emissions around the sampling site. Based on a mercury emission inventory of China in 2014 (Wu et al., 2016), the total GEM emission in Shanghai was approximately 5 tons/yr. Since our sampling site is located in Shanghai, it seems unlikely that the GEM emission within a $0.4^\circ \times 0.4^\circ$ grid of the site can reach more than 10 tons, even higher than the total of Shanghai. To clarify this, we checked the EDGAR (Emissions Database for Global Atmospheric Research) global emission inventory (<http://edgar.jrc.ec.europa.eu/overview.php?v=4tox2>), which included a variety of emission sectors as shown in the table below. We also selected a $0.4^\circ \times 0.4^\circ$ grid of the site as shown in the figure below. The latest year of the EDGAR mercury emission dataset is 2012.

It is calculated that the total GEM emissions in this grid box is about 105kg/yr, of which power industry and cement production are the major contributors. In this regard, the emissions around the sampling site is not significant.

The sampling site is located beside Dianshan Lake as seen in the photos below. No strong point sources and high buildings are around the site and could be regarded as an ideal suburban site in the YRD region.

Sector	Emissions (kg/yr)
Cement	28.49
Power-industry	53.87
Residential	10.05
Glass	0.03
Transportation	3.67
Waste	9.38
Total	105.49





7. Section 2.4: you should show the arrival heights of the backward trajectories and the threshold concentrations.

Response: Thanks for the suggestion. The last paragraph in Section 2.4 has been revised as “In this study, we set the threshold concentration as the mean value of the whole sampling period. The mean GEM, PBM, and GOM concentrations were 2.77 ng/m^3 , 60.8 pg/m^3 , and 82.1 pg/m^3 , respectively. The HYSPLIT (HYbrid Single-Particle Lagrangian Integrated Trajectory) model is applied for calculating air mass backward trajectories (Draxler and Rolph, 2012). The model was run online at the NOAA ARL READY Website using the meteorological data archives of Air Resource Laboratory (ARL). The meteorological input data used in the model was obtained from NCEP (National Centers for Environmental Prediction)’s global data assimilation system (GDAS) with a horizontal resolution of $0.5^\circ \times 0.5^\circ$. In this study, 72-hours back trajectories were calculated at 500m AGL (above ground level) and the cell size was set as $0.5^\circ \times 0.5^\circ$.

8. Line 193: standard errors of the means should be also presented here. You should also define the characteristic of the site. Is it a remote site or suburban site? I would prefer a suburban characteristic of the sampling site. Then, comparisons between previous observations in urban, suburban and remote areas are meaningful.

Response: The standard errors of the means have been added and the sentence has been revised as “The annual average concentrations of GEM, PBM, and GOM at DSL were $2.77 \pm 1.36 \text{ ng/m}^3$, $60.8 \pm 67.4 \text{ pg/m}^3$, and $82.1 \pm 115.4 \text{ pg/m}^3$, respectively.” in the revision. The characteristic of the site has already been defined as suburban in Table 1.

9. Line 210: a description of elevated Hg concentrations in both cold and warm seasons is confusing. What is the statistical test for the seasonal variations?

Response: The table below shows the statistical test with the p-value among the four seasons for GEM concentration. It indicates the GEM concentration in autumn is statistically different from that of spring, summer, and winter ($p < 0.05$), while there are no significant differences

among spring, summer, and winter ($p>0.05$). In this regard, we revised the description as “Statistical test showed that no significant differences of the seasonal variations of GEM concentrations among spring, summer, and winter were observed (Table S1). This was different from many urban and remote sites in China, such as Guiyang, Xiamen, and Mt. Changbai, where GEM showed significantly higher concentrations in cold seasons than those in warm seasons (Feng et al., 2004; Xu et al., 2015; Fu et al., 2012).” in the revision.

Table R1. P-value between seasons for GEM concentration

	spring	summer	autumn	winter
spring				
summer	$p>0.05$			
autumn	$p<0.05$	$p<0.05$		
winter	$p>0.05$	$p>0.05$	$p<0.05$	

10. Line 214-216: here references are needed.

Response: Thanks for the suggestion. The references have been added in the revision.

11. Line 224-225: does a highest GOM concentration observed in winter support the effect of atmospheric oxidation at the sampling site. Generally, modeling studies argued that the oxidation rate of GEM should be highest in summer. Also, GOM observed peaked in morning (10:00), similar to GEM. This is in contrast with many previous studies that showed highest concentrations at noon, which could support a strong transformation between GEM and GOM.

Response: Thanks for the comments. The atmospheric oxidation was lowest in winter due to the relatively weak solar radiation. Thus, the high GOM concentrations observed in winter probably were attributed to the influence of strong anthropogenic emissions (such as the enhanced coal combustion in winter) and unfavorable meteorological conditions.

As for similar peaks of GOM and GEM in this study, we think this is also likely attributed to the influence of anthropogenic emissions as GOM derived largely from anthropogenic emissions in addition to the secondary formation.

In the revised manuscript, we have stated more clearly about the diurnal pattern of mercury species.

12. Line 241: are there any previous studies showed the diurnal patterns of anthropogenic emissions. The difference in Hg concentrations between daytime and night needs a statistical test.

Response: To our best knowledge, no diurnal patterns of anthropogenic Hg emissions are available from previous studies. The figure below is the hourly profile of major emission sectors (including power plants, industries, residential and transportation) for allocating emissions in China (data from Prof. Qiang Zhang from Tsinghua University). It could be seen that all emissions peak during daytime, reflecting the strong influences from human activities. We also performed statistical analysis and confirmed that the difference of Hg concentrations between daytime and night was significant ($p < 0.05$).

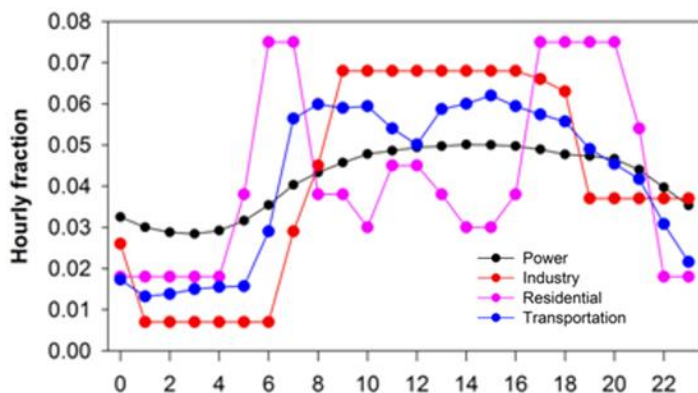


Figure R1. Hourly profile of major emission sectors in China

13. Line 257-258: PBM showed the highest in southwest, west and northwest winds, this is not consistent with the PSCF result. Please explain.

Response: Thanks for the comment. We think that there are two main reasons. 1) The wind rose plot was based on instantaneous wind directions, which revealed the relationship between PBM concentrations and wind direction/wind speed at a local scale. The PSCF analysis was based on three-days backward trajectories, which revealed the transport routes of air masses and potential sources regions at a much larger scale. Thus, it is possible that the wind rose plot and PSCF didn't show very consistent results. 2) As shown in Fig 5 (a), the frequency of the wind from southwest directions only accounted for about 6% of the total winds, which could impact the results of PSCF. As the PSCF analysis applied a weighting factor to reduce the uncertainty when a small number of trajectories crossed a particular cell. This might cause the PSCF values to be underestimated in the southwest, west and northwest wind directions.

14. Line 272: a description of PBL should be presented before the abbreviation. What methods did you use to determine the PBL? It is also appropriate to separate the shallow PBL from the PSCF analysis.

Response: We added the sentence “The data of the height of planetary boundary layer (PBL) were retrieved from the U.S. National Oceanic and Atmospheric Administration (<https://ready.arl.noaa.gov/READYmet.php>).” in Section 2 in the revision. When performing

the PSCF analysis, the starting heights were set as 500m, thus precluding the events under the shallow PBL conditions.

15. Line 300-301: I do not agree East China Sea is an important source region of the site given the PSCF values ranging from 0.2 to 0.4. There are also studies of atmospheric Hg in East China Sea, which highlighted that outflows of Hg from mainland China drive the increase of Hg concentrations.

Response: Thanks for the comment. The PSCF pattern in Fig. 7 of the original manuscript was based on an annual basis of Hg, indicating moderate PSCF values as the reviewer commented. If by referring to seasonal potential source regions of GEM as shown in the figure below, we did observe some high PSCF values (>0.5) over the East China Sea. We believe these signals imply the impact of ship emissions, but not the impact of ocean emissions. However, we do agree with the reviewer that East China Sea is not an important source region as the mainland evidently showed much higher and widespread PSCF signals. To avoid misunderstanding, we revised the sentence as “In addition, the East China Sea (including the offshore areas and open ocean) showed sporadic high PSCF signals of GEM in all four seasons (Fig. S1), indicating possible influences from shipping activities.” in the revision.

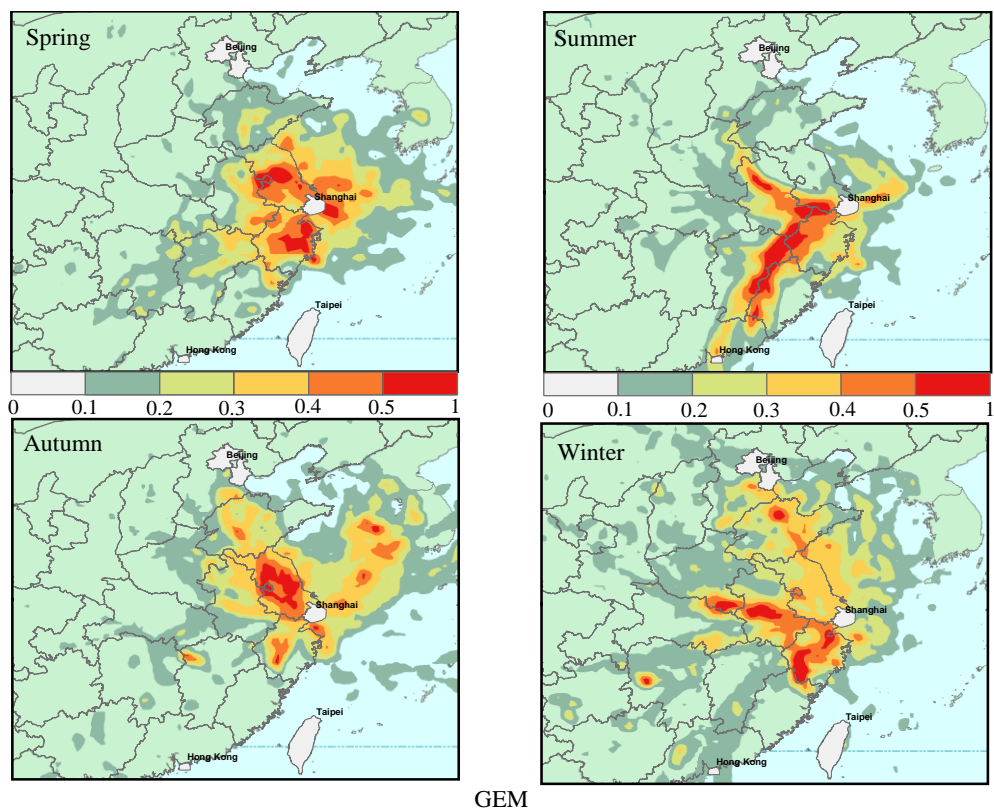


Figure S1. Potential source regions of seasonal GEM at the sampling site according to PSCF analysis.

16. Line 314-315: what I see from Figure 7 is that GOM and GEM share the similar source regions, and what is different is that of PBM.

Response: Thanks for pointing this out. We revised the description as “The PSCF pattern of GOM was as similar as that of GEM but different from that of PBM.” in the revision.

17. Line 355-356: relative fraction of wind in south, southwest and west wind directions are similar in the four GOM/PBM groups, and why? Long-rang transport sources are also located in these directions.

Response: Thanks for the comment. We agree with the reviewer that the long-range transport sources could be also derived from the south, southwest and west directions. However, it is generally regarded that the long-range transport extent from the wind directions mentioned above was less than from northern China. Thus, this may explain that the frequency of south, southwest and west wind directions showed no clear trend as the GOM/PBM ratios increased. In this section, we have testified that the GOM/PBM ratio can be used as a quick tracer for identifying the relative importance of long-range transport vs. local sources. However, this is just a qualitative method, but not a quantitative solution for separating different sources. Explicit source apportionment should require chemical transport modeling, however, this is out the scope of this study.

In the revised manuscript, we have added in the end of this paragraph that “In general, the GOM/PBM ratio can be used as a qualitative tracer for identifying the relative importance of long-range transport vs. local sources. However, when the influences from long-range transport and local emission were close, the result could be ambiguous based on this method and this may require further efforts such as chemical transport modeling”.

18. Line 359-382: low GEM concentrations were mostly related to high CO and SNA concentrations. Does this support that local-regional emissions are more important? This is contradictory to low GOM/PBM ratios, which indicates a progress of long-range transport.

Response: Thanks for the comments. In Shanghai, when high CO and SNA concentrations occurred, these events were generally related to the impact of long-range transport from northern China, especially in winter, but seldom from local emissions. In this study, GEM showed an increasing trend as the GOM/PBM ratios increased while both CO and SNA decreased. Thus, the low GEM concentrations were mostly related to high CO and SNA concentrations, suggesting the long-range transport from northern China was not the major cause of high GEM concentrations. In Fig. 9 of the manuscript, lower GEM concentrations corresponded to lower GOM/PBM ratios, further corroborating the influence of long-range transport was not crucial on GEM. Hence, there is no contradiction between the results based on different methods.

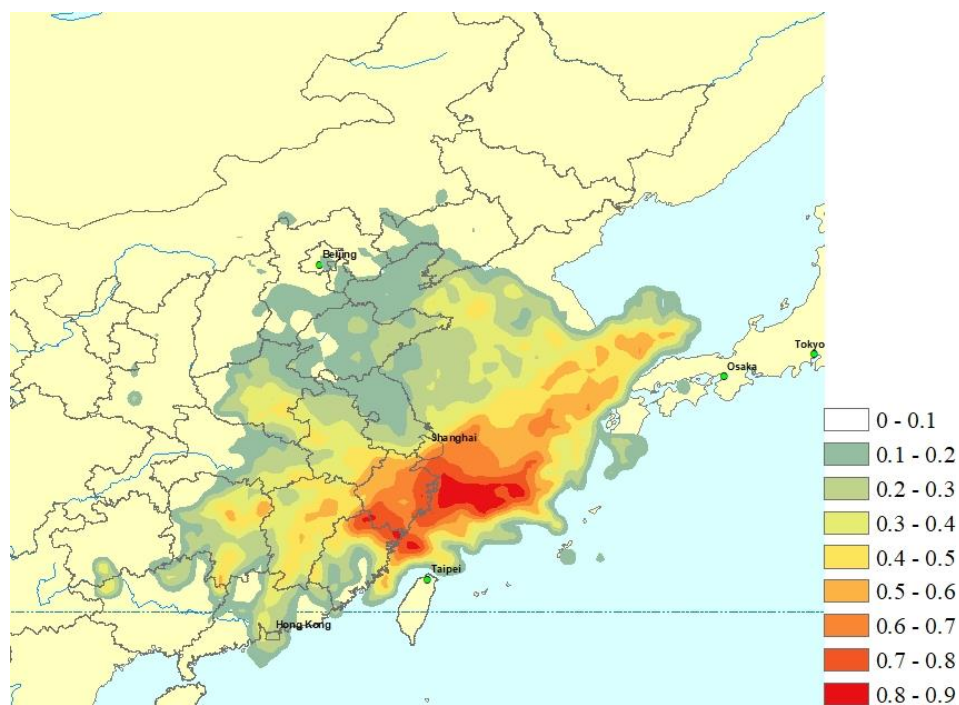
19. Section 3.3.3: why did not apportion the major sources of PBM and GOM?

Response: Thanks for this good suggestion. Actually, we've tried hard to apportion the major sources of PBM and GOM by using PMF. However, we found the results difficult to explain. We think that the possible reasons are that the concentrations of PBM and GOM fluctuated much stronger than other atmospheric species such as soluble ions, organic/elemental carbon, and elements. Due to the relatively short residence time in the atmosphere, it seems not suitable by digesting PBM and GOM into the PMF analysis. Thus, we didn't include source apportionment of PBM and GOM in this study.

20. Line 401-406: factor 2 could be mostly related to oil combustion in motor vehicle in urban areas and shipping emissions over the Dianshan Lake.

Response: Thanks for the comment. In order to determine whether factor 2 represents shipping emissions, the time-series of GEM concentrations from the shipping factor based on the PMF modeling were extracted and digested into the PSCF modeling. The figure below showed the potential sources regions were mainly located over the East China Sea, which indicated factor 2 from PMF should be representative of the shipping sector. At the same time, we recognized oil combustion in motor vehicle and shipping emissions over the Dianshan Lake certainly contributed to Hg pollution, but the existing ships in Dianshan Lake are far from being comparable to that of the adjacent East China Sea, and the proportion of mobile oil combustion is relatively small in YRD (5.34%)(Tang et al., 2018), thus we think that factor 2 should be likely related to ship emission over the offshore and open areas of the East China Sea as well as oil combustion in motor vehicles and inland shipping activities.

In the revised manuscript, we have made clarification about the explanation of factor 2 by PMF modeling.



21. Section 3.4.1: I do not agree variations of GEM and GOM concentration can support a strong conversion of GEM to GOM. Did you observe a strong negative correlation between GEM and GOM concentrations?

Response: Thanks for comments. Strong negative correlation between GEM and GOM concentrations were usually observed at remote and high-altitude sites, where the impact of anthropogenic emissions is weak. As a suburban site located in one of the most industrialized regions of China, it is difficult to see such a strong negative correlation between GEM and GOM as the reviewer mentioned. However, from Figure 11, we can still see that when GEM concentration began to decline from 6:00, the concentrations of GOM continued to rise until it reached the peak value at around 10:00, and the levels of ozone and temperature also kept rising during this period. This phenomenon has been repeatedly observed during the study period, revealing the acceleration of the conversion process of GEM to GOM under favorable atmospheric conditions of higher O₃ concentration and ambient temperature. However, we understand that GOM could be directly emitted from various emission sources and the formation mechanism of GOM is complicated and we are not trying to elucidate it based on limited measured parameters.

In the revised manuscript, we have revised the title of Section 3.4 as “Factors affecting the formation and transformation of mercury species”. In the context of this section, we have adjusted the writings to focus on the crucial factors affecting the formation and transformation of mercury species but not the intrinsic mechanisms.

22. 452-469: Figure 12 is meaningless. Anyone could expect a similar trend between GOM concentrations and GOM/PBM ratios.

Response: Thanks for the comments. We do agree with the reviewer that the relationship between GOM concentrations and GOM/PBM ratios could be expected. Actually, Figure 12 more focus on the multi-relationship among GOM, GOM/PBM, O₃, and temperature. We intended to explore some crucial factors affecting the concentrations of GOM such as temperature and the levels of oxidants.

References:

- Draxler, R. R., & Rolph, G. D. (2012). HYSPLIT (HYbrid Single-Particle Lagrangian Integrated Trajectory) Model access via NOAA ARL READY Website. NOAA Air Resources Laboratory, Silver Spring, MD. <http://ready.arl.noaa.gov/HYSPLIT.php>. Accessed March 2012.
- Feng, X. B., Shang, L. H., Wang, S. F., Tang, S. L., and Zheng, W.: Temporal variation of total gaseous mercury in the air of Guiyang, China, J. Geophys. Res.-Atmos., 109, 10.1029/2003jd004159, 2004.
- Friedli, H. R., Arellano, A. F., Geng, F., Cai, C., and Pan, L.: Measurements of atmospheric mercury in Shanghai during September 2009, Atmospheric Chemistry and Physics, 11, 3781-3788, 10.5194/acp-11-3781-2011, 2011.

Fu, X. W., Feng, X. B., Zhu, W. Z., Zheng, W., Wang, S. F., and Lu, J. Y.: Total particulate and reactive gaseous mercury in ambient air on the eastern slope of the Mt. Gongga area, China, *Appl. Geochem.*, 23, 408-418, 10.1016/j.apgeochem.2007.12.018, 2008.

Fu, X. W., Feng, X., Shang, L. H., Wang, S. F., and Zhang, H.: Two years of measurements of atmospheric total gaseous mercury (TGM) at a remote site in Mt. Changbai area, Northeastern China, *Atmospheric Chemistry and Physics*, 12, 4215-4226, 10.5194/acp-12-4215-2012, 2012.

Fu, X. W., Zhang, H., Yu, B., Wang, X., Lin, C. J., and Feng, X. B.: Observations of atmospheric mercury in China: a critical review, *Atmospheric Chemistry and Physics*, 15, 9455-9476, 10.5194/acp-15-9455-2015, 2015.

Tang, Y., Wang, S. X., Wu, Q. R., Liu, K. Y., Wang, L., Li, S., Gao, W., Zhang, L., Zheng, H. T., Li, Z. J., and Hao, J. M.: Recent decrease trend of atmospheric mercury concentrations in East China: the influence of anthropogenic emissions, *Atmospheric Chemistry and Physics*, 18, 8279-8291, 10.5194/acp-18-8279-2018, 2018.

Xu, L. L., Chen, J. S., Yang, L. M., Niu, Z. C., Tong, L., Yin, L. Q., and Chen, Y. T.: Characteristics and sources of atmospheric mercury speciation in a coastal city, Xiamen, China, *Chemosphere*, 119, 530-539, 10.1016/j.chemosphere.2014.07.024, 2015.

Zhang, L., Wang, S. X., Wang, L., and Hao, J. M.: Atmospheric mercury concentration and chemical speciation at a rural site in Beijing, China: implications of mercury emission sources, *Atmospheric Chemistry and Physics*, 13, 10505-10516, 10.5194/acp-13-10505-2013, 2013.

Zhu, J., Wang, T., Talbot, R., Mao, H., Hall, C. B., Yang, X., Fu, C., Zhuang, B., Li, S., Han, Y., and Huang, X.: Characteristics of atmospheric Total Gaseous Mercury (TGM) observed in urban Nanjing, China, *Atmospheric Chemistry and Physics*, 12, 12103-12118, 10.5194/acp-12-12103-2012, 2012.

Zhu, J., Wang, T., Bieser, J., and Matthias, V.: Source attribution and process analysis for atmospheric mercury in eastern China simulated by CMAQ-Hg, *Atmospheric Chemistry and Physics*, 15, 8767-8779, 10.5194/acp-15-8767-2015, 2015.

Response to Reviewer #2's Comments

Anonymous Referee #2:

The paper analyzed speciated Hg concentrations at a site in eastern China and applied various data analysis methods, including potential source contribution function (PSCF) and positive matrix factorization (PMF), to examine the sources and transformation processes involved. The speciated Hg concentrations collected at this site are likely some of the highest that have been observed worldwide including within Asia, and this warrants a detailed investigation into the causes in order to address the Hg pollution issue in China. However, I did not get a clear understanding of the sources contributing to such high speciated Hg concentrations. I think this is partly due to incomplete understanding of Hg emissions in China, which leads to uncertainties in the interpretation of the sources. The omission of the PMF analysis for GOM and PBM is also contributing to a lack of understanding of the anthropogenic sources. The alternative explanation in the paper for the extremely high GOM concentrations is the oxidation of GEM. However, the discussion seems too speculative, as it doesn't account for the many physical and chemical parameters that are involved in the Hg transformation process. This is a complicated process, and the way that it is examined in the paper (methodology and data) does not further the understanding of GEM oxidation. Considering the high levels of anthropogenic Hg emissions across China, I suggest focusing your analysis on anthropogenic sources and making sure that all of these sources have been carefully considered.

We sincerely thank for the reviewer's in-depth comments and helpful suggestions on this manuscript. Based on the specific comments, we have responded to all the comments point-by-point and made corresponding changes in the manuscript as highlighted in red color. The reviewer has raised a number of issues and we quite agree. We feel the substantial revisions based on the reviewer's comments have greatly improved the quality of this manuscript. Please check the detailed responses to all the comments as below.

Specific comments:

1. Line 26: what is meant by quasi-local? Please explain what local sources were affecting this site.

Response: The sampling site is located in the suburbs of Shanghai. At the scale of the Yangtze River Delta (YRD) region, the main emission sectors of GEM were coal-fired power plants, coal-fired industrial boilers, residential coal combustion, cement clinker production, and mobile oil combustion (Wang et al., 2016). We also calculated the total mercury emissions in a region of $0.4^\circ \times 0.4^\circ$ covering the sampling site based on the EDGAR emission inventory. The emissions for GEM were around 105 kg/yr, indicating that no strong mercury emissions are around this site. The major emission sectors are from the power industries and cement production.

Usually local emissions refer to the scale of one city. Since the sampling site is located at the conjunction of Shanghai, Jiangsu, and Zhejiang provinces, quasi-local mean the emissions around the site covering multiple cities in Shanghai, Jiangsu, and Zhejiang. In the revised manuscript, we have defined it more clearly.

2. Lines 29-30: “Besides the common anthropogenic emission sectors...” I think that it is better to list the anthropogenic sources in the abstract because it informs stakeholders about the major sources of Hg in China so that appropriate policies can be developed to manage Hg pollution.

Response: Thanks for the suggestion. This sentence is revised as “Besides the common anthropogenic emission sectors (i.e., industrial and biomass burning, coal combustion, iron and steel production, cement production, and incineration), ...” in the revision.

3. Line 55: “mercury will experience the chemical and physical speciation and its forms were essential to understand its biogeochemical cycle”. I suggest revising this to, “mercury undergoes speciation which plays an important role in its biogeochemical cycle.”

Response: Thanks for the suggestion. This sentence has been revised as “mercury undergoes speciation which plays an important role in its biogeochemical cycle.” in the revision.

4. Line 76: The treaty name is Minamata Convention on Mercury.

Response: The treaty name has been corrected as “Minamata Convention on Mercury” in the revision.

5. Lines 77-79: “the situation of mercury pollution is still grim, especially in Asia, which contribute about half of the global mercury emissions (Wu et al., 2006)” I suggest changing this to “the mercury pollution issue is still grim especially in Asia,: : :” Could you use a more recent reference to describe the current Hg emissions in Asia?

Response: Thanks for the reviewer’s suggestions. The reference has been updated and the sentence has been revised as “However, the mercury pollution issue is still grim especially in Asia, which contribute about half of the global mercury emissions (Pacyna et al., 2016).” in the revision.

6. Lines 83-85: I’ve seen several papers analyzing the sources and processes of speciated Hg in China. Could you discuss the major findings from these studies and explain how this paper is different or builds on the current knowledge?

Response: Thanks for the suggestion and we have added the major findings from some recent papers about the sources and processes of speciated Hg in China as below.

“Early field measurements in urban Shanghai found that the sources of TGM were most likely derived from coal fired power plants, smelters and industrial activities (Friedli et al., 2011). The study in urban Nanjing indicated that natural sources were important while most sharp peaks of TGM were caused by anthropogenic sources (Zhu et al., 2012). Modeling of atmospheric mercury in eastern China simulated by the CMAQ-Hg model showed that natural

emissions were the most important source for GEM in eastern China with a contribution of 36.6% (Zhu et al., 2015). One study at Chongming (an island belonging to Shanghai) observed a downward trend for GEM concentrations from 2014 to 2016 due to the reduction of domestic emissions (Wang et al., 2016). Studies conducted in Changbai Mountain (Wan et al., 2009) and Xiamen (Xu et al., 2015) used Principal Components Analysis (PCA) to identify potential sources of atmospheric mercury, but the specific contributions of each source couldn't be quantified due to the limitation of the PCA method. Overall, studies with respect to the specific sources and their quantified contribution to atmospheric mercury in the suburbs of East China and the formation and transformation processes among Hg species in the atmosphere are still lacking.” in the revision.

7. Line 128: Did you perform any quality control on the speciated Hg data, e.g. determining field blanks? Some of the 2-h GOM and PBM concentrations were extremely high; I wonder if they may be outliers? You mentioned that the air inlet is on the rooftop of a building. What kind of building is this and is there the possibility that ventilation exhaust from the building caused the high Hg concentrations? Depending on the building, indoor air can be very polluted.

Response: Yes, a series of work have been done to ensure the quality of the measurement. Before sampling, denuders and quartz filters were prepared and cleaned according to the methods in Tekran technical notes. The Tekran 2573B instrument routinely undergoes automated daily calibrations using internal GEM permeation source and external manual calibration when necessary. Two-point calibrations (including zero calibration and span calibration) were performed separately for each pure gold cartridge. Manual injections were performed to evaluate these automated calibrations using the standard saturated mercury vapor. We noticed that sometimes the concentrations of GOM and PBM were extremely high. After ascertaining that the instrument was in normal operation during those episodes, we find that these high values are continuous, but not suddenly rising or falling. Thus, we think the data under these conditions are valid. We did find some extremely high values, which were about several times higher than the previous hour. As for these data, we think they are outliers and have already been excluded in the data analysis.

The Tekran instrument along with other instruments were set up on the top roof of a four-story building. This supersite is carefully maintained by SEMC. The building is purely used for atmospheric monitoring without any other usage. There are no human activities inside the building except that when the maintenance people enter the building. There is only routinely one guard responsible for the running of the building and he doesn't live inside the building. Thus, we can say that there are almost no emissions inside the building and the ventilation exhaust shouldn't be the cause of high Hg concentrations.

In the revised manuscript, we have added more description about the supersite in Section 2.

8. Line 166: “we set the threshold concentration as the mean value of the whole sampling period.” Are these the mean Hg concentrations and what are the values?

Response: Yes, the mean concentrations of GEM, PBM, and GOM are used. We added the sentence “The mean GEM, PBM, and GOM concentrations were 2.77 ng/m³, 60.8 pg/m³, and 82.1 pg/m³, respectively.” in the revision.

9. Line 167: Please describe how the back trajectories were calculated and the relevant model inputs and parameters.

Response: We have added more detailed description about the simulation of back trajectories as below.

The HYSPLIT (HYbrid Single-Particle Lagrangian Integrated Trajectory) model is applied for calculating air mass backward trajectories (Draxler and Rolph, 2012). The model was run online at the NOAA ARL READY Website using the meteorological data archives of Air Resource Laboratory (ARL). The meteorological input data used in the model was obtained from NCEP (National Centers for Environmental Prediction)’s global data assimilation system (GDAS) with a horizontal resolution of 0.5° × 0.5°. In this study, 72-hours back trajectories were calculated at 500m AGL (above ground level) and the cell size was set as 0.5°×0.5°

10. Line 187: The description of the PMF analysis is overly general; there needs to be a more detailed description of the model runs. Did you perform only a single run or multiple runs with different number of factors to come up with the optimal solution? How did you decide how many factors to keep? Did you do any analysis to assess the performance of the model? The quality of the PMF results depends on the input data and other considerations. Were there any procedures followed to ensure the quality of the input data?

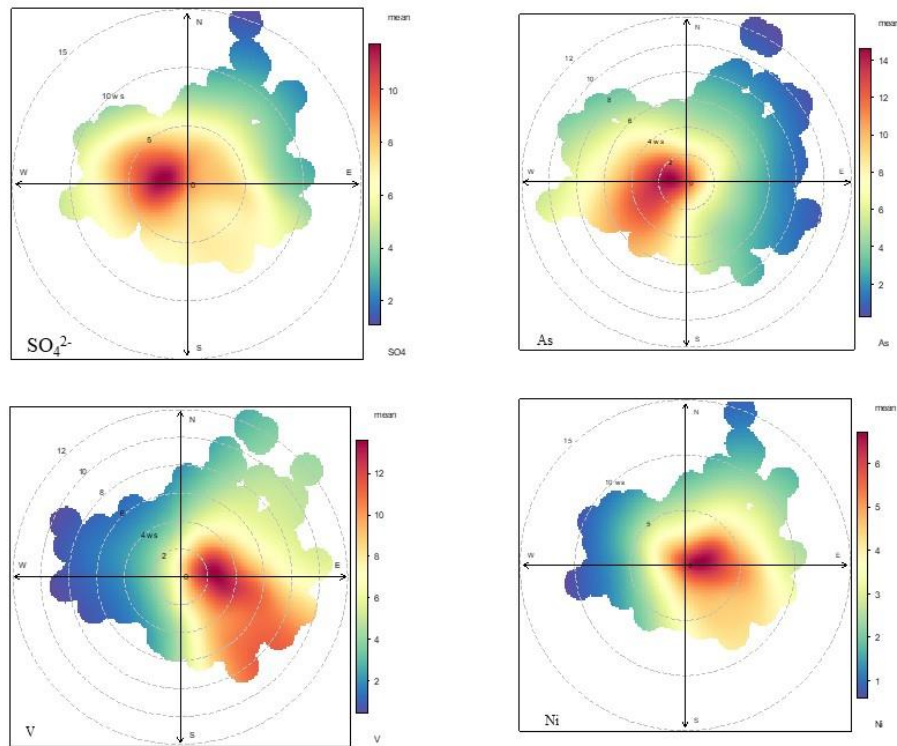
Response: We have added more detailed description of the PMF running as suggested in Section 2.5.

“In this study, the number of factors from 3 to 8 was examined with the optimal solutions determined by the slope of the Q value versus the number of factors. For each run, the stability and reliability of the outputs were assessed by referring to the Q value, residual analysis, and correlation coefficients between observed and predicted concentrations. Finally, a 6-factor solution, which showed the most stable results and gave the most reasonable interpretation, was chosen. Before running the model, a dataset including unique uncertainty values of each data point was created and digested into the model. The error fraction was assumed to be 15% of concentrations for GEM and 10% of concentrations for the other compounds (Xu et al., 2017), the missing data were excluded and the total number of samples was 3526.”

We added additional analysis to assess the performance of the model as below.

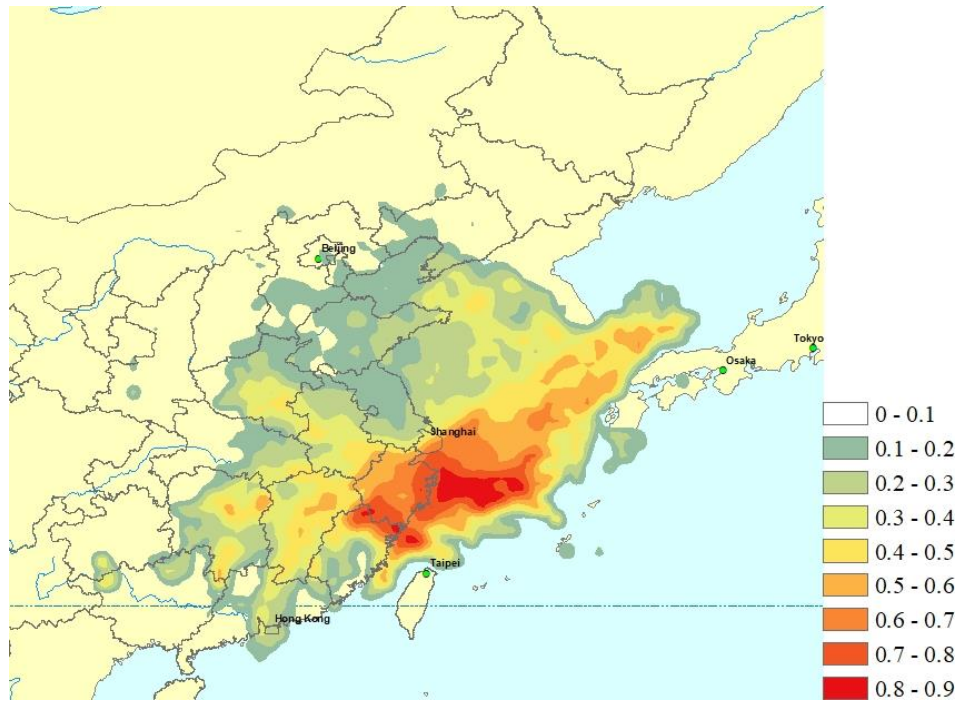
(1) In order to validate the PMF results, wind roses of SO₄²⁻, As, Ni, and V are plotted in the figure below. SO₄²⁻ and As shared similar patterns with high concentrations mainly from the southwest. SO₄²⁻ and As are tracers for coal combustion. PMF identified combustion is the biggest source of GEM. Thus, this confirmed that the major sources of GEM are located in the southwest region. Ni and V showed similar patterns with high concentrations mainly from the

northeast, east, and southeast. PMF identified a shipping source from the ocean. The wind rose plots of Ni and V also confirmed the identification of the shipping factor.



(2) In order to determine whether factor 2 represents shipping emissions, the time-series of GEM concentrations from the shipping factor based on the PMF modeling were extracted and digested into the PSCF modeling. The figure below showed the potential sources regions were mainly located over the East China Sea, which indicated factor 2 from PMF should be representative of the shipping sector. At the same time, we recognized oil combustion in motor vehicle and shipping emissions over the Dianshan Lake certainly contributed to Hg pollution, but the existing ships in Dianshan Lake are far from being comparable to that of the adjacent East China Sea, and the proportion of mobile oil combustion is relatively small in YRD (5.34%)(Tang et al., 2018), thus we think that factor 2 should be likely related to ship emission over the offshore and open areas of the East China Sea as well as oil combustion in motor vehicles and inland shipping activities.

In the revised manuscript, we have made clarification about the explanation of factor 2 by PMF modeling.



11. Lines 192-193: Please include the standard deviation for the concentrations.

Response: The standard deviation for the concentrations have been included, the sentence has been revised as “The annual average concentrations of GEM, PBM, and GOM at DSL were $2.77 \pm 1.36 \text{ ng/m}^3$, $60.8 \pm 67.4 \text{ pg/m}^3$, and $82.1 \pm 115.4 \text{ pg/m}^3$, respectively.” in the revision.

12. Lines 203-205: “The abnormally high GOM concentrations observed in this study were likely attributed to both strong primary emissions and secondary formation” I am skeptical that this is due to secondary formation because as discussed in the seasonal concentrations in the next paragraph, it is the winter concentrations that were much higher than other seasons. During the winter, secondary formation from GEM oxidation is likely not significant. I suggest focusing on primary emissions during the wintertime and determining the major sources (e.g. coal combustion, oil combustion, residential wood burning, etc.) and conditions during winter that could lead to strong pollution episodes (e.g. stagnant atmosphere, changes in air mass patterns, etc.). Is DSL a high elevation area? If so, could transport from the free troposphere contribute to the extremely high GOM concentrations?

Response: Thanks for the comment. We do agree with the reviewer that high GOM concentrations are dominated by primary emissions, especially in wintertime. We revised the sentence as “The abnormally high GOM concentrations observed in this study were likely dominated by strong primary emissions.” in the revision.

The DSL site is not a high-altitude site (~ 14 meter above sea level), so we don't think transport from the free troposphere can significantly contribute to the atmospheric mercury concentrations under most circumstances. However, we do appreciate for this comment on the possibility of mercury transport from the free troposphere in the future studies.

13. Lines 227-228: Have you ruled out other possible reasons, e.g. forest fire emissions, combustion and industrial emissions, etc.? The lower concentrations in summer compared to winter could be simply due to increased atmospheric mixing, wet deposition (have you analyzed rainfall data?), dry deposition, changes in air mass patterns, etc. More detailed analysis is needed before arriving at the conclusion that GEM oxidation is causing the high GOM concentrations.

Response: Thanks for the comments and we do agree with the reviewer that we didn't fully consider the factors influencing the concentrations of GOM. As for the reviewer's concern, forest fire emissions were not the emission source in the Yangtze River Delta region. Combustion and industrial emissions were the major emission sectors in the Yangtze River Delta region. Those emissions are almost constant among the 12 months (Tang et al., 2018). Thus, the lower concentrations of GOM in summer compared to winter should be largely due to the more favorable meteorological conditions as the reviewer mentioned. At the same time, GOM concentrations in summer were higher than spring and autumn, which should be partly ascribed to the secondary transformation from GEM. In this Section, we just generally describe the seasonal pattern of Hg species. More detailed analysis of the impact of meteorological conditions on Hg species and the related formation mechanisms are presented in the following sections.

In the revised manuscript, this sentence is changed as "GOM concentrations in summer were much lower than that in winter, which were largely due to the more favorable meteorological conditions. However, GOM concentrations in summer were higher than spring and autumn, which should be partly ascribed to the secondary transformation from GEM. More detailed analysis of the impact of meteorological conditions on Hg species and the related formation mechanisms are presented in the following sections.".

14. Lines 238-240: Do these sites have similar/different characteristics as the DSL site? What about the distance between the listed sites and DSL? I think these factors may explain the diurnal variations.

Response: The listed sites are all urban site, of which the site in Nanjing also belongs to the Yangtze River Delta region and is about 300km from the DSL site. The similar meteorology and emission characteristics within the Yangtze River Delta region may explain the similar diurnal patterns of Hg species between DSL and Nanjing. As for Guiyang, and Guangzhou, they are much far away from DSL with distances of around 1000 – 2000km. Different meteorology and emission characteristics may explain the different diurnal patterns between those sites and DSL. In the revised manuscript, we have explained more clearly about the comparison of diurnal patterns among various sites.

15. Lines 240-245: It appears GEM and GOM have similar diurnal variations and both peaked at 10 AM. This suggests they were affected by the same sources. Could you elaborate what are the stronger emissions from both human activities and natural releases in this area that are causing the high GEM concentrations? Did you consider traffic emissions as a potential source because of higher traffic volumes in the morning which is consistent with the morning peak in the concentrations? I also think more investigation is needed before you can state that the high GOM concentrations are the result of GEM oxidation. To support this statement requires

additional data on the oxidants of GEM and model simulations of the chemical reactions. Based on the diurnal variation, the 10 AM peak does not seem consistent with GEM oxidation because the photochemistry is driven by solar irradiance which peaks at noon. The GOM peak would likely be at noon or later, but in your case, the peak occurs earlier than noontime. Also, have you considered all possible sources of Hg and are there any unknown sources (sources that are not reported in the emissions inventory)?

Response: Thanks for the comments. According to the emissions inventory in the YRD region, the main anthropogenic emission sectors of GEM included coal-fired power plants (39.33%), coal-fired industrial boilers (27.53%), residential coal combustion (1.12%), cement clinker production (13.2%), iron and steel production (6.46%), and mobile oil combustion (5.34%) (Tang et al., 2018). Natural emissions included primary natural release and re-emission of legacy Hg stored in the terrestrial and water surface (Cheng et al., 2014). According to the emissions inventory, traffic emissions only accounted for 5.34% of the total GEM annual emission in the YRD region (Tang et al., 2018). We did consider whether the traffic emissions cause the morning peak of Hg concentrations, however, if it is true, Hg concentrations should also rise during the evening rush hours, which is not shown in the figure. We agree with the reviewer that more investigation is needed before we can draw the conclusion that the high GOM concentrations are the result of GEM oxidation. Thus, we revised the description as “GOM and GEM showed similar diurnal variations and both peaked at 10:00, probably suggesting that GOM and GEM were affected by common sources (e.g. coal-fired power plants and industrial boilers).” in the revision.

16. Lines 253-257: Both GEM and GOM appeared to be 2 and 8 times higher, respectively, when winds came from the southwest quadrant than other directions. I think more analysis is needed to identify the sources from this southwest region that is causing the mean GOM concentrations to increase to 100 pg/m³. Since wind speed and wind direction data were used, the sources are likely local which narrows down the area of investigation.

Response: According to the PMF source apportionment results, industrial and biomass burning (47.8%) was the biggest source of GEM at the sampling site. When referring to the emissions inventory in the YRD region, the main anthropogenic emission sectors of GEM were coal-fired power plants and coal-fired industrial boilers, accounting for 66.9% of the total GEM emissions in YRD (Wang et al., 2016). Thus, it is reasonable to conclude that the high GEM and GOM concentrations from the southwest were caused by coal-fired power plants and coal-fired industrial boilers.

17. Lines 262-265: This is too general. I think that you need to extract the relevant details from this reference, e.g. Hg flux data from the southwest region vs. north/northwest regions. Did the reference discuss what is causing the Hg in the soil, e.g. local contamination, atmospheric deposition, etc.?

Response: Thanks for the suggestion. According to the study of (Wang et al., 2016), it could be seen that the mean annual Hg air-soil flux in the southwest region of our sampling site (e.g. Zhejiang province) ranged from 8.75 to 15 ng m⁻² h⁻¹, while that in the north/northwest region (e.g. Jiangsu province) ranged from 2.5 to 8.75 ng m⁻² h⁻¹ (left figure). The reference didn't discuss in details about the factors affecting the levels of Hg in soil, but mentioned that soil Hg

contents in forest ecosystems are 2-4 times higher than that in grassland and cropland. The land type of the southwest region is mainly mountain forests while that of the north/northwest region is mainly flat cropland and grassland. This may partly explain the relatively high mercury concentrations observed from the southwest.

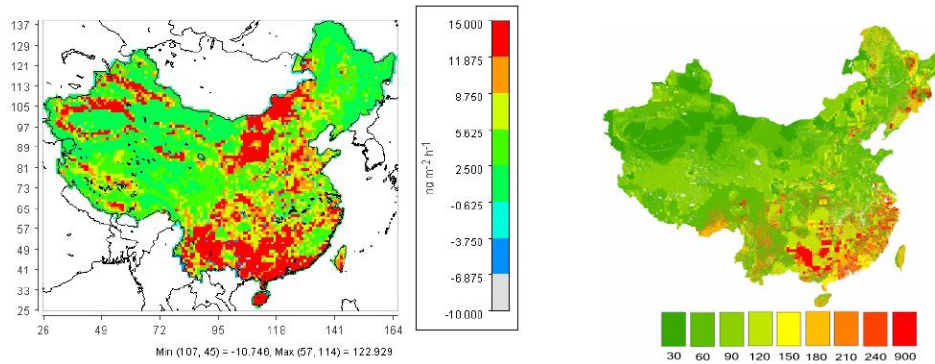


Figure R1. (left) mean annual air–soil flux; (right) Hg concentrations (ng g^{-1} in surface soil (0–20 cm) of China.

In the revised manuscript, we added the sentence “A modeling study simulated that the mean annual Hg air-soil flux in the southwest region of our sampling site (e.g. Zhejiang province) ranged from 8.75 to 15 $\text{ng m}^{-2} \text{h}^{-1}$, while that in the north/northwest region (e.g. Jiangsu province) ranged from 2.5 to 8.75 $\text{ng m}^{-2} \text{h}^{-1}$ (Wang et al., 2016). Hence, emissions from natural sources, such as soils, vegetations and water, should play an important role in the observed high atmospheric Hg concentrations from the south and southeast.” in the revision.

18. Lines 270-271: “This relationship between GEM and temperature can only be interpreted as the impact of natural source emissions.” I think this is one possible interpretation, but not the only interpretation. Temperature can co-vary with other parameters. Also, natural source emissions should be revised to surface emissions because it may have originated from anthropogenic sources by process of deposition.

Response: Thanks for the comment and we agree that this is just a possible interpretation but not the only one. And we have changed the term “natural source emissions” as “surface emissions” and elsewhere throughout the manuscript. We revised the description as “This relationship between GEM and temperature can be likely interpreted as the impact of surface emissions.” in the revision.

19. Lines 275-277: “The GOM concentration showed a clearly positive correlation with temperature in summer. This should be related to the in situ oxidation of GEM under high temperature” The correlation between GOM and temperature does not necessarily indicate oxidation of GEM. Temperature is only one parameter involved in Hg chemistry; there are many other physical and chemical parameters that are influencing the chemistry but they have not been considered in this analysis.

Response: Thanks for the comment and we do agree with the reviewer that the conclusion cannot be drawn based on inadequate evidence. Given the limited parameters measured in this study, it is difficult for us to investigate other physical and chemical parameters that impact the mercury chemistry. When higher temperature occurs, the atmospheric oxidation ability is usually enhanced due to enhanced solar radiation, thus resulting a larger extent of GEM oxidation. Thus, we think the positive relationship between GOM and temperature may imply the oxidation of GEM to GOM to some degree. But of course, GOM has a significant source of direct emissions as mentioned by the reviewer above. Thus, we revised the description as “The GOM concentration showed a clearly positive correlation with temperature in summer. Higher temperature in summer in the Yangtze River Delta region is mostly associated with ozone pollution days (Lu et al., 2018), thus implying higher GOM could be partially related to the in situ oxidation of GEM in addition to its sources from direct emissions.” in the revision.

20. Lines 293-295: “However, as shown in Fig. 1, southern provinces such as Zhejiang and Jiangxi were estimated to release only 25 tons/yr atmospheric Hg from anthropogenic activities, being far less than the northern provinces such as Jiangsu and Shandong (77 tons/yr)... If only the anthropogenic emissions of GEM were considered, the occurrence of stronger PSCF signals in southern provinces seemed unreasonable.” 25 tons/yr of Hg emissions from anthropogenic sources is still very high if you were to compare that to emissions in North America and Europe. I don’t think you can rule out the impact of anthropogenic Hg sources in the southern region on this site, even though the PSCF values are higher in the northern region. Also, have you considered possible transport of GOM from the free troposphere especially when the trajectory endpoints reach high altitudes?

Response: Thanks for the comments. In this discussion, we are not trying to rule out the impact of anthropogenic Hg sources. What we wanted to clarify is that in addition to the direct emissions from anthropogenic sources, surface emissions are also important. As the sampling site is not a high-altitude site, we did not consider the impact of possible transport GOM from the free troposphere. But this suggestion is of great valuable, and inspiring for our future work.

In the revised manuscript, we have deleted the term “only” to avoid any misunderstandings.

21. Lines 297-298: “In this regard, the re-emission of GEM from natural surfaces in southern areas should be a crucial source, corroborating the discussion in Section 3.2.” How do you know this when you don’t have the Hg emissions from natural surfaces to compare against anthropogenic emissions? More data are needed before you can arrive at this conclusion.

Response: Thanks for the comments and suggestions. Based on the study by (Wang et al., 2016), the mean annual Hg air-soil flux in the southwest region of our sampling site ranged from 8.75 to 15 ng m⁻² h⁻¹. By using this value, we can estimate that the total Hg emissions from soils were in the range of 6.9 - 13.9 tons/yr for Zhejiang province. As for the anthropogenic Hg emission of Zhejiang in 2014, it was approximately 15tons/yr (Wu et al., 2016). Thus, the magnitude of mercury from natural surfaces is comparable to that from anthropogenic sources.

In the revised manuscript, we have added more discussions to support this conclusion.

22. Lines 315-316: “the potential source regions of GOM were more from southern China rather than from northern China, which might be due to the higher atmospheric oxidants levels in the southern regions.” This is highly speculative and needs to be supported with data.

Response: Thanks for the comments. We deleted this sentence and changed the description as “The PSCF patterns of GOM were similar with that of GEM but different from that of PBM.” in the revision.

23. Lines 322-328: “...leading to the formation of GOM dominated by mainland oxidants rather than the ocean oxidants.” This discussion needs to be revised because I don’t think you can differentiate between mainland oxidants (i.e. ozone) and oceanic oxidants (i.e. bromine). There are many potential oxidants of GEM aside from ozone and bromine. Modeling studies indicate that oxidation of GEM by bromine can occur globally not just in the marine regions. I feel there is too much speculation on the discussion of GEM oxidation. Instead of this reason, have you considered that GOM may have originated from mainland and then was transported into the sea before arriving at the site?

Response: Thanks for the comments. We do agree with the reviewer that mainland oxidants and oceanic oxidants were not differentiated and this paragraph is speculative. Hence, we deleted the sentence “It should be noted that the signals from the ocean in summer were weaker than in the other seasons. This was likely due to the particularly high ozone concentrations over land in summer (Lu et al., 2018), leading to the formation of GOM dominated by mainland oxidants rather than the ocean oxidants.” to avoid inappropriate conclusion.

24. Lines 367-369: “This corroborated the discussion above that the GOM/PBM ratio was a reliable tracer for assessing the relative importance of regional/long-range transport vs. local atmospheric processing.” I am skeptical about this because of the mixing between regionally-transported air masses and local air. I think it is more complicated, and there are many processes affecting GOM and PBM concentrations at a particular site.

Response: Thanks for the comments and we do agree that there are too many processes affecting the formation of GOM and PBM. As for the ratio of GOM/PBM, it has been used to investigate the relative importance of local sources relative to regional transport in a number of studies based on the fact that the atmospheric residence time of GOM is generally regarded to be shorter than that of PBM (Lee et al., 2016; Zhang et al., 2013; Zhu et al., 2014). However, the GOM/PBM ratio can be only regarded as a qualitative tracer but not a quantitative method for identifying the relative importance of long-range transport vs. local sources.

In Section 3.3.2, by introducing more atmospheric species such as CO and SNA, we found that all the evidences were consistent. But still, this section didn’t aim to sort out the complicated processes that affect GOM and PBM.

25. Line 388: “six-factor solution was selected based on the results of multiple model runs”. The details of these model runs should be included in the methods.

Response: The details of model runs have been included in the methods. We added the sentences “In this study, the number of factors from 3 to 8 was examined with the optimal

solutions determined by the slope of the Q value versus the number of factors. For each run, the stability and reliability of the output were assessed by referring to the Q value, residual analysis and correlation coefficients between observed and predicted concentrations. Finally, a 6-factor solution, which showed the most stable results and gave the most reasonable interpretation, was chosen. Before running the model, a dataset including unique uncertainty values of each data point was created and inserted into the model, the error fraction was assumed to be 15% of concentrations for GEM and 10% of concentrations for other compounds (Xu et al., 2017), the missing data were excluded and the total number of samples was 3526.” in the revision.

26. Lines 391-392: “since no tracers for the natural emissions (e.g. soils, vegetations, and ocean) were available in this study, the identification of natural mercury sources was not possible.” What about Na and Cl ions for identifying marine sources and Ca and K for soil and vegetation?

Response: Thanks for the comment. We have tried multiple runs by setting up different number of factors. However, the model didn’t resolve specific factors for natural emissions. We think the possible reasons are as below. Na has sources from soil dust, road dust, and industrial fly ash in addition to marine sources. Cl is significantly impacted by coal burning and waste incineration. Ca and K both have sources from construction activities. Hence, the miscellaneous sources of those elements precluded the PMF model to resolve the natural sources of mercury.

As suggested by another reviewer, we applied the PCA (Principal Component Analysis) to identify the potential sources of GEM by adding temperature. Four factors are resolved, which totally explained 75.32% of the variance as shown in the table below.

Factor 1 accounted for 34.15% of the total variance with high loadings for SO₂, SO₄²⁻, NH₄⁺, K⁺, Pb, Se, and As, which is explained as coal combustion mixed with biomass burning.

Factor 2 accounted for 14.85% of the total variance with high loadings for temperature, O₃, and NH₃, which is explained as surface emissions. Factor 3 explained 13.43% of the total variance, showed high loading of Ni and V, which indicated the contribution of ship emissions. Factor 4 explained 12.89% of the total variance, with high loading of Fe and Ca, indicating the contribution of cement production. Table R2 PCA factor loading for GEM at DSL.

	Factor 1	Factor 2	Factor 3	Factor 4
GEM	0.50	0.25	0.11	0.07
SO ₂	0.69	-0.20	-0.18	0.35
NO ₂	0.38	-0.49	0.35	0.39
SO ₄ ²⁻	0.84	0.13	0.15	0.00
NH ₄ ⁺	0.88	-0.12	0.18	0.07
K ⁺	0.77	-0.25	0.04	0.39
Pb	0.80	-0.17	0.04	0.32
Se	0.87	-0.05	0.01	0.29
As	0.82	-0.23	0.06	0.33
O ₃	0.06	0.79	-0.30	0.03
NH ₃	0.03	0.73	0.36	-0.04
Temperature	-0.23	0.82	0.17	-0.03
Ni	0.24	-0.02	0.85	0.22
V	-0.03	0.11	0.90	-0.05
Fe	0.50	-0.12	0.24	0.74
Ca	0.26	0.08	0.00	0.90
Explained variance %	34.15	14.85	13.43	12.89

27. 3.3.3. Source apportionment by PMF: Why was the PMF analysis only performed on GEM data and not GOM and PBM? I think GOM and PBM needs to be included due to the extremely high concentrations at this site. Anthropogenic emissions of GOM and PBM should not be ruled out. One of the major goals of the Minamata Convention is to reduce anthropogenic Hg emissions. Thus, it seems logical to carry out source apportionment analysis on GOM and PBM and attempt to identify the sources contributing to such high concentrations.

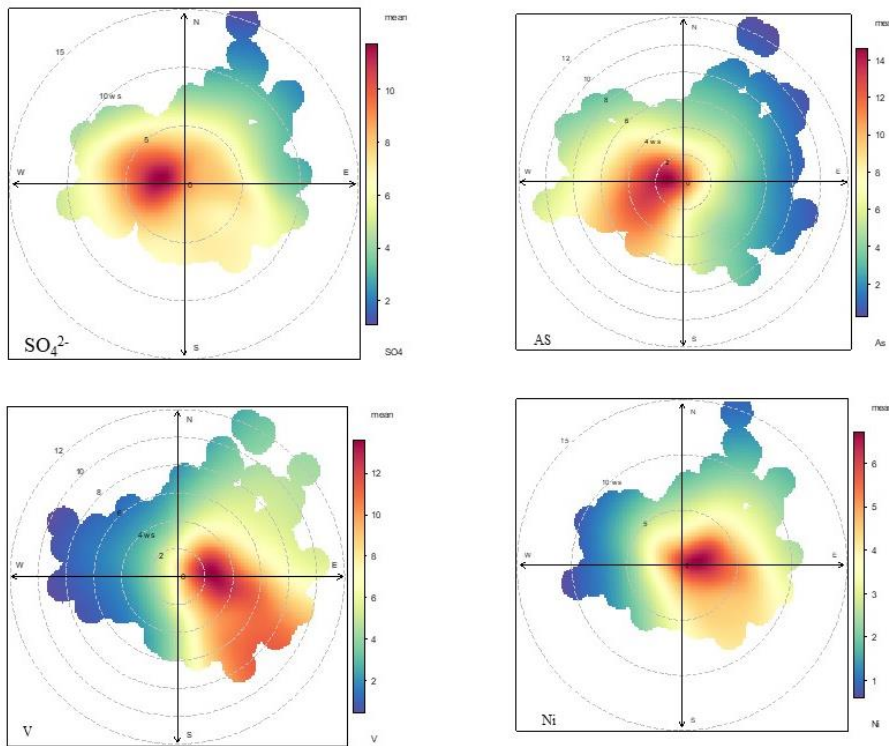
Response: Thanks for this good suggestion. Actually, we've tried hard to apportion the major sources of PBM and GOM by using PMF. However, we found the results difficult to explain. We think that the possible reasons are that the concentrations of PBM and GOM fluctuated much stronger than other atmospheric species such as soluble ions, organic/elemental carbon,

and elements. Due to the relatively short residence time in the atmosphere, it seems not suitable by digesting PBM and GOM into the PMF analysis. Thus, we didn't include source apportionment of PBM and GOM in this study.

28. Another suggestion is to confirm whether the sources identified from PMF are located in the southwest region, where you previously identified as the wind direction sector associated with the highest concentrations. Aside from using the ions and trace metals data for PMF analysis, the data can be used in the previous wind direction and PSCF analyses and also in the time-series analyses with speciated Hg. The concentration spikes in GOM (800-1000 pg/m³ at times) as shown in the time-series plots are very concerning, and I would look further into what is the cause of this.

Response: Thanks for the suggestion. In order to discuss where the sources identified from PMF came from, wind roses of SO₄²⁻, As, Ni, and V are plotted in the figure below. SO₄²⁻ and As shared similar patterns with high concentrations mainly from the southwest. SO₄²⁻ and As are tracers for coal combustion. PMF identified combustion is the biggest source of GEM. Thus, this confirmed that the major sources of GEM are located in the southwest region.

Ni and V showed similar patterns with high concentrations mainly from the northeast, east, and southeast. PMF identified a shipping source from the ocean. The wind rose plots of Ni and V also confirmed the identification of the shipping factor.



29. Lines 435-438: "Accordingly, as an anthropogenic emitting tracer, the concentration of carbon monoxide was basically stable and even showing a downward trend, which suggested that anthropogenic activities were not the main driving force for the increase of GOM." I am skeptical about this. Is CO a tracer for all types of industries or only those involving combustion? The point that CO was stable and not increasing with GOM doesn't necessarily imply no

anthropogenic influence. CO is stable likely because it is continuously supplied by the high density of combustion activities in this region.

Response: Thanks for the comments. CO is generally regarded as a tracer for industries involving combustion. According to the inventory of Hg emissions in the YRD region, the main sources of Hg were related to the industries involving coal combustion (Wang et al., 2016). Thus the level of CO concentration could be used to represent the intensity of anthropogenic emissions to some extent. We agree with the reviewer that CO was stable and not increasing with GOM doesn't necessarily imply no anthropogenic influence. In Figure 11, although GOM didn't co-vary with CO, we didn't mean to say "no anthropogenic influence". In the revised manuscript, this sentence is revised as "Accordingly, as an anthropogenic emitting tracer, the concentration of carbon monoxide was basically stable and even showing a downward trend, which suggested some other factors accounted for the increase of GOM in addition to the anthropogenic emissions" to avoid any misunderstandings.

30. Lines 438-469: The discussion on GEM oxidation by ozone is too speculative. As mentioned, there are many potential oxidants of GEM, but they were not analyzed in this work. I think the understanding of Hg transformation is very complicated, and this discussion does not really acknowledge that

Response: Thanks for the comments. Severe ozone pollution frequently occurred in the YRD due to strong anthropogenic emission intensities (Lu et al., 2018). In this study, high GOM concentrations were observed (Fig. 2). GOM concentration showed a clearly positive correlation with temperature in summer, the summer mean GOM concentration was higher than spring and autumn, a clear positive correlation between GOM and O₃ were also observed in both statistical analysis (Fig. 12) and episode events (Fig. 11). In this regard, we think that the atmospheric oxidants should play an important role in GEM oxidation. But of course, we understand that the formation mechanism of GOM is complicated and we are not trying to elucidate it based on limited measured parameters. In the revised manuscript, we have revised the title of Section 3.4 as "Factors affecting the formation and transformation of mercury species". In the context of this section, we have adjusted the writings to focus on the crucial factors affecting the formation and transformation of mercury species but not the intrinsic mechanisms.

References

- Cheng, I., Zhang, L. M., Mao, H. T., Blanchard, P., Tordon, R., and Dalziel, J.: Seasonal and diurnal patterns of speciated atmospheric mercury at a coastal-rural and a coastal-urban site, *Atmospheric Environment*, 82, 193-205, 10.1016/j.atmosenv.2013.10.016, 2014.
- Draxler, R. R., & Rolph, G. D. (2012). HYSPLIT (HYbrid Single-Particle Lagrangian Integrated Trajectory) Model access via NOAA ARL READY Website. NOAA Air Resources Laboratory, Silver Spring, MD. <http://ready.arl.noaa.gov/HYSPLIT.php>. Accessed March 2012.
- Friedli, H. R., Arellano, A. F., Geng, F., Cai, C., and Pan, L.: Measurements of atmospheric mercury in Shanghai during September 2009, *Atmospheric Chemistry and Physics*, 11, 3781-3788, 10.5194/acp-11-3781-2011, 2011.

- Lee, G.-S., Kim, P.-R., Han, Y.-J., Holsen, T. M., Seo, Y.-S., and Yi, S.-M.: Atmospheric speciated mercury concentrations on an island between China and Korea: sources and transport pathways, *Atmospheric Chemistry and Physics*, 16, 4119-4133, 10.5194/acp-16-4119-2016, 2016.
- Lu, X., Hong, J., Zhang, L., Cooper, O. R., Schultz, M. G., Xu, X., Wang, T., Gao, M., Zhao, Y., and Zhang, Y.: Severe Surface Ozone Pollution in China: A Global Perspective, *Environmental Science & Technology Letters*, 10.1021/acs.estlett.8b00366, 2018.
- Pacyna, J. M., Travnikov, O., De Simone, F., Hedgecock, I. M., Sundseth, K., Pacyna, E. G., Steenhuisen, F., Pirrone, N., Munthe, J., and Kindbom, K.: Current and future levels of mercury atmospheric pollution on a global scale, *Atmos. Chem. Phys.*, 16, 12495-12511, 10.5194/acp-16-12495-2016, 2016.
- Tang, Y., Wang, S. X., Wu, Q. R., Liu, K. Y., Wang, L., Li, S., Gao, W., Zhang, L., Zheng, H. T., Li, Z. J., and Hao, J. M.: Recent decrease trend of atmospheric mercury concentrations in East China: the influence of anthropogenic emissions, *Atmospheric Chemistry and Physics*, 18, 8279-8291, 10.5194/acp-18-8279-2018, 2018.
- Wan, Q., Feng, X. B., Lu, J. L., Zheng, W., Song, X. J., Han, S. J., and Xu, H.: Atmospheric mercury in Changbai Mountain area, northeastern China I. The seasonal distribution pattern of total gaseous mercury and its potential sources, *Environmental Research*, 109, 201-206, 10.1016/j.envres.2008.12.001, 2009.
- Wang, X., Lin, C.-J., Yuan, W., Sommar, J., Zhu, W., and Feng, X.: Emission-dominated gas exchange of elemental mercury vapor over natural surfaces in China, *Atmospheric Chemistry and Physics*, 16, 11125-11143, 10.5194/acp-16-11125-2016, 2016.
- Wu, Q., Wang, S., Li, G., Liang, S., Lin, C.-J., Wang, Y., Cai, S., Liu, K., and Hao, J.: Temporal Trend and Spatial Distribution of Speciated Atmospheric Mercury Emissions in China During 1978–2014, *Environmental science & technology*, 50, 13428-13435, 10.1021/acs.est.6b04308, 2016.
- Zhang, L., Wang, S. X., Wang, L., and Hao, J. M.: Atmospheric mercury concentration and chemical speciation at a rural site in Beijing, China: implications of mercury emission sources, *Atmospheric Chemistry and Physics*, 13, 10505-10516, 10.5194/acp-13-10505-2013, 2013.
- Zhu, J., Wang, T., Talbot, R., Mao, H., Hall, C. B., Yang, X., Fu, C., Zhuang, B., Li, S., Han, Y., and Huang, X.: Characteristics of atmospheric Total Gaseous Mercury (TGM) observed in urban Nanjing, China, *Atmospheric Chemistry and Physics*, 12, 12103-12118, 10.5194/acp-12-12103-2012, 2012.
- Zhu, J., Wang, T., Talbot, R., Mao, H., Yang, X., Fu, C., Sun, J., Zhuang, B., Li, S., Han, Y., and Xie, M.: Characteristics of atmospheric mercury deposition and size-fractionated particulate mercury in urban Nanjing, China, *Atmospheric Chemistry and Physics*, 14, 2233-2244, 10.5194/acp-14-2233-2014, 2014.
- Zhu, J., Wang, T., Bieser, J., and Matthias, V.: Source attribution and process analysis for atmospheric mercury in eastern China simulated by CMAQ-Hg, *Atmos. Chem. Phys.*, 15, 8767-8779, 10.5194/acp-15-8767-2015, 2015.
- Xu, L. L., Chen, J. S., Yang, L. M., Niu, Z. C., Tong, L., Yin, L. Q., and Chen, Y. T.: Characteristics and sources of atmospheric mercury speciation in a coastal city, Xiamen, China, *Chemosphere*, 119, 530-539, 10.1016/j.chemosphere.2014.07.024, 2015.

Xu, X., Liao, Y., Cheng, I., and Zhang, L.: Potential sources and processes affecting speciated atmospheric mercury at Kejimkujik National Park, Canada: comparison of receptor models and data treatment methods, *Atmospheric Chemistry and Physics*, 17, 1381-1400, 10.5194/acp-17-1381-2017, 2017.

Response to Reviewer#3's comments

Anonymous Referee #3:

This manuscript presents an analysis of speciated atmospheric mercury (Hg), i.e. gaseous elemental mercury (GEM), particulate-bound mercury (PBM), and gaseous oxidized mercury (GOM), during June 2015 to May 2016 at the Dianshan Lake Station (DSL), Shanghai, east China. The topic is relevant to the Atmospheric Chemistry and Physics. However, the scientific contribution is hindered by a lack of methodology description in certain sections, some debatable analysis, some overreaching conclusions, and the quality of presentation. My specific comments and suggestions are listed below.

We sincerely thank for the reviewer's in-depth comments and helpful suggestions on this manuscript. Based on the specific comments, we have responded to all the comments point-by-point and made corresponding changes in the manuscript as highlighted in red color. The reviewer has raised a number of issues and we quite agree. We feel the substantial revisions based on the reviewer's comments have greatly improved the quality of this manuscript. Please check the detailed responses to all the comments as below.

1. re-emissions from surfaces.

It is concluded that "GEM at DSL exhibited high concentrations in both warm and cold seasons, which was due to the strong re-emission fluxes from natural surfaces in summer..." (L506) However, there is no quantitative analysis to support this claim. The authors pointed out that "It has to be noted that since no tracers for the natural emissions (e.g. soils, vegetations, and ocean) were available in this study, the identification of natural mercury sources was not possible." (L390). The reviewer believes that temperature could be used to identify reemission with factor analysis approaches, such as Principal Component Analysis (PCA).

Response: Thanks for the suggestion. We applied the PCA to identify the potential sources of GEM by adding temperature. Four factors are resolved, which totally explained 75.32% of the variance as shown in the table below.

Factor 1 accounted for 34.15% of the total variance with high loadings for SO_2 , SO_4^{2-} , NH_4^+ , K^+ , Pb , Se , and As , which is explained as coal combustion mixed with biomass burning. Factor 2 accounted for 14.85% of the total variance with high loadings for temperature, O_3 , and NH_3 , which was explained as surface emissions. Factor 3 explained 13.43% of the total variance and showed high loadings for Ni and V , which indicated the contribution of ship emissions. Factor 4 explained 12.89% of the total variance and showed high loadings for Fe and Ca , indicating the contribution of cement production.

In the revised manuscript, we have added PCA analysis to perform source apportionment with PMF.

Table R1. PCA analysis for GEM at DSL.

	Factor 1	Factor 2	Factor 3	Factor 4
GEM	0.50	0.25	0.11	0.07
SO ₂	0.69	-0.20	-0.18	0.35
NO ₂	0.38	-0.49	0.35	0.39
SO ₄ ²⁻	0.84	0.13	0.15	0.00
NH ₄ ⁺	0.88	-0.12	0.18	0.07
K ⁺	0.77	-0.25	0.04	0.39
Pb	0.80	-0.17	0.04	0.32
Se	0.87	-0.05	0.01	0.29
As	0.82	-0.23	0.06	0.33
O ₃	0.06	0.79	-0.30	0.03
NH ₃	0.03	0.73	0.36	-0.04
Temperature	-0.23	0.82	0.17	-0.03
Ni	0.24	-0.02	0.85	0.22
V	-0.03	0.11	0.90	-0.05
Fe	0.50	-0.12	0.24	0.74
Ca	0.26	0.08	0.00	0.90
Explained variance %	34.15	14.85	13.43	12.89

2. formation of GOM and PBM, local vs. regional events.

a. L359-369, CO and SNA concentrations were used to show that “GOM/PBM ratio was a reliable tracer for assessing the relative importance of regional/long-range transport vs. local atmospheric processing.” (L368). Because CO and SNA concentrations are available, perhaps there is little need to use the GOM/PBM ratio, or GEM/CO ratio could be used as in previous studies of atmospheric Hg.

Response: Thank for the suggestion. We used CO and SNA to supplement the results based on the application of the ratio of GOM/PBM. The results by using CO and SNA or GOM/PBM are generally consistent, thus our study can be served as a reference that the GOM/PBM ratio could be used a tracer for assessing the relative importance of regional/long-range transport vs. local atmospheric processing even when data such as CO and SNA are not available.

b. Local vs. regional events. The authors stated that “Fig. 12 also demonstrated the increases of GOM along with the ratios of GOM/PBM. The lower ratios of GOM/PBM were associated with lower temperature and O₃ concentrations, indicating the more probable long range/regional events during the cold seasons with relatively weak photochemistry. On the contrary, the higher ratios of GOM/PBM were associated with higher temperature and O₃ concentrations, indicating the more probable local events during the warm seasons with relatively strong photochemistry.” (L460) This reasoning seems to suggest that “long range/regional events” and “local events” dominate during the cold and warm seasons respectively. The authors may want to present evidence that the study site was shielded from long range transport in some seasons, because most receptors are under the influence of long-range transport all the time. In my view, air mass from all directions would have higher temperature and O₃ concentrations in summer thus “relatively strong photochemistry” than those in winter, regardless “local” or “long range/regional events”. Therefore, higher temperature and O₃ concentrations in warm season would indicate “relatively strong photochemistry” but not “local events”. Similarly, lower temperature and O₃ concentrations in cold season would indicate “relatively weak photochemistry” but not “long range/regional events”. The authors may want to amend this section and the related conclusions.

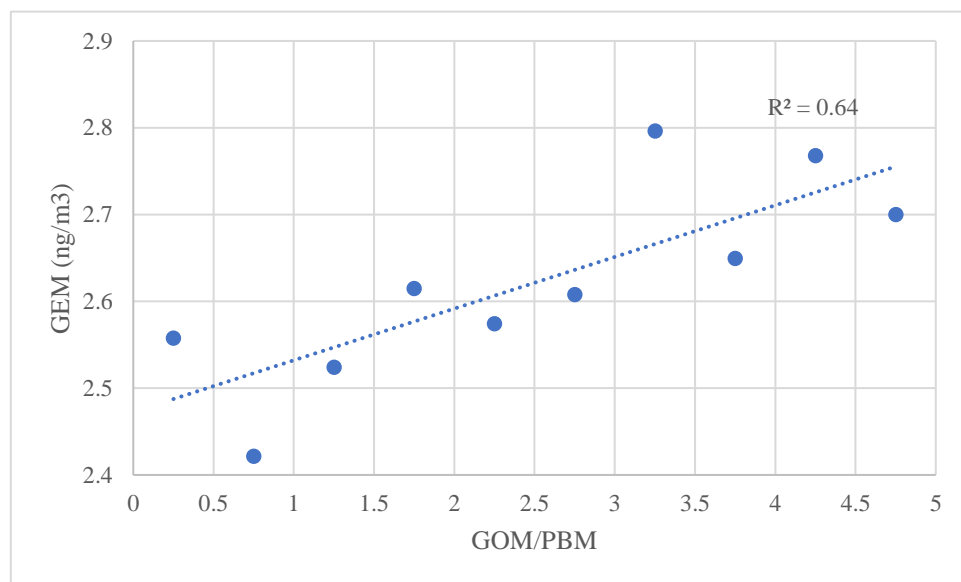
Response: Thanks for the reviewer’s in-depth comments and we totally agree. We revised the description as “Fig. 12 also suggested that the lower ratios of GOM/PBM were associated with lower temperature and O₃ concentrations, indicating relatively weak photochemistry during the cold seasons. On the contrary, the higher ratios of GOM/PBM were associated with higher temperature and O₃ concentrations, indicating relatively strong photochemistry during the warm seasons” in the revision.

c. GEM levels. It was concluded that “GEM as a function of the GOM/PBM ratios indicated that when the quasi-local sources dominated, GEM concentrations were relatively higher than those events under the regional/long-range transport conditions” (L522-524). L370-382, “In the GOM/PBM ratio bins of less than 2.5, GEM fluctuated with the mean values less than 2.6 ng/m³. The mean GEM concentration increased from 2.61 ng/m³ in the GOM/PBM ratio bin of 2.5-3.0 to 2.8 ng/m³ in the bin of 3.0-3.5, and then remain relatively stable when the GOM/PBM ratio bins higher than 3.0.” Indeed, this is the only noticeable increase in GEM (a 7% increase from the bin of 2.5-3.0 to that of 3.0-3.5) among 10 bins, while the change in GEM concentrations between the first and last bin is less than 5%. Nonetheless, the authors stated that “Generally, GEM showed an increasing trend as the GOM/PBM ratios increased while both SNA and CO decreased. The elevation of GEM concentrations tended to be associated with the impact of quasi-local sources. In contrast, under the high SNA and CO conditions when GOM/PBM ratios were lower, GEM was relatively low, suggesting its formation was not favored via the regional/long-range transport.” The authors may need to report the statistical trend (e.g. regression) if any, and clarity what type of GEM “formation was not favored via the

regional/long-range transport”, and explain why GEM would change with the strength of photochemistry. In case GEM is high in summer due to re-emission when GOM is also high due to higher oxidant levels, then the common course is meteorological conditions, namely ambient temperature, an analysis taking into account seasonal trend of all variables involved could be more appropriate, instead of the seemingly speculative approach employed.

Response: Thanks for the insightful comments. The regression analysis between GEM and GOM/PBM was shown in the figure below. Correlation coefficients of the regression reached 0.64, suggesting the positive correlation between GEM concentrations and GOM/PBM ratios. By stating “GEM formation was not favored via the regional/long-range transport” in the original writings, we meant to say that when the impact of long-range transport was important, GEM concentrations were observed to be relatively low. The usage of the word “formation” might lead to misunderstandings here, so we revised the sentence as “In contrast, under the high SNA and CO conditions when GOM/PBM ratios were lower, GEM showed relatively low concentrations. This suggested the regional/long-range transport didn’t favor the elevation of GEM concentrations.”.

The seasonal relationship between temperature and Hg concentrations have been discussed in details in Section 3.1. Generally, the GEM concentrations increased as the temperature increased, which is interpreted to be likely from the surface emissions. GOM concentration showed a clearly positive correlation with temperature, which might be related to the in situ oxidation of GEM under high temperature.



3 PBM formation

1) L476, "Fig. 13 shows the statistical pattern of the variation of PBM and GOM in the ascending bins of PM2.5. It was obvious that the concentrations of PBM increased with the concentrations of PM2.5, which was due to both primary emissions and the subsequent process of Hg species adsorbed on particulate matters." The authors may want to provide more evidence or citation to support that increasing PBM with increasing PM2.5 concentrations "was due to

both primary emissions and the subsequent process of Hg species adsorbed on particulate matters”

Response: Thanks for the suggestion. Previous studies have shown that PBM can be emitted directly from various anthropogenic sources such as coal-fired power plants and industries (Liu et al., 2018; Wu et al., 2016). In addition, a number of studies concluded that gas-particle partitioning of TGM is an important pathway of PBM formation in urban areas of China (Shon et al., 2005; Fu et al., 2015). The high levels of particles in Eastern China probably facilitated the formation of PBM (Fu et al., 2015).

In the revised manuscript, we have added references in the related paragraphs in Section 3.4.2.

2) L480, “When PM_{2.5} concentrations were at relatively low levels under 75 µg/m³, GOM concentrations increased with PM_{2.5}. However, when PM_{2.5} concentrations exceeded 75 µg/m³, GOM exhibited a slightly decreasing trend as PM_{2.5} increased. It seemed that when the concentration of PM_{2.5} reached a certain value, the formation of GOM was inhibited to some extent, which was likely due to the adsorption of GOM onto the particles.” “Statistical analysis showed that when PM_{2.5} reached a certain value, GOM was inhibited to some extent due to the gas-particle partitioning process.” (L34-35) Those statements/conclusions seem to be debatable. As seen in Fig 13, when PM_{2.5} concentrations exceeded 75 µg/m³, GOM decreased till PM_{2.5} reached 105 µg/m³ then increased, instead of a slightly decreasing trend. The authors may need to report the statistical trend (e.g. regression) if any and rephrase the statements about inhibitive effects in discussion and conclusion, or omit this passage. Based on an analysis of a three-day episode (December 30, 2015 to January 1, 2016), the authors concluded that “Under high PM_{2.5} concentrations, high humidity and low temperature conditions, the gas-particle partitioning process was obvious at DSL, which might be an important pathway for the formation of PBM.” (L532) The authors may want to provide more in-depth analysis of the reliance of PBM on PM_{2.5} concentrations when temperature and relative humidity levels favor formation of PBM, and justify the use of a three-day episode in winter to represent the year-long study period. My scan of Fig 6 suggests that only in autumn the PBM levels increase with decreasing ambient temperature, not in other three seasons including winter (the three-day episode).

Response: Thanks for the comments. We do agree with the reviewer that the description about the trends of GOM and PM_{2.5} seems to be debatable. Thus, the sentence has been changed as “However, when PM_{2.5} concentrations increased to 75-105 µg/m³, GOM exhibited as obvious decreasing trend as PM_{2.5} increased.” and added the sentences “when PM_{2.5} concentrations exceeded 105 µg/m³, GOM exhibited a slightly increasing trend as PM_{2.5} increased. High PM_{2.5} concentrations in China always related to severe anthropogenic emissions (Auzmendi-Murua et al., 2014), so the moderate increasing trend of GOM in these bins should be attributed to the impact of strong primary emissions.” in the revision.

Previous study in an island between China and Korea has demonstrated that the partition coefficient of mercury gas-particle partitioning in atmosphere was negative correlated with atmospheric temperature and positively correlated with relative humidity (Lee et al., 2016). From the seasonal statistical analysis in Fig 6, the autumn PBM levels showed a clear decreasing trend with increasing ambient temperature, while the spring and winter PBM

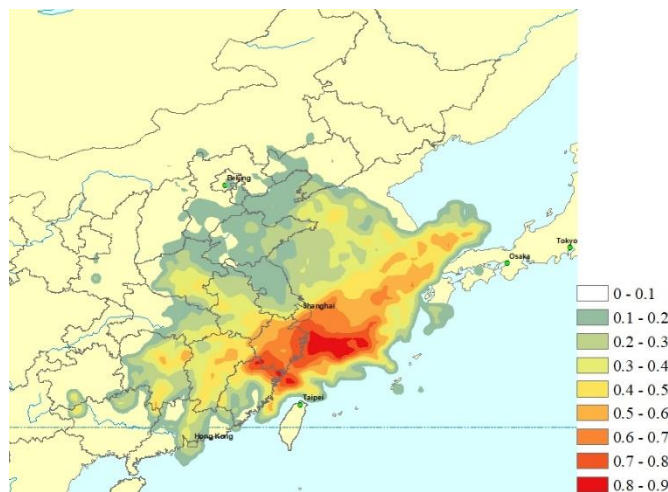
showed a moderate decreasing trend with increasing ambient temperature. We think that this phenomenon can demonstrate the influence of gas-particle partitioning process and temperature on the PBM concentration during the whole study period to some extent.

3) contribution of the shipping sector

It is concluded that “shipping emissions” contributed to 20% of GEM based on PMF (L30, L526). However, there is a lack of data support. The authors may want to a) identify the port on Fig 1, b) find out the Hg emission value at and near this port (I believe that researchers from Tsinghua University have some related publications), and compare the shipping sector emission with emissions from other sources, c) for each sample, plot the time series of contribution to GEM by this factor and the wind or air mass direction to verify that this factor indeed represents the shipping sector.

Response: Thanks for the suggestion. The ports in the YRD region has been added in Fig 1. However, Hg emissions at the port level are not available as the public emission inventories are always grided.

As the reviewer suggested, we have extracted the time-series of GEM concentrations from the shipping factor based on the PMF modeling. We use this time-series into the PSCF modeling. The figure below showed the potential sources regions were mainly located over the East China Sea, which indicated Factor 2 from PMF should be representative of the shipping sector.



2. The title reads, “Characteristics of atmospheric mercury in East China: implication on sources and formation of mercury species over a regional transport intersection zone”. The authors may want to justify the use of data from a single site to represent 1) atmospheric Hg in East China, and 2) regional transport intersection zone, or rephrase the title. Similarly, some conclusions are a bit over-reaching, e.g. “shipping emission was found to be an important source (19.6%) of atmospheric mercury in East China” (L30)

Response: Thanks for the suggestion. The title is changed as “Characteristics of atmospheric mercury in the suburbs of East China: implication on sources and formation of mercury species over a regional transport intersection zone”.

In the original abstract, the sentence before the writing “Besides the common anthropogenic emission sectors, shipping emission was found to be an important source (19.6%) of atmospheric mercury in East China” is “Six sources and their contributions to anthropogenic GEM were identified.”. The PMF modeling only resolve source apportionment to anthropogenic mercury. However, based on the original data analysis and additional PCA analysis, we found the observed mercury has sources from natural emissions. Thus, the number 19.6% only pointed to anthropogenic emissions, but not all the mercury emissions. In the revised abstract, we have changed “atmospheric mercury” to “anthropogenic mercury” for clarification.

3. Seasonal trend of Hg species

The differences in seasonal mean TGM concentrations could be too small (max=2.88 ng/m³, min=2.63 ng/m³, the difference is 9%; summer 2.87 ng/m³, spring 2.73 ng/m³, difference 5%) and statistically not significant to support the conclusion of “GEM concentrations were elevated in both cold and warm seasons” (L21) and “GEM at DSL exhibited high concentrations in both warm and cold seasons, which was due to the strong re-emission fluxes from natural surfaces in summer and enhanced coal combustion for residential heating over northern China in winter.” (L506). The authors may want to conduct comparison of multiple means (e.g. under ANOVA) for each of the three Hg species, and rephrase the discussion and conclusion in case the seasonal means are not statistically significant. Furthermore, please comment on the reasons of small difference among the four seasonal means if coal combustion for residential heating is enhanced in winter and re-emission fluxes from natural surfaces is strong in summer

Response: The table below showed the p-value by t-test between seasons for GEM concentrations, which suggested that the GEM concentration in autumn is statistically different from that of spring, summer, and winter ($p<0.05$), while there are no significant differences among spring, summer, and winter ($p>0.05$). In this regard, we revised the description as “Statistical test showed no significant differences of the seasonal variations of GEM concentrations among spring, summer, and winter were observed (Table S1). This was different from many urban and remote sites in China, such as Guiyang, Xiamen, and Mt. Changbai, where GEM showed significantly high concentrations in cold seasons than those in warm seasons (Feng et al., 2004; Xu et al., 2015; Fu et al., 2012). The relatively high GEM concentrations during the cold season in China should be attributed to the increases of energy consumption (Fu et al., 2015). In this study, GEM concentration in summer was comparable to that in winter, which was likely attributed to the strong natural mercury emissions (e.g. soils, vegetations, and water) due to elevated temperature in summer (Liu et al., 2016)” in the revision.

Table R1. P-value between seasons for GEM concentration

	spring	summer	autumn	winter
spring				

summer	p>0.05			
autumn	p<0.05	p<0.05		
winter	p>0.05	p>0.05	p<0.05	

4. Methodology is missing at numerous places. e.g. 1) please explain how to plot “Mean concentrations of (b) GEM, (c) PBM, and (d) GOM as a function of wind speed and wind directions” (L700) in the Method section and why Figures 5(b), (c) and (d) do not represent the frequency of wind directions shown in Figure 5 (a), in the Results section. 2) details of the backward trajectory simulation should be provided, including the model being used, run time, and start height, each with a justification, 3) where and how to use the “weighting function (w_{ij})” (L162), 4) PMF, the treatment of missing data if any, and the total number of samples, 5) what is “the uncertainty of the j th pollutant on the i th measurement” (L187) in your study, 6) how to evaluate whether PMF is able to reproduce the observed Hg concentrations (e.g. time series and/or seasonal means), 7) how was hourly or bi-hourly PBL (assume it means Planetary Boundary Layer) height measured or estimated, 8) how was “secondary inorganic aerosols (SNA)” (L359) or “SNA (sulfate, nitrate, and ammonium) in PM2.5” (L715) monitored, 9) how to conduct analysis with bi-hourly Hg data and hourly data of meteorological parameters and other air pollutants.

Response:

1) Figure 5 (b), (c), and (d) were plotted by the software R-studio. The radii of the circles in Figure 5 (b), (c), and (d) represent the value of wind speed. Figure 5 (b), (c), and (d) showed the relationship of Hg concentrations with wind speed and wind directions. As for Figure 5(a), the radii of the circles represent the frequency of wind directions but not the value of wind speed. In the revised manuscript, we have stated more clearly in the caption of Figure 5.

2) The details of the backward trajectory simulation have now been added into the Method section.

The HYSPLIT (HYbrid Single-Particle Lagrangian Integrated Trajectory) model is applied for calculating air mass backward trajectories (Draxler and Rolph, 2012). The model was run online at the NOAA ARL READY Website using the meteorological data archives of Air Resource Laboratory (ARL). The meteorological input data used in the model was obtained from NCEP (National Centers for Environmental Prediction’s global data assimilation system (GDAS) with a horizontal resolution of $0.5^\circ \times 0.5^\circ$. In this study, 72-hours back trajectories were calculated at 500m AGL (above ground level) and the cell size was set as $0.5^\circ \times 0.5^\circ$.

3) w_{ij} is an empirical value to reduce the uncertainties of PSCF values in certain grid cells that are associated with a small number of endpoints. The values of w_{ij} have been shown in Eq. (2) in the manuscript and w_{ij} is multiplied by $PSCF_{ij}$ to derive the weighted PSCF values.

In this revision, we have stated clearly about the calculation.

4) we added the details of PMF model runs in the Method section. In this study, the number of factors from 3 to 8 was examined with the optimal solutions determined by the slope of the Q value versus the number of factors. For each run, the stability and reliability of the output were assessed by referring to the Q value, residual analysis and correlation coefficients between observed and predicted concentrations. Finally, a 6-factor solution, which showed the most stable results and gave the most reasonable interpretation, was chosen. Before running the model, a data set including unique uncertainty values of each data point was created and inserted into the model, the error fraction was assumed to be 15% of concentrations for GEM and 10% of concentrations for other compounds (Xu et al., 2017), the missing data were excluded and the total number of samples is 3526.

5) The error fraction was set as 15% of concentrations for GEM and 10% of concentrations for other compounds (Xu et al., 2017).

6) In this study, the number of factors from 3 to 8 was examined with the optimal solutions determined by the slope of the Q value versus the number of factors. For each run, the stability and reliability of the output were assessed by referring to the Q value, residual analysis and correlation coefficients between observed and predicted concentrations. Finally, a 6-factor solution, which showed the most stable results and gave the most reasonable interpretation, was chosen. These procedures guaranteed the PMF was able to reproduce the observed Hg concentrations.

7) The data of the height of planetary boundary layer (PBL) were retrieved from the U.S. National Oceanic and Atmospheric Administration
(<https://ready.arl.noaa.gov/READYamet.php>).

8) Water-soluble inorganic anions (SO_4^{2-} , NO_3^- , Cl^-) and cations (K^+ , Mg^{2+} , Ca^{2+} , NH_4^+) in $\text{PM}_{2.5}$ were simultaneously monitored by the Monitor for Aerosols and Gases in ambient Air (MARGA) at the temporal resolution of one hour. The details of the instrument have been described in the first paragraph of Section 2.3.

9) To conduct data analysis with bi-hourly Hg data and hourly data of meteorological parameter, we first converted hourly meteorological data to bi-hourly meteorological data. Briefly, the hourly meteorological data was converted into the X and Y vectors. Then wind speed at the X and Y vectors were averaged and final we can get the average wind speed and wind direction based on the trigonometric function.

5. GOM and PBM could be included in PMF source apportionment. The results (e.g. sample by sample GEM, GOM, PBM, CO, SNA etc contributions in each factor) might help the identification of age of the air mass, as well as sources and processes related with Hg.

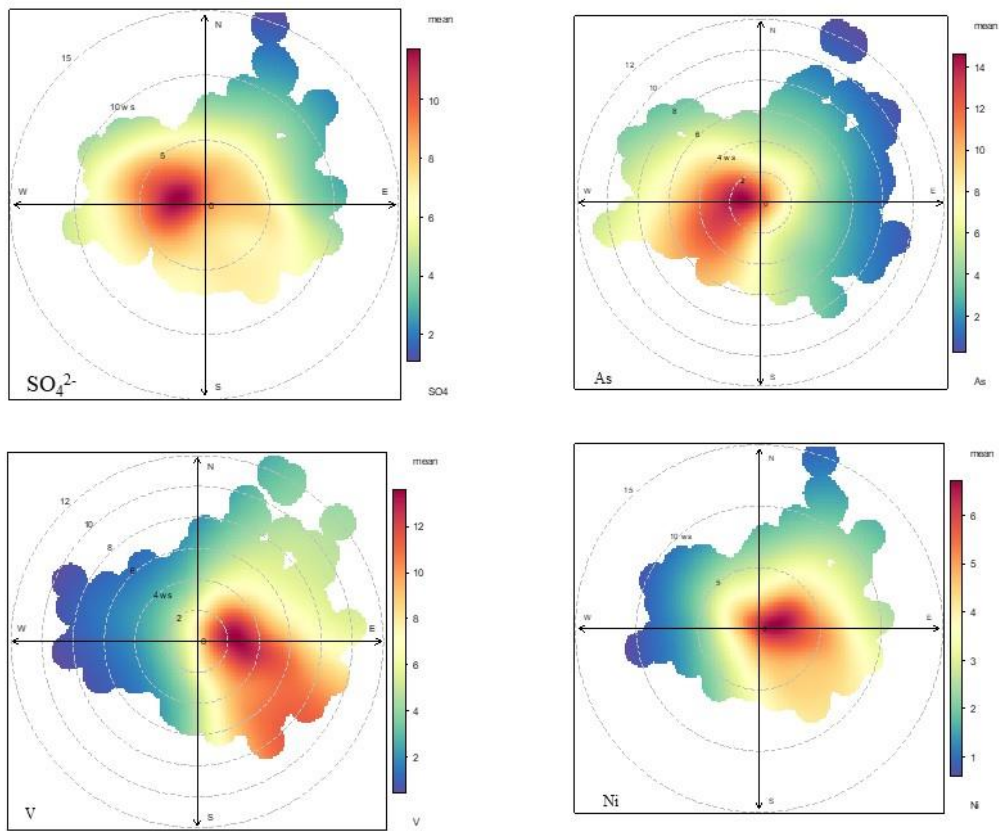
Response: Thanks for this suggestion. Actually, we've tried hard to apportion the major sources of PBM and GOM by using PMF. However, we found the results difficult to explain. We think that the possible reasons are that the concentrations of PBM and GOM fluctuated much stronger than other atmospheric species such as soluble ions, organic/elemental carbon, and elements. Due to the relatively short residence time in the atmosphere, it seems not suitable by digesting

PBM and GOM into the PMF analysis. Thus, we didn't include source apportionment of PBM and GOM in this study.

6. Interpretation of PMF results. This section could be improved by a more in-depth analysis and/or citation of existing literature. Overall, the analysis seems to be subjective at times, leading to invalid or overreaching statements/conclusions based on measurements at one site, a small difference in seasonal or binned concentrations, speculative approaches, or a short episode of a few days. It is recommended to clarify the meaning of local and regional events, whether "local" means local man-made emissions, local re-emission, local photochemical reactions, all of the above; or different item in different sections. Time series (Fig 2) or box plots (Fig 3) of temperature, relative humidity, CO, PM2.5 mass, SNA (sulfate, nitrate, and ammonium, or secondary inorganic aerosols), O₃, and GOM/PBM ratios could be employed to depict seasonal trend of those variables, which may help to differentiate the association from causation.

Response: Thanks for the comments. In this study, local sources represented all emission sources in local area. GOM/PBM ratios together with CO, and SNA were used to reveal the relative importance of local sources vs. long-range transport.

In order to validate the PMF results, wind roses of SO₄²⁻, As, Ni, and V are plotted in the figure below. SO₄²⁻ and As shared similar patterns with high concentrations mainly from the southwest. SO₄²⁻ and As are tracers for coal combustion. PMF identified combustion is the biggest source of GEM. Thus, this confirmed that the major sources of GEM are located in the southwest region. Ni and V showed similar patterns with high concentrations mainly from the northeast, east, and southeast. PMF identified a shipping source from the ocean. The wind rose plots of Ni and V also confirmed the identification of the shipping factor.



Clarification issues

1. The following items could be included in Fig 1, 1) location of the sampling site, 2) location of the shipping port, 3) the name of all provinces within e.g. 2000 or 3000 km of the sampling site, 4) a scale in the lower-right box, 5) the meaning of the upper-right box, 6) the meaning of the short black line.

Response: Thanks for the suggestion. Due to the conversion problems from text to pdf, some items in the figure were not properly shown in the original submission. Now we have corrected the errors and added marks as the reviewer suggested.

- 1) The location of the sampling site has been marked with a pentagram in Fig. 1.
- 2) The locations of the shipping ports has been marked by the purple triangle marks in Fig. 1.
- 3) The name of all provinces within e.g. 2000 or 3000 km of the sampling site have been added in Fig 1.
- 4) the plotting scale of the lower-right box has been added.
- 5) The upper-right box showed the compass of the map but failed to display, there must be an error in the file conversion.

6) That line was due to an error in file conversion and it is corrected now.

2. The provincial level Hg emissions in Wu et al. (2016) could be provided as supplemental information.

Response: The provincial level Hg emissions in Wu et al. (2016) have been provided as supplemental information in the revision.

3. Please provide the distance between the sampling site and the nearest coastal line, and comment on whether the sampling site is capable of capturing the land-sea circulation.

Response: The distance between the sampling site and coastal lines is about 50 km. One recent study reported that shipping emissions influenced the air quality in not only coastal areas but also the inland areas hundreds of kilometers away from the sea in China, as shown in the figure below (Lv et al., 2018). In this regard, our sampling site is well capable of capturing the land-sea circulation.

In the revised manuscript, we have added more descriptions about the sampling site.

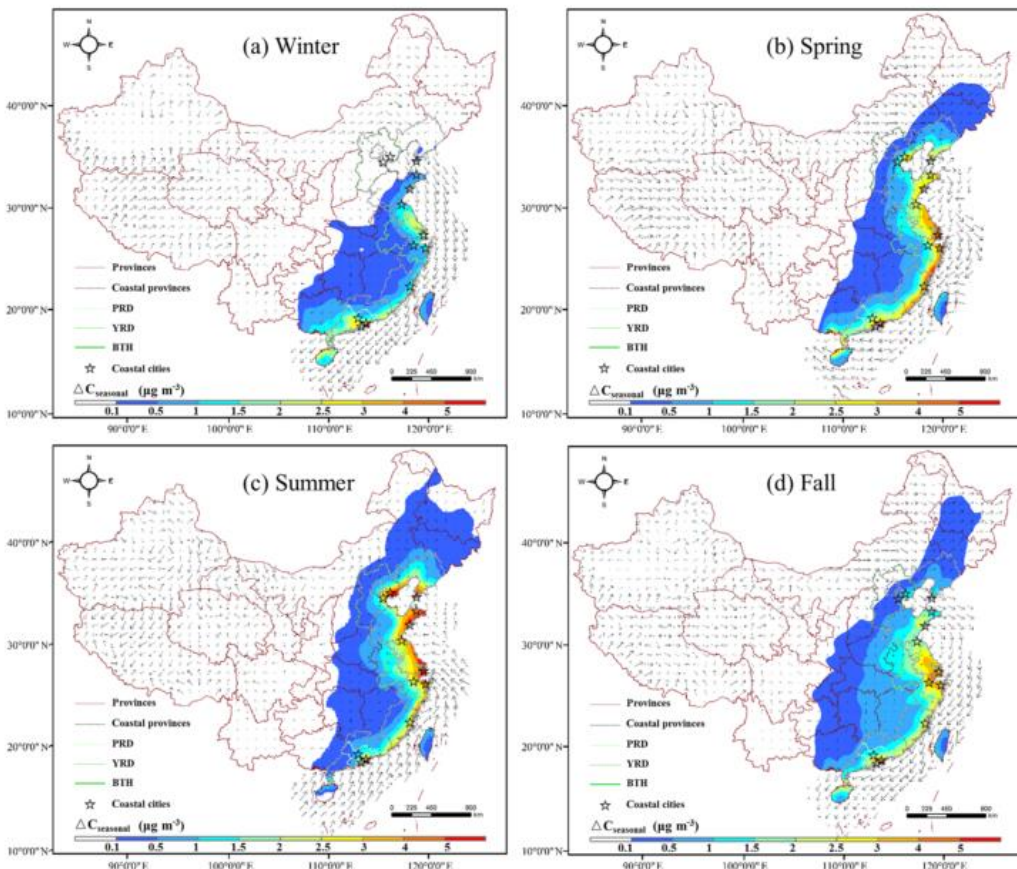


Figure 5. Contributions of shipping emissions to the seasonal mean PM_{2.5} concentrations (base case- no ship case): (a) winter, (b) spring, (c) summer and (d) fall. Arrows represent the WRF modeled seasonal mean surface wind field.

4. L147, “meteorological data”, please provide the height of the instrument about ground level, and comment on whether the instrument is capable of capturing the meteorological condition in the study area.

Response: The instrument was set up on the top roof of a four-story building, which is a supersite carefully maintained by Shanghai Environmental Monitoring Center (SEMC). The height of the instrument is about 14 m above the ground. The sampling site is located in the rural areas and beside the shore of Dianshan Lake. There are no tall buildings or mountains nearby, making sure that this site is capable of capturing the meteorological conditions in the study area.

5. L149, other pollutants, please provide the reporting or averaging intervals of CO, ozone and PM_{2.5} mass measurements.

Response: Thanks for the suggestion. The average intervals of CO, ozone, and PM_{2.5} mass measurements were one hour. We revised the description as “Atmospheric ozone (O₃) concentration was continuously measured using Thermo Fisher 49i, which operates on the principle that ozone molecules absorb UV light at a wavelength of 254 nm. The ambient carbon monoxide (CO) and PM_{2.5} concentrations were measured by Thermo Fisher 48Itle and Thermo Fisher 1405F, respectively. All data were averaged at the intervals of one hour.” in the revision

6. L205 and L362, please explain what is “secondary formation”.

Response: In Line 205, it means the oxidation process of GEM to GOM. In Line 362, it means secondary particle formation. We have expressed more clearly about this term in the revision.

7. L302-304, “The potential source regions of all year round PBM were mainly from northeastern China, including Jiangsu, Anhui, Shandong, and Hebei provinces.” Please justify the classification that Jiangsu and Anhui belong to northeastern China.

Response: Thanks for the comments. The classification of the provinces in the original manuscript is not well defined. We revised the description as “The potential source regions of all year round PBM were mainly from the north of Jiangsu and Anhui provinces, and from northeastern China, including Shandong and Hebei provinces.”

8. section 3.2.2 (L333), all eight wind directions should be included in the discussion. The authors many want to point out that there is little difference in the wind direction distribution between the GOM/PBM bins of 1-2 and 2-3.

Response: Thanks for the suggestion. We revised the sentence as “As shown in Fig. 8, the frequency of south, southwest, west, and northeast winds showed no clear trend as the GOM/PBM ratios increased.” in the revision.

9. Figure 2, please explain the meaning of the red-dish line.

Response: The red-dashed line represented the mean concentrations of each season. We added the sentence “The red-dashed lines represent the mean concentrations of Hg species in each season.” in the caption of Figure 2.

10. Figures 5 (b), (c), (d), what is the meaning of “15 ws”?

Response: “15 ws” in Figures 5(b), (c), (d) meaning the wind speed is 15 m/s. The radii of the circle in Figures 5 (b), (c), (d) represent the value of wind speed.

11. Figures 9 and 12, please explain the meaning of the bars.

Response: The bars in Figures 9 and 12 represent one standard error of the parameters in each bin. It has been clarified in the captions of the figures now.

12. Figure 12 caption, “Temperature as a function of the GOM/PBM ratios” Please explain why temperature would change with changing GOM/PBM ratios in the main body.

Response: This expression is not appropriate. We have changed it as “Temperature variations in each bin of the GOM/PBM ratios”.

13. Figure 13, please explain the meaning of the shaded areas.

Response: The shaded areas in Figure 13 represented one standard error of GOM and PBM concentrations.

Editorial suggestions:

1. The significant number seems to be excessive at times, e.g. one decimal will suffice when presenting Hg concentrations.

Response: Thanks for the comment. We do agree with the reviewer that the significant number is excessive at times. After referring to a number of related papers, we revised the significant number as one decimal for GOM and PBM concentrations and two decimals for GEM concentrations in the revised manuscript.

2. Avoid the use of first person, i.e. “we”.

Response: Thanks for the suggestion. All statements involving the use of first person have been revised in the revision.

3. Please define all abbreviations, e.g. PSCF, PBL, RH, in the main body instead of the headings.

Response: Thanks for the suggestion. All abbreviations have been defined in the main body instead of the headings in the revised manuscript.

4. Inconsistent expressions, e.g. “Equation 1” (L160), “as below” (L163), “shown as Eq. (3)” (L173); “secondary inorganic aerosols (SNA)” (L359), “SNA (sulfate, nitrate, and ammonium) in PM2.5” (L715); RGM (Figure 6).

Response: Thanks for the suggestions. All the inconsistent expressions have been revised in the revision.

5. There are quite a few awkward sentences, e.g. 34-35, L171-172, L268-270, L393 (“Se, As, and Pb, which were typical tracers of coal combustion”), L403-404, L443.

Response: Thanks for pointing it out. The awkward sentences have been adjusted.

6. There are quite a few awkward phrases, e.g. “obvious” (L35 and other places), “comprehensive” (L86, suggest to remove), “Xij is” (L175) should be “where Xij is”, “about” (L305 and other places, suggest to replace with “approximately”), “As similar as Fig. 9” (L452), “CN” in Table 1 should be replaced with “China”.

Response: Thanks for pointing it out. The awkward phrases have been replaced or removed according to the suggestions of the reviewer.

7. The manuscript could be shortened by 1) removing some unnecessary material (e.g. L170-186, those model descriptions could be removed by citing the Users Guide by USEPA or other publications), 2) condense the discussion and conduction sections.

Response: Thanks for the suggestions. We have revised the manuscript as suggested.

8. Figure 2, the seasons seem to be incorrect.

Response: Thanks for pointing this out. The seasons in Figure 2 have been corrected in the revised manuscript.

9. Figure 4 caption, suggest to remove “The red line and black line represented the corresponding diurnal variation of RH and wind speed, respectively.” because there are legends to represent each and all variables.

Response: Thanks for the suggestion. The sentence has been removed in the caption of the figure.

10. Figure 6, the ranges should be, <13, 13-15, 15-17, etc.

Response: Thanks for the suggestion. The presenting of the ranges has been changed in the revision.

11. Figure 8, the ranges should be 0-1, 1-2, 2-3, >3.

Response: The presenting of the ranges has been changed according to the suggestion of the reviewer in the revision.

References:

Auzmendi-Murua, I., Castillo, A., and Bozzelli, J. W.: Mercury Oxidation via Chlorine, Bromine, and Iodine under Atmospheric Conditions: Thermochemistry and Kinetics, *Journal of Physical Chemistry A*, 118, 2959-2975, 10.1021/jp412654s, 2014.

Draxler, R., and Rolph, G.: HYSPLIT - Hybrid Single Particle Lagrangian Integrated Trajectory Model, 2012.

Feng, X. B., Shang, L. H., Wang, S. F., Tang, S. L., and Zheng, W.: Temporal variation of total gaseous mercury in the air of Guiyang, China, *J. Geophys. Res.-Atmos.*, 109, 10.1029/2003jd004159, 2004.

- Fu, X. W., Feng, X., Shang, L. H., Wang, S. F., and Zhang, H.: Two years of measurements of atmospheric total gaseous mercury (TGM) at a remote site in Mt. Changbai area, Northeastern China, *Atmospheric Chemistry and Physics*, 12, 4215-4226, 10.5194/acp-12-4215-2012, 2012.
- Fu, X. W., Zhang, H., Yu, B., Wang, X., Lin, C. J., and Feng, X. B.: Observations of atmospheric mercury in China: a critical review, *Atmospheric Chemistry and Physics*, 15, 9455-9476, 10.5194/acp-15-9455-2015, 2015.
- Lee, G.-S., Kim, P.-R., Han, Y.-J., Holsen, T. M., Seo, Y.-S., and Yi, S.-M.: Atmospheric speciated mercury concentrations on an island between China and Korea: sources and transport pathways, *Atmospheric Chemistry and Physics*, 16, 4119-4133, 10.5194/acp-16-4119-2016, 2016.
- Liu, K., Wang, S., Wu, Q., Wang, L., Ma, Q., Zhang, L., Li, G., Tian, H., Duan, L., and Hao, J.: A Highly Resolved Mercury Emission Inventory of Chinese Coal-Fired Power Plants, *Environmental science & technology*, 52, 2400-2408, 10.1021/acs.est.7b06209, 2018.
- Liu, M. D., Chen, L., Wang, X. J., Zhang, W., Tong, Y. D., Ou, L. B., Xie, H., Shen, H. Z., Ye, X. J., Deng, C. Y., and Wang, H. H.: Mercury Export from Mainland China to Adjacent Seas and Its Influence on the Marine Mercury Balance, *Environmental science & technology*, 50, 6224-6232, 10.1021/acs.est.5b04999, 2016.
- Lv, Z. F., Liu, H., Ying, Q., Fu, M. L., Meng, Z. H., Wang, Y., Wei, W., Gong, H. M., and He, K. B.: Impacts of shipping emissions on PM_{2.5} pollution in China, *Atmospheric Chemistry and Physics*, 18, 15811-15824, 10.5194/acp-18-15811-2018, 2018.
- Shon, Z. H., Kim, K. H., Kim, M. Y., and Lee, M.: Modeling study of reactive gaseous mercury in the urban air, *Atmospheric Environment*, 39, 749-761, 10.1016/j.atmosenv.2004.09.071, 2005.
- Wu, Q. R., Wang, S. X., Li, G. L., Liang, S., Lin, C. J., Wang, Y. F., Cai, S. Y., Liu, K. Y., and Hao, J. M.: Temporal Trend and Spatial Distribution of Speciated Atmospheric Mercury Emissions in China During 1978-2014, *Environmental science & technology*, 50, 13428-13435, 10.1021/acs.est.6b04308, 2016.
- Xu, L. L., Chen, J. S., Yang, L. M., Niu, Z. C., Tong, L., Yin, L. Q., and Chen, Y. T.: Characteristics and sources of atmospheric mercury speciation in a coastal city, Xiamen, China, *Chemosphere*, 119, 530-539, 10.1016/j.chemosphere.2014.07.024, 2015.
- Xu, X. H., Liao, Y. Y., Cheng, I., and Zhang, L. M.: Potential sources and processes affecting speciated atmospheric mercury at Kejimkujik National Park, Canada: comparison of receptor models and data treatment methods, *Atmospheric Chemistry and Physics*, 17, 1381-1400, 10.5194/acp-17-1381-2017, 2017.

1 **Characteristic of atmospheric mercury in the suburbs of East China: implication**
2 **on sources and formation of mercury species over a regional transport intersection**
3 **zone**

4 Xiaofei Qin¹, Xiaohao Wang², Yijie Shi¹, Guangyuan Yu¹, Na Zhao¹, Yanfen Lin², Qingyan Fu²,
5 Dongfang Wang², Zhouqing Xie³, Congrui Deng^{1,*}, Kan Huang^{1,*}

6 ¹*Center for Atmospheric Chemistry Study, Shanghai Key Laboratory of Atmospheric Particle
7 Pollution and Prevention (LAP³), Department of Environmental Science and Engineering, Fudan
8 University, Shanghai, 200433 China*

9 ²*Shanghai Environmental Monitoring Center, Shanghai, 200030 China*

10 ³*School of Earth and Space Sciences, University of Science and Technology of China, Hefei, Anhui,
11 230026 China*

12

13 Correspondence: congruideng@fudan.edu.cn, huangkan@fudan.edu.cn

14

15 **Abstract**

16 Mercury (Hg) is a global pollutant of great concern in East Asia, which is considered to be the largest
17 mercury-emitting region in the world. In this study, atmospheric gaseous elemental mercury (GEM),
18 gaseous oxidized mercury (GOM), and particulate-bound mercury (PBM) were measured
19 continuously over a regional transport intersection zone **in the suburbs of** East China to reveal the
20 sources and formation of mercury species. The annual mean concentrations of GEM, PBM, and
21 GOM reached 2.77 ng/m³, 60.8 pg/m³, and 82.1 pg/m³, respectively. GEM concentrations were
22 elevated in **winter, summer, and spring while lower in autumn**. This seasonal pattern of GEM
23 suggested that the re-emissions from natural surfaces **played** a significant role in the fluctuation of
24 atmospheric mercury in addition to anthropogenic sources. Relationship between Hg species and
25 wind directions indicated the high Hg concentrations were related to winds from the south,
26 southwest, and north of the measurement site. An application of the GOM/PBM tracer method and
27 trajectory-based source region identification **distinguished the relative importance of** long-range
28 transport from northern China and quasi-local emission sources **on the magnitudes of Hg species**. It
29 was revealed that GEM concentrations were higher when quasi-local sources dominated compared

30 to the dominance of long-range transport events. Six sources and their contributions to
31 anthropogenic GEM were identified. Besides the common anthropogenic emission sectors (*i.e.*
32 **industrial and biomass burning, coal combustion, iron and steel production, cement production, and**
33 **incineration**), shipping emission was found to be an important source (19.6%) of **anthropogenic**
34 mercury in East China, where marine vessel shipping activities are intense. **In addition, a**
35 **considerable natural source of GEM was identified.** Concurrences of high GOM concentrations with
36 elevated O₃ and temperature, along with the lagged variation of GEM and GOM during daytime
37 demonstrated the very high GOM concentrations were **partially** ascribed to the intense in situ
38 oxidation of GEM. Statistical analysis showed that when PM_{2.5} reached a certain **threshold** value,
39 GOM was inhibited to some extent due to the gas-particle partitioning process. This process was
40 **controlled** under the conditions of high PM_{2.5} concentrations, high humidity, and low temperature.
41

42 **1. Introduction**

43 Mercury (Hg) is a global pollutant of great concerns for environment and human health. Based
44 on its physical and chemical properties, atmospheric mercury is operationally divided into three
45 forms, *i.e.* gaseous elemental mercury (GEM), particulate-bound mercury (PBM), and gaseous
46 oxidized mercury (GOM). GEM is the predominant form in the atmosphere (>90%), while PBM
47 consists of a small quantity of the total mercury as well as for GOM. Elemental mercury in the
48 atmosphere is relatively stable, which means that it has a long lifetime of 0.5-2 year and can
49 transport globally before they are oxidized and removed from the atmosphere via wet and dry
50 depositions (Marsik et al., 2007). In contrast, GOM and PBM would be rapidly wiped out from the
51 atmosphere after emission due to their significantly greater reactivity, deposition velocities, and
52 water solubility .

53 Both natural processes and anthropogenic activities release mercury into the atmosphere.
54 Natural sources of mercury include the ocean volatilization, volcanic eruption, evasion from soils
55 and vegetation, geothermal activities, and weathering minerals (Pirrone et al., 2010;Simoneit et al.,
56 2004). Re-emissions of mercury that previously deposited onto the environmental surfaces are also
57 considered as natural source. **As for the anthropogenic emission sources of mercury, coal**
58 **combustion, non-ferrous smelters, cement production, waste incineration, and mining** are
59 considered to be the main sources. After being emitted into the atmosphere, **mercury undergoes**

60 speciation which plays an important role in its biogeochemical cycle. Previous studies suggest that
61 the oxidation of GEM in the terrestrial environments was generally initiated by O₃ and OH radicals
62 (Mao et al., 2016). Atomic bromine (Br) and bromine monoxide (BrO) are two additional oxidation
63 agents in the marine atmosphere (Xiao et al., 2018; Wang et al., 2016). Observational studies of
64 GOM in the polar regions (Choi et al., 2013; Ye et al., 2016) and in the subtropical marine boundary
65 layer (Cheng et al., 2014; Zhu et al., 2014) as well as atmospheric modeling studies about mercury
66 cycling (Feng et al., 2004; Shon et al., 2005) have considered Br to be an important oxidant of GEM.
67 (Wang et al., 2014) even reported that Br is the primary oxidant of GEM in tropical marine boundary
68 layer (MBL). However, it still remain unknown and controversial about the speciation and
69 quantification of the GEM+O₃ products, and the reaction of GEM+OH is still under huge debate
70 between theoretical and experimental studies due to the lacking of mechanisms consistent with
71 thermochemistry (Xiao et al., 2018). As the GEM converts into GOM, a part of GOM will be
72 adsorbed onto particulate matter since it has high water solubility and relatively strong surface
73 adhesion properties (Liu et al., 2010). GEM accounts for the vast majority of total mercury in the
74 atmosphere, and its concentration is an order of magnitude higher than that of GOM and PBM.
75 Generally, the levels of GEM could be affected by various emission sources, redox reactions, and
76 foliar uptake, while the GOM species from the GEM oxidation and subsequent formation of PBM
77 by adsorption on the particle matters can significantly affect their ambient concentrations, especially
78 in regions with high GEM levels.

79 Many efforts have been made by governments to reduce mercury emissions. In October 2013,
80 128 countries signed a global treaty “Minamata Convention on Mercury” in order to reduce mercury
81 emissions from anthropogenic activities (Zhu et al., 2016). However, the mercury pollution issue is
82 still grim especially in Asia, which contribute approximately half of the global mercury emissions
83 (Pacyna et al., 2016). Mainland China plays an important role in the biogeochemical cycling of
84 mercury, since approximately 27% of the global total atmospheric mercury exhausts are from this
85 area (Hui et al., 2017). The Yangtze River Delta (YRD) is one of the most industrialized and
86 urbanized regions in China. Early field measurements in urban Shanghai found that the sources of
87 TGM were most likely derived from coal fired power plants, smelters and industrial activities
88 (Friedli et al., 2011). One study in urban Nanjing indicated that natural sources were important while
89 most sharp peaks of TGM were caused by anthropogenic sources (Zhu et al., 2012). Modeling of

90 atmospheric mercury in eastern China simulated by the CMAQ-Hg model showed that natural
91 emissions with a contribution of 36.6% were the most important source for GEM in eastern China
92 (Zhu et al., 2015). One study at Chongming (an island belonging to Shanghai) observed a downward
93 trend for GEM concentrations from 2014 to 2016 due to the reduction of domestic emissions (Wang
94 et al., 2016). Studies conducted in Changbai Mountain (Wan et al., 2009) and Xiamen (Xu et al.,
95 2015) used Principal Components Analysis (PCA) to identify potential sources of atmospheric
96 mercury, but the specific contributions of each source couldn't be quantified due to the limitation of
97 the PCA method. Overall, studies with respect to the specific sources and their quantified
98 contributions to atmospheric mercury in the suburbs of East China and the formation and
99 transformation processes among Hg species in the atmosphere are still lacking.

100 In this study, one-year measurements of GEM, GOM, and PBM were conducted at Dianshan
101 Lake Station (DSL), a suburban site in Shanghai. DSL is located in the junction of Shanghai,
102 Zhejiang, and Jiangsu provinces and is close to the East China Sea (ECS). Few local sources and
103 multiple surroundings make DSL a unique location for studying the main pollution sources and
104 transport pathways of Hg. In this paper, the relationship between Hg and meteorological conditions
105 was revealed; and the oxidation process of GEM to GOM and the adsorption process of GOM on
106 ambient particles were discussed. We also assessed the potential contributing sources of Hg, locating
107 the high potential sources regions and identifying the specific source and their contributions. This
108 study demonstrated the characteristics of atmospheric mercury over an intersection zone and
109 provided insights into the formation of GOM and PBM, and revealed the considerable contribution
110 from shipping activities over the coastal area.

111

112 **2. Materials and methods**

113 **2.1. Site description**

114 The field observation was conducted on the top of a four-story building (~14 m) at a super site
115 which is located in the west of Shanghai, and nearby the Dianshan Lake in Qingpu district (Fig. 1).
116 This supersite is carefully maintained by Shanghai Environmental Monitoring Center (SEMC). The
117 building is purely used for atmospheric monitoring without any other usage. DSL lies at suburbs of
118 Shanghai and there are no large point sources around within 20 kilometers, ensuring this site is
119 capable of capturing the meteorological conditions in the study area. Beside the measurement site

120 is Dianshan Lake, which is the largest freshwater lake in Shanghai with a total area of 62 square
121 kilometers, and next to the site is a highway with moderate traffic. The total GEM emission within
122 a 20 km cycle around the site was around 100kg/yr, indicating weak local human activities. The
123 distance between the sampling site and coastal lines is about 50 km, making it capable of capturing
124 the land-sea circulation. Its special geographical location (at the junction of Shanghai, Zhejiang and
125 Jiangsu provinces) makes it possible to receive the air masses from all these populous regions. In
126 addition, this site is located at the typical outflow path from East China to the Pacific Ocean. The
127 red dots in Fig. 1 represent the amount of atmospheric Hg emitted by anthropogenic activities of
128 each provinces in 2014 (Wu et al., 2016). The emission intensities of anthropogenic Hg in China
129 were higher in the north and lower in the south. The atmospheric Hg emissions by province in 2014
130 are listed in Table S1.

131

132 **2.2 Measurement of atmospheric mercury species**

133 Atmospheric mercury species (GEM, GOM, and PBM) were collected and measured from June
134 2015 to May 2016 using the Tekran 2537B/1130/1135 system (Tekran Inc., Canada). The Tekran
135 system has been widely used and the details have been described elsewhere (Landis and Keeler,
136 2002). In general, GEM, GOM, and PBM in the atmosphere were collected by dual gold cartridges,
137 KCl-coated annular denuder, and regenerable quartz fiber filter, respectively. In this study, GEM
138 was collected at an interval of 5 minutes with a flow rate of 1 L/min, while GOM and PBM were
139 collected at an interval of 2 hours with a flow rate of 10L/min. After the collection, all mercury
140 species were thermally decomposed to Hg^0 immediately and measured by cold vapor atomic
141 fluorescence spectroscopy (CVAFS). GEM concentrations were expressed in ng/m³, while GOM
142 and PBM were in pg/m³ at standard temperature of 273.14K and pressure of 1013 hPa.

143 A series of work need to be done to ensure the accuracy and validity of the measurement. The
144 KCl-coated denuder, Teflon coated glass inlet, and impactor plate were replaced weekly and quartz
145 filters were replaced monthly. Before sampling, denuders and quartz filters were prepared and
146 cleaned according to the methods in Tekran technical notes. The Tekran 2537B analyzer was
147 routinely calibrated using its internal permeation source every 47 hours, and was also cross-
148 calibrated every 3 months against an external temperature controlled Hg vapor standard. Two-point
149 calibrations (including zero calibration and span calibration) were performed separately for each

150 pure gold cartridge. Manual injections were performed to evaluate these automated calibrations
151 using the standard saturated mercury vapor.

152 Quality control on data were also performed during the data analysis. Some extremely high
153 concentrations (especially for GOM and PBM) were occasionally observed. If the values were
154 several times higher than the previous hour, those data were regarded as outliers and were excluded
155 in the data analysis.

156

157 **2.3 Measurement of other air pollutants and meteorological parameters**

158 Water-soluble inorganic anions (SO_4^{2-} , NO_3^- , Cl^-) and cations (K^+ , Mg^{2+} , Ca^{2+} , NH_4^+) in $\text{PM}_{2.5}$
159 were simultaneously monitored by the Monitor for Aerosols and Gases in ambient Air (MARGA)
160 at the resolution of one hour. Ambient air was drawn into a sampling box at a flow rate of 16.7L/min.
161 After removing the water-soluble gases by an absorbing liquid, a supersaturation of water vapor
162 induced the particles in the airflow to grow into droplets, and then the droplets were collected and
163 transported into the analytical box which contains two ion chromatograph systems for the
164 determination of the water-soluble ions in $\text{PM}_{2.5}$.

165 Heavy metals (Pb, Fe, K, Ba, Cr, Se, Cd, Ag, Ca, Mn, Cu, As, Hg, Ni, Zn, V) in $\text{PM}_{2.5}$ were
166 measured hourly using the Xact-625 Ambient Metals Monitor (Cooper Environmental services,
167 Beaverton, OR, USA), which is a sampling and analyzing X-ray fluorescence spectrometer designed
168 for online measurements of particulate elements. In this study, ambient air was sampled at a flow
169 rate of 16.7L/min and the particles were collected onto a Teflon filter tape. Then the filter tape was
170 moved into the spectrometer, where it was illuminated with an X-ray tube under three excitation
171 conditions and the excited X-ray fluorescence was measured by a silicon drift detector. Daily
172 advanced quality assurance checks were performed during 30 minutes after midnight to monitor
173 shifts in the calibration.

174 The hourly meteorological data **including** air temperature, relative humidity (RH), wind
175 speed, and wind direction were simultaneously monitored at the observation site by the automatic
176 weather station (AWS). **The data of the height of planetary boundary layer (PBL) were retrieved**
177 **from the U.S. National Oceanic and Atmospheric Administration**
178 (<https://ready.arl.noaa.gov/READYmet.php>). Atmospheric ozone (O_3) concentration was
179 continuously measured using Thermo Fisher 49i, which operates on the principle that ozone

180 molecules absorb UV light at a wavelength of 254 nm. The ambient carbon monoxide (CO) and
181 PM_{2.5} concentrations were measured by Thermo Fisher 48Itle and Thermo Fisher 1405F,
182 respectively. All data were averaged at the intervals of one hour.

183

184 **2.4 Potential source contribution function (PSCF)**

185 PSCF is a useful tool to diagnose the possible source areas with regard to the levels of air
186 pollutants when setting a contamination concentration threshold at the receptor site. Back trajectory
187 models are used to simulate the airflows. The principle of PSCF is to calculate the ratio of the total
188 number of back trajectory segment endpoints in a grid cell (i, j) which exceed the threshold
189 concentration (m_{ij}) to the total number of back trajectory segment endpoints in this grid cell (i, j)
190 during the whole sampling period (n_{ij}) as expressed by Equation (1) (Zhang et al., 2017; Cheng et
191 al., 2015).

192

$$PSCF_{ij} = \frac{m_{ij}}{n_{ij}} \quad (1)$$

193 When a particular cell is associated with a small number of endpoint, weighting function (w_{ij})
194 is applied to reduce this uncertainty and the value of w_{ij} is shown in Equation (2) (Fu et al., 2011),
195 in which N_{ave} is the mean n_{ij} of all grid cells with n_{ij} greater than zero. $PSCF_{ij}$ is multiplied by w_{ij} to
196 derive the weighted PSCF values.

197

$$w_{ij} = \begin{cases} 1.0, & N_{ij} > 3N_{ave} \\ 0.7, & 3N_{ave} > N_{ij} > 1.5N_{ave} \\ 0.4, & 1.5N_{ave} > N_{ij} > N_{ave} \\ 0.2, & N_{ave} > N_{ij} \end{cases} \quad (2)$$

199 In this study, we set the threshold concentration as the mean value of the whole sampling period.
200 The mean GEM, PBM, and GOM concentrations were 2.77 ng/m³, 60.8 pg/m³, and 82.1 pg/m³,
201 respectively. The HYSPLIT (HYbrid Single-Particle Lagrangian Integrated Trajectory) model is
202 applied for calculating air mass backward trajectories (Draxler and Rolph, 2012). The model was
203 run online at the NOAA ARL READY Website using the meteorological data archives of Air
204 Resource Laboratory (ARL). The meteorological input data used in the model was obtained from
205 NCEP (National Centers for Environmental Prediction)'s global data assimilation system (GDAS)
206 with a horizontal resolution of 0.5° × 0.5°. In this study, 72-hours back trajectories were calculated
207 at 500m AGL (above ground level) and the cell size was set as 0.5°×0.5°.

208

209 **2.5 Positive matrix factorization (PMF)**

210 The PMF model is widely used to quantitatively determine the source contributions of specific
211 air pollutants (Gibson et al., 2015). The essential principle of PMF is that the concentration of each
212 sample is determined by source profiles and different contributions. The equation of the PMF model
213 is shown as Equation (3):

214
$$X_{ij} = \sum_{k=1}^P g_{ik} f_{kj} + e_{ij} \quad (3)$$

215 Where X_{ij} is the concentration of the j th contamination at the receptor site in the i th sample. g_{ik}
216 represent the contribution of the k th factor on the i th sample, f_{kj} is used to express the mass fraction
217 of the j th contamination in the k th factor, P is the number of factors, which represent pollution
218 sources, e_{ij} is the residual for each measurement or model error.

219 Before the model determines the optimal non-negative factor contributions and factor profiles,
220 an objective function, which is the sum of the square difference between the measured and modeled
221 concentrations weighted by the concentration uncertainties, has to be minimized (Cheng et al., 2015).

222 The equation that determines the objective function is given by Equation (4):

223
$$Q = \sum_{i=1}^n \sum_{j=1}^m \left(\frac{X_{ij} - \sum_{k=1}^P A_{ik} F_{kj}}{S_{ij}} \right)^2 \quad (4)$$

224 where X_{ij} is the ambient concentration of the j th pollutant in the i th sample (m and n represent the
225 total number pollutants and samples, respectively). A_{ik} is the contribution of the k th factor on the i th
226 sample and F_{kj} is the mass fraction of the j th pollutant in the k th factor. S_{ij} is the uncertainty of the
227 j th pollutant on the i th measurement, P is the number of factors, which imply the pollutant sources.

228 In this study, the number of factors from 3 to 8 was examined with the optimal solutions determined
229 by the slope of the Q value versus the number of factors. For each run, the stability and reliability
230 of the outputs were assessed by referring to the Q value, residual analysis, and correlation
231 coefficients between observed and predicted concentrations. Finally, a 6-factor solution, which
232 showed the most stable results and gave the most reasonable interpretation, was chosen. Before
233 running the model, a dataset including unique uncertainty values of each data point was created and
234 digested into the model. The error fraction was assumed to be 15% of concentrations for GEM and
235 10% of concentrations for the other compounds (Xu et al., 2017), the missing data were excluded
236 and the total number of samples was 3526.

237

238 **3. Results and discussion**

239 **3.1. Characteristics of atmospheric mercury species**

240 Fig. 2 displays the time series of atmospheric GEM, PBM, and GOM concentrations during 1
241 June, 2015 to 31 May, 2016 at DSL. The annual average concentrations of GEM, PBM, and GOM
242 at DSL were $2.77 \pm 1.36 \text{ ng/m}^3$, $60.8 \pm 67.4 \text{ pg/m}^3$, and $82.1 \pm 115.4 \text{ pg/m}^3$, respectively. As shown in
243 Table 1, the levels of GEM and PBM in this study were lower than some sites in China by a factor
244 of 2-7, such as rural Miyun, suburban Xiamen, and urban Guiyang (Xu et al., 2015;Fu et al., 2011).
245 However, compared to the studies conducted in urban and rural areas abroad such as New York
246 (Choi et al., 2013), Chicago (Gratz et al., 2013), and Nova Scotia (Cheng et al., 2014), the
247 concentrations of GEM and PBM in the suburbs of Shanghai were much higher by a factor of 1-3
248 and 3-8, respectively. Different from GEM and PBM, the GOM concentrations at DSL were higher
249 than all the Chinese sites and other sites around the world listed in Table 1. The mean GOM
250 concentration in this study (82.1 pg/m^3) was even higher than that in Guiyang (35.7 pg/m^3), where
251 the emissions of GEM and GOM were quite intense due to the massive primary emission sources
252 such as coal-fired power plants and cement plants (Fu et al., 2011). The abnormally high GOM
253 concentrations observed in this study were likely dominated by strong primary emissions.

254 The monthly patterns of GEM, PBM, and GOM during the whole sampling period are shown
255 in Fig. 3. The seasonal mean GEM concentrations were slightly higher in winter (2.88 ng/m^3) and
256 summer (2.87 ng/m^3) than in spring (2.73 ng/m^3) and autumn (2.63 ng/m^3), with the highest monthly
257 mean value of 3.19 ng/m^3 in June and the lowest of 2.39 ng/m^3 in March. Statistical test showed that
258 no significant differences of the seasonal variations of GEM concentrations among spring, summer,
259 and winter were observed (Table S2). This was different from many urban and remote sites in China,
260 such as Guiyang, Xiamen, and Mt. Changbai, where GEM showed significantly high concentrations
261 in cold seasons than those in warm seasons (Feng et al., 2004;Xu et al., 2015;Fu et al., 2012). The
262 relatively high GEM concentrations during the cold season in China should be attributed to the
263 increases of energy consumption (Fu et al., 2015). In this study, GEM concentration in summer was
264 comparable to that in winter, which was likely attributed to the strong natural mercury emissions
265 (e.g. soils, vegetations, and water) due to elevated temperature in summer (Liu et al., 2016). The
266 seasonal mean PBM concentrations were the highest in winter (93.5 pg/m^3) while the lowest in
267 summer (35.7 pg/m^3), and moderate in autumn (56.8 pg/m^3) and spring (51.6 pg/m^3), with the

268 highest monthly mean value of 109.4 pg/m³ in January and the lowest of 28.9 pg/m³ in September.
269 This seasonal pattern was consistent with other sites in China such as Beijing and Nanjing (Zhu et
270 al., 2014; Zhang et al., 2013). PBM concentrations at low altitude sites in the Northern Hemisphere
271 were commonly enhanced in winter, which was ascribed to intense emissions from residential
272 heating, the reduction of wet scavenging processes, enhanced gas-particle partitioning of
273 atmospheric mercury under low temperature, etc. (Rutter and Schauer, 2007). As for GOM, its
274 seasonal mean concentrations were the highest in winter (124.0 pg/m³), followed by summer (77.3
275 pg/m³), spring (68.1 pg/m³), and autumn (61.0 pg/m³). **GOM concentrations in summer were much**
276 **lower than that in winter, which were largely due to the more favorable meteorological conditions.**
277 However, GOM concentrations in summer were higher than spring and autumn, which should be
278 partly ascribed to the secondary transformation from GEM. More detailed analysis of the impact of
279 meteorological conditions on Hg species and the related formation mechanisms are presented in the
280 following sections.

281 Fig. 4 shows the diurnal variation of GEM, PBM, and GOM during the whole sampling period.
282 To ensure the time resolutions were consistent among all three mercury species, the temporal
283 resolution of measured GEM was converted from 5 minutes to a two-hour average. As shown in Fig.
284 4, GEM concentrations were higher during daytime with the maximum in the morning at around
285 10:00 and minimum in the midnight at around 02:00. The diurnal trends of GOM were as similar as
286 that of GEM, except that the minimum GOM occurred at around 20:00 in the evening. The diurnal
287 trends of PBM were different from those of GEM and GOM, exhibiting relatively higher
288 concentrations during nighttime. The PBM maximum occurred in the early morning at around 6:00
289 and the minimum was observed in the afternoon at 18:00. The diurnal trends of GEM, PBM, and
290 GOM were as similar as those in Nanjing (Zhu et al., 2012), but different from those in Guiyang,
291 Xiamen, and Guangzhou (Feng et al., 2004; Chen et al., 2013). **Since DSL and Nanjing both belongs**
292 **to the Yangtze River Delta region, the similar meteorology and emission characteristics within the**
293 **Yangtze River Delta region may explain the similar diurnal patterns of Hg species between DSL**
294 **and Nanjing.** The elevated GEM concentrations at DSL during daytime were likely related to the
295 stronger emissions from both human activities and natural releases. **GOM and GEM showed similar**
296 **diurnal variations and both peaked at 10:00, probably suggesting that GOM and GEM were affected**
297 **by common sources (e.g. coal-fired power plants and industrial boilers).** The high PBM

298 concentrations at night were likely derived from the adsorption of Hg species onto the preexisting
299 particles and the subsequent accumulation in the shallow nocturnal boundary layer. Fig. 4 shows
300 that wind speed was relatively low while high for relative humidity at night, which were conducive
301 to the adsorption of GOM onto the particles.

302

303 **3.2. Relationship between Hg species and meteorological factors**

304 Fig. 5 shows the relationship between wind direction/speed and atmospheric mercury species.
305 As shown in Fig. 5a, the prevailing wind at DSL during the study period came from the east,
306 accounting for approximately one-third of all the wind directions. Winds also prevailed from the
307 north with a fraction of 16%. Wind speed from all directions during the study period was mainly in
308 the range of 0-6 m/s, of which wind speed higher than 4 m/s mainly derived from the east. GEM as
309 a function of wind directions showed that the highest GEM concentrations were linked to the winds
310 from the south and southwest with the mean value of 3.92 ng/m³, while the mean GEM
311 concentration from the other wind sectors was 2.71 ng/m³ (Fig. 5b). GOM showed similar wind-
312 concentration patterns as GEM. While PBM showed high concentrations from the north/northwest
313 and south/southwest (Fig. 5c &5d). By referring to Fig. 1, the anthropogenic mercury emissions in
314 northern China were generally higher than southern China. Hence, the observation of high
315 atmospheric Hg concentrations from the north was expected. In this regard, the even higher
316 atmospheric Hg concentrations from the south and southeast than from the north cannot be simply
317 explained by anthropogenic emission sources, implying that there must be additional Hg emission
318 sources. (Feng et al., 2004) reported that the Hg concentrations in the surface soils of southern China
319 were generally higher than the northern China. A modeling study simulated that the mean annual
320 Hg air-soil flux in the southwest region of our sampling site (e.g. Zhejiang province) ranged from
321 8.75 to 15 ng m⁻² h⁻¹, while that in the north/northwest region (e.g. Jiangsu province) ranged from
322 2.5 to 8.75 ng m⁻² h⁻¹ (Wang et al., 2016). Hence, emissions from natural sources, such as soils,
323 vegetations and water, should play an important role in the observed high atmospheric Hg
324 concentrations from the south and southeast.

325 In order to confirm this conjecture, the relationship between temperature and Hg concentrations
326 at DSL was investigated. Seasonal temperature in ascending order was divided into different groups
327 and the corresponding mean Hg concentrations were plotted in Fig. 6. In spring, the GEM

concentrations increased as the temperature increased. As for the other season, when the temperature increased to a certain value, the trends of GEM variations were as similar as spring. This relationship between GEM and temperature can be likely interpreted as the impact of surface emissions. It must be noted that the height of PBL increased as the temperature increased, while at the same time, GEM still showed a significant upward trend. This suggested that the atmospheric dilution effect caused by the developing boundary layer was far from offsetting the increase of surface emissions caused by increased temperature. The GOM concentration showed a clearly positive correlation with temperature in summer. Higher temperature in summer in the Yangtze River Delta region is mostly associated with ozone pollution days (Lu et al., 2018), thus implying higher GOM could be partially related to the in situ oxidation of GEM in addition to its sources from direct emissions. In the other seasons, no clear correlations between GOM and temperature were observed. As for PBM, it appeared to have weakly negative correlations with the height of PBL, suggesting the atmospheric diffusion conditions were influential on the concentrations of PBM.

341

342 **3.3. Tracing sources of Hg species**

343 **3.3.1. Potential source regions of Hg species**

344 PSCF was applied to identify the potential source regions of the three Hg species. As for GEM,
345 the major source areas were located in Anhui, Jiangxi, and Zhejiang provinces, and there were also
346 signals from Shandong province (Fig. 7a). As for the seasonal pattern (Fig. S1), the potential source
347 regions of GEM in spring were mainly from Jiangsu and Zhejiang provinces. In summer, the PSCF
348 hotspots were identified in Anhui and Jiangxi provinces. Jiangsu province was likely to become the
349 main potential source region of GEM in autumn. In winter, Anhui and Zhejiang provinces showed
350 relatively high PSCF values. In addition, there were also signals from Henan and Shandong
351 provinces, suggesting the importance of long-range transport in wintertime. There existed
352 substantial high PSCF signals in the southern areas, even stronger than those in the north. However,
353 as shown in Fig. 1, southern provinces such as Zhejiang and Jiangxi were estimated to release 25
354 tons/yr atmospheric Hg from anthropogenic activities, being far less than the northern provinces
355 such as Jiangsu and Shandong (77 tons/yr) (Wu et al., 2016). If only the anthropogenic emissions
356 of GEM were considered, the occurrence of stronger PSCF signals in southern provinces seemed
357 unreasonable. Based on the mean annual Hg air-soil flux of 8.75 to 15 ng m⁻² h⁻¹ in the southwest

358 region of our sampling site (Wang et al., 2016), it was estimated that the total Hg emissions from
359 soils were in the range of 6.9 - 13.9 tons/yr for Zhejiang province. As for the anthropogenic Hg
360 emission of Zhejiang province in 2014, it was approximately 15tons/yr (Wu et al., 2016). Thus, the
361 magnitude of mercury from natural surfaces was comparable to that from anthropogenic sources. In
362 this regard, the re-emission of GEM from natural surfaces in southern areas should be an important
363 source, corroborating the discussion in Section 3.2. In addition, the East China Sea (including the
364 offshore areas and open ocean) showed sporadic high PSCF signals of GEM in all four seasons (Fig.
365 S1), indicating possible influences from shipping activities. The detailed estimation of variable
366 sources would be discussed in Section 3.3.3.

367 The PSCF pattern of PBM was quite different from that of GEM (Fig. 7b). The potential source
368 regions of all year round PBM were mainly from the north of Jiangsu and Anhui provinces, and
369 from northeastern China, including Shandong and Hebei provinces. These provinces were regarded
370 as the main Hg sources areas in China and accounted for approximately 25.2% of the Chinese
371 anthropogenic atmospheric Hg emissions (Wu et al., 2016). As for the seasonal PSCF patterns of
372 PBM (Fig. S2), its potential source regions in spring, autumn, and winter shared certain
373 commonalities that exhibited the consistent PSCF patterns as the annual pattern. The exception was
374 found for summer, which showed high PSCF values mainly in the southern areas of Shanghai. This
375 might be attributed to that the prevailing winds in summer were from the south, southeast, and
376 southwest where Zhejiang and Jiangxi provinces were important mercury source regions.

377 The potential source regions of all year round GOM were mainly located in Anhui and Zhejiang
378 provinces and the coastal areas along Jiangsu province (Fig. 7c). The PSCF pattern of GOM was as
379 similar as that of GEM but different from that of PBM. The potential source regions of GOM were
380 more from southern China rather than from northern China, which might be due to the higher
381 atmospheric oxidant levels in the southern regions. Especially in summer, the potential sources
382 regions of GOM concentrated in Zhejiang and Jiangxi provinces (Fig. S3). In the other seasons,
383 there were somewhat different PSCF patterns observed. In detail, while significant PSCF signals
384 from the inland areas were found, moderate PSCF signals over the East China Sea and Yellow Sea
385 also observed in spring. In autumn, the high PSCF values mainly occurred in Zhejiang province and
386 there were also moderate signals over the Yellow Sea. In winter, the high PSCF values spread from
387 the coastal areas of Jiangsu to a vast ocean of the Yellow Sea. One previous study suggested that the

388 marine boundary layer could provide considerable amounts of oxidants such as chlorine and
389 bromine, which were beneficial for the production of GOM by oxidizing GEM (Auzmendi-Murua
390 et al., 2014) and this may explain the substantial PSCF signals over the ocean.

391 The results of the PSCF analysis suggested the significant influences of adjacent areas of
392 Shanghai on contributing to all the atmospheric mercury species. It was also illustrated that the long-
393 range and regional transport via both land transport and sea breeze were important.

394

395 **3.3.2. Comparison between the impact of quasi-local sources and regional/long-range
396 transport on atmospheric mercury**

397 According to the relationship between wind direction and Hg species as well as the PSCF
398 analysis discussed above, the elevated GEM, GOM, and PBM concentrations at the observation site
399 were generally related to the wind sectors from the southwest and north. In order to reveal the
400 relative importance of local sources and regional transport, the ratio of GOM/PBM was applied as
401 an indicator based on the fact that the residence time of GOM is generally considered to be shorter
402 than that of PBM. If regional/long-range transport was evident, the ratio of GOM/PBM should be
403 lower due to that GOM was more quickly scavenged than PBM during the transport, and vice versa
404 when local sources dominated. In this regard, the ratios of GOM/PBM during the whole study period
405 were grouped into four categories, i.e. 0-1, 1-2, 2-3, and higher than 3. The corresponding frequency
406 of wind direction in each category was compared in Fig. 8. It was clear that the higher GOM/PBM
407 ratios were associated with more frequent winds from the east and southeast. The frequency of these
408 two wind sectors increased significantly from 27% under the GOM/PBM ratios less than 1 to 52%
409 under the GOM/PBM ratios higher than 3. Winds from the east and southeast were typically
410 characterized of relatively clean air masses, suggesting the local sources around the observational
411 site should dominate. In contrast, the lower GOM/PBM ratios were associated with more frequent
412 winds clockwise from the west to the north and the frequency of these wind sectors decreased
413 significantly from 44% under the GOM/PBM ratios less than 1 to 21% under the GOM/PBM ratios
414 higher than 3. These winds were indicative of the long-range/regional transport from northern China
415 and were associated with the relatively low GOM/PBM ratios. According to the PSCF results above,
416 the potential source areas of Hg species (GEM, GOM and PBM) derived mostly from the south and
417 southwest of the sampling site. As shown in Fig. 8, the frequency of south, southwest, **west, and**

418 northeast winds showed no clear trend as the GOM/PBM ratios increased. This suggested the
419 emissions of Hg in these directions of the sampling site were complicated, and the phenomenon
420 above can not be simply explained by the impact of local sources or regional transport. In general,
421 the GOM/PBM ratio can be used as a qualitative tracer for identifying the relative importance of
422 long-range transport vs. local sources. However, when the influences from long-range transport and
423 local emission were close, the result could be ambiguous based on this method and this may require
424 further efforts such as chemical transport modeling.

425 The relationships among GEM, CO, secondary inorganic aerosols (SNA) and GOM/PBM
426 ratios were further investigated. Fig. 9 displays the concentrations of GEM as a function of
427 GOM/PBM ratios colored by CO. The sizes of the circles represented the corresponding
428 concentrations of SNA in PM_{2.5}. CO was commonly used as a tracer of fuel combustion and SNA
429 were derived from secondary particle formation via the gas-to-particle conversion. CO and SNA
430 were collectively used as proxies of the extent of anthropogenic air pollutants and especially for
431 evaluating the extent of regional/long-range transport. As shown in Fig. 9, GEM showed an overall
432 increasing trend as the GOM/PBM ratios increased. In addition, it could be clearly seen that the
433 lower GOM/PBM ratios were associated with higher CO and SNA concentrations and vice versa.
434 This corroborated the discussion above that the GOM/PBM ratio was a reliable tracer for assessing
435 the relative importance of regional/long-range transport vs. local atmospheric processing.

436 In the GOM/PBM ratio bins of less than 2.5, GEM fluctuated with the mean values less than
437 2.6 ng/m³. The mean GEM concentration increased from 2.61 ng/m³ in the GOM/PBM ratio bin of
438 2.5-3.0 to 2.8 ng/m³ in the bin of 3.0-3.5, and then remain relatively stable when the GOM/PBM
439 ratio bins higher than 3.0. Generally, GEM showed an increasing trend as the GOM/PBM ratios
440 increased while both SNA and CO decreased. The elevation of GEM concentrations tended to be
441 associated with the impact of quasi-local sources. In contrast, under the high SNA and CO
442 conditions when GOM/PBM ratios were lower, GEM showed relatively low concentrations. This
443 suggested the regional/long-range transport didn't favor the elevation of GEM concentrations. It has
444 been recognized that the common regional/long-range transport pathways on contributing to the
445 particulate pollution events of Shanghai were from the north and northwest originating mostly from
446 the North China Plain. The relatively lower GEM concentrations under the regional/long-range
447 transport conditions corroborated the PSCF analysis that only moderate probabilities of GEM source

448 regions from northern China were found (Fig. 7a).

449

450 3.3.3. Source apportionment by combined PMF and PCA

451 PMF modeling has been widely used to apportion the sources of atmospheric pollutants. In this
452 study, GEM together with heavy metals and soluble ions, measured online synchronously, were
453 introduced into the EPA PMF5.0 model to apportion the major anthropogenic sources of GEM. A
454 six-factor solution was selected based on the results of multiple model runs, which can well explain
455 the measured concentrations of the introduced species. The profiles of six identified PMF factors
456 and contributions of major anthropogenic sources to GEM are shown in Fig. 10. It has to be noted
457 that since no tracers for the natural emissions (e.g. soils, vegetations, and ocean) were available in
458 this study, the identification of natural mercury sources was not possible **based on the PMF modeling**.

459 Factor 1 had high loadings for Se, As, Pb, NO_3^- , SO_4^{2-} , and NH_4^+ . Se, As, and Pb were typical
460 tracers of coal combustion. SO_4^{2-} and NO_3^- were also formed from the gaseous pollutants emitted
461 from coal burning. Hence, this factor was defined as coal combustion sources and accounted for
462 12.3% of the **anthropogenic GEM**. **Fig. S4 plotted wind roses of specific aerosol species. Of which,**
463 **SO_4^{2-} and As shared similar patterns with high concentrations mainly from the southwest.** Since
464 **combustion was an important source of GEM, this confirmed that the major sources of GEM were**
465 **located in the southwest region.**

466 Factor 2 displayed particularly high loadings for Ni and V. The major sources of Ni in the
467 atmosphere can be derived from coal and oil combustions (Tian et al., 2012), and oil combustion
468 accounted for 85% of anthropogenic V emissions in the atmosphere (Duan and Tan, 2013). In
469 general, Ni and V have been considered as good tracers of heavy oil combustion, which has been
470 commonly used in marine vessels (Viana et al., 2009). Thus, this factor was identified as shipping
471 emissions. The sampling site is adjacent to the East China Sea and is located in Shanghai which has
472 the largest port in the world. **Fig. S4 showed similar patterns of Ni and V with high concentrations**
473 **mainly from the northeast, east, and southeast.** To further validate this factor, the time-series of GEM
474 concentrations from the shipping factor based on the PMF modeling were extracted and digested
475 into the PSCF modeling (Fig. S5), showed that the potential sources regions were mainly located
476 over the East China Sea and coastal regions. This indicated factor 2 from PMF should be
477 representative of the shipping sector as well as oil combustion in motor vehicles and inland shipping

478 activities. Overall, this factor accounted for 19.6% of anthropogenic GEM and ranked as the second
479 largest emission sector, highlighting the urgent need of controlling the marine vessel emissions.

480 Factor 3 showed high loadings for Ca and moderate loadings for Ba and Fe. Ca and Fe are rich
481 elements in crust that can be used for cement production. As mercury could be released during
482 industrial processes of cement production, Factor 3 was assigned as cement production and
483 accounted for a minor fraction of 6.3 % of the anthropogenic GEM.

484 Factor 4 was characterized by high loadings of Cr and moderate loadings of Mn, Fe, Ni, and
485 Cu. These species together served as markers of metals smelting. Metals smelting were known to
486 be large sources of Hg emitted to the atmosphere (Pirrone et al., 2010), especially in the YRD, one
487 of the most developed and industrialized areas in China. This factor accounted for 7.6% of the
488 anthropogenic GEM.

489 Factor 5 had high loadings of Cl⁻. Waste incineration is an important source of enriched
490 chloride over land. Factor 5 was identified to be waste incineration, which contributed 6.4% of the
491 anthropogenic GEM.

492 Factor 6 was characterized by high loadings of Cd, Ag, K⁺, and Na⁺. The major sources of Cd
493 in China were iron and steel smelting industries (Duan and Tan, 2013). Ag was mainly used in
494 industrial applications, including electronic appliances and photographic materials. K⁺ was a typical
495 tracer of biomass burning, which often stemmed from agriculture waste burning over the Yangtze
496 River Delta and the North China Plain. In this regard, Factor 6 was considered as a combined source
497 of the industrial and biomass burning emission sectors. It was estimated to contribute 47.8% of the
498 anthropogenic GEM.

499 As discussed in the above sections, surface emissions were likely to be important sources of
500 the observed atmospheric mercury. As PMF modeling didn't resolve the natural sources of mercury,
501 the PCA (Principal Component Analysis) was applied for further source apportionment by
502 introducing the temperature parameter. Four factors are resolved, which totally explained 75.32%
503 of the variance as shown in Table 2. Factor 1 accounted for 34.15% of the total variance with high
504 loadings for SO₂, SO₄²⁻, NH₄⁺, K⁺, Pb, Se, and As, which was explained as coal combustion mixed
505 with biomass burning. Factor 2 accounted for 14.85% of the total variance with high loadings for
506 temperature, O₃, and NH₃, which was explained as surface emissions. Factor 3 explained 13.43%
507 of the total variance and showed high loadings for Ni and V, which indicated the contribution of

508 ship emissions. Factor 4 explained 12.89% of the total variance and showed high loading for Fe and
509 Ca, indicating the contribution of cement production.

510

511

512 **3.4. Factors affecting the formation and transformation of mercury species**

513 **3.4.1. Factors affecting the formation of GOM**

514 A typical case from July 24 to July 27, 2015 was chosen to investigate the possible formation
515 process of GOM. As shown in Fig. 11, the shaded episodes represented nighttime from 18:00 to
516 6:00 the next day. Both GEM and GOM exhibited rising trends during nighttime (Fig. 11a), which
517 was ascribed to nighttime accumulation effect due to the very shallow boundary layer (Fig. 11c).
518 Starting from 6:00 in the morning, GEM concentrations began to gradually decline as the boundary
519 layer developed. In contrast, the concentrations of GOM continued to rise from 6:00 until it reached
520 the peak value at around 10:00. During this period, the levels of ozone and temperature also kept
521 rising until surpassed 200 $\mu\text{g}/\text{m}^3$ and 34°C, respectively. Accordingly, as an anthropogenic emitting
522 tracer, the concentration of carbon monoxide was basically stable and even showing a downward
523 trend, which suggested some other factors accounted for the increase of GOM in addition to the
524 anthropogenic emissions. This phenomenon clearly revealed the acceleration of the conversion
525 process of GEM to GOM under favorable atmospheric conditions of higher O₃ concentration and
526 ambient temperature. In the case of atmosphere dilution by the rise of PBL, the fact that GOM was
527 not falling but rising suggested the great influence of this process on ambient GOM concentrations.
528 Similar observation has been found at the high-altitude Pic du Midi observatory in southern France
529 (Fu et al., 2016), which was almost impervious to anthropogenic emission sources. The important
530 role of GEM oxidation in our sampling site, which located in one of the most developed industrial
531 areas in China, was most likely due to the presence of sufficient oxidants in this area. Severe ozone
532 pollution frequently occurred in the YRD due to strong anthropogenic emission intensities (Lu et
533 al., 2018). Previous studies suggested that the primary oxidants in the terrestrial environment were
534 O₃ and OH radicals (Shon et al., 2005), while Br was an important oxidant in the subtropical marine
535 boundary layer (Obrist et al., 2011). It was possible that, in addition to O₃ and OH radicals, Br might
536 also be an important inducing species to the oxidation of GEM as the DSL site is adjacent to the
537 East China Sea.

538 Fig. 12 statistically analyzed the relationship among GOM, O₃, and temperature. Temperature
539 was plotted against a range of GOM/PBM bins colored by O₃ and the size of the circles represented
540 the concentrations of GOM. In general, as temperature and O₃ increased, the concentrations of GOM
541 were subject to substantial enhancement. For instance, when temperature (O₃) was below 12°C (65.7
542 µg/m³), GOM averaged 37.8 pg/m³. While temperature (O₃) increased to above 20°C (91.5 µg/m³),
543 GOM rose to 168.8 pg/m³, yielding a factor of 1- 5 GOM increases. This further confirmed the case
544 study above that the levels of oxidants under favorable environmental conditions were crucial for
545 the formation of GOM. Fig. 12 also suggested that the lower ratios of GOM/PBM were associated
546 with lower temperature and O₃ concentrations, indicating relatively weak photochemistry during
547 the cold seasons. On the contrary, the higher ratios of GOM/PBM were associated with higher
548 temperature and O₃ concentrations, indicating relatively strong photochemistry during the warm
549 seasons. This suggested that the formation of GOM was more favored by local atmospheric
550 processing rather than the transport. This study demonstrated the abnormally high GOM
551 concentrations observed at DSL were largely ascribed to local oxidation reactions. However, the
552 explicit formation mechanism of GOM need to be investigated by measuring more detailed
553 components of GOM and atmospheric oxidants.

554

555 3.4.2. Factors affecting the transformation of PBM

556 Previous studies have shown that PBM can be emitted directly from various anthropogenic
557 sources such as coal-fired power plants and industries (Liu et al., 2018; Wu et al., 2016). In
558 addition, gas-particle partitioning was considered to be an important pathway for the formation of
559 PBM (Shon et al., 2005; Amos et al., 2012). Since most of the areas in the YRD belong to non-
560 attainment areas in regard of particulate pollution and the concentrations of GOM were particularly
561 high at DSL as discussed above, the role of gas-particle partitioning in the formation of PBM should
562 be investigated. Previous studies reported that the concentrations of PM_{2.5} in eastern and northern
563 China are highest in the world (Auzmendi-Murua et al., 2014), elevated atmospheric particulate
564 matter probably facilitates the formation of PBM in the atmosphere in China (Fu et al., 2015). Fig.
565 13 shows the statistical pattern of the variation of PBM and GOM in the ascending bins of PM_{2.5}.
566 The concentrations of PBM increased with the concentrations of PM_{2.5}, which was due to both
567 primary emissions and the subsequent process of Hg species adsorbed on particulate matters. The

568 trend of GOM was somehow different from that of PBM. When PM_{2.5} concentrations were at
569 relatively low levels under 75 $\mu\text{g}/\text{m}^3$, GOM concentrations increased with PM_{2.5}. However, when
570 PM_{2.5} concentrations increased to 75–105 $\mu\text{g}/\text{m}^3$, GOM exhibited a clear decreasing trend as PM_{2.5}
571 increased. It seemed that when the concentration of PM_{2.5} reached a certain value, the formation of
572 GOM was inhibited to some extent, which was likely due to the adsorption of GOM onto the
573 particles. When PM_{2.5} concentrations exceeded 105 $\mu\text{g}/\text{m}^3$, GOM exhibited a slightly increasing
574 trend as PM_{2.5} increased. High PM_{2.5} concentrations in China always related to severe anthropogenic
575 emissions (Auzmendi-Murua et al., 2014), so the moderate increasing trend of GOM in these bins
576 should be attributed to the impact of strong primary emissions.

577 A short episode from December 30, 2015 to January 1, 2016 was chosen to further investigate
578 this phenomenon. As shown in Fig. 14, in Stage 1, the concentrations of PM_{2.5} were below 100
579 $\mu\text{g}/\text{m}^3$, PBM and GOM shared the similar temporal variation as PM_{2.5}. In Stage 2, as PM_{2.5} kept
580 climbing, GOM began to show somewhat negative correlation with PM_{2.5}, but not significant. The
581 reason might be that the relatively high temperature and low humidity during this period were not
582 conducive to the transfer of GOM to particle matters. In Stage 3, GOM decreased as PM_{2.5} continued
583 to increase, showing a clear anti-correlation. During this period, PBM showed a consistent trend
584 with PM_{2.5} and CO. Temperature was relatively low but with relatively high humidity. This
585 phenomenon clearly demonstrated the process of gas-particle partitioning of PBM formation. In
586 stage 4, GOM and PBM showed similar decreasing trend with PM_{2.5} and CO. The low GOM
587 concentrations, low humidity, and high temperature resulted in no significant signs of GOM
588 adsorption to PM_{2.5} in this stage. In general, under high PM_{2.5} and GOM concentrations, high
589 humidity and low temperature conditions in our sampling site, clear processes of gas-particle
590 partitioning were observed .

591

592 4. Conclusions

593 In this study, a year-long observation of three atmospheric Hg species was conducted at the
594 Dianshan Lake (DSL) Observatory, located on the typical transport routes from mainland China to
595 the East China Sea. During the whole measurement period, the mean GEM, PBM, and GOM
596 concentrations were 2.77 ng/m³, 60.8 pg/m³, and 82.1 pg/m³, respectively.

597 Different from many sites in China, GEM at DSL exhibited high concentrations in winter,

598 summer, and spring, which was due to the strong re-emission fluxes from natural surfaces in summer
599 and enhanced coal combustion for residential heating over northern China in winter. The relatively
600 high GOM concentrations in summer indicated that the formation of GOM from GEM oxidation
601 was likely crucial. PBM exhibited high concentrations in winter, indicating the impact from long-
602 range transport. The diurnal patterns of GEM and GOM were similar with relatively high levels
603 during daytime. For GEM, this was likely attributed to both human activities and re-emission from
604 natural surfaces during daytime. For GOM, in addition to direct emissions, high concentrations
605 during daytime were partially ascribed to photochemical oxidation of GEM. The PBM
606 concentrations were higher during nighttime, which was ascribed to the accumulation effect within
607 the shallow nocturnal boundary layer.

608 The relationship between meteorological factors and atmospheric Hg species showed that the
609 high Hg concentrations were generally related to the winds from the south, southwest, and north
610 and positively correlated with temperature. Both anthropogenic sources and natural sources
611 contributed to the atmospheric mercury pollution at DSL. Higher GOM/PBM ratios corresponded
612 to lower CO and SNA concentrations and vice versa. The ratio of GOM/PBM can be used as a tracer
613 for distinguishing local sources and regional/long-range transport based on the fact that the
614 residence time of GOM was shorter than that of PBM. GEM as a function of the GOM/PBM ratios
615 indicated that when the quasi-local sources dominated, GEM concentrations were relatively higher
616 than those events under the regional/long-range transport conditions. According to the PMF source
617 apportionment results, six sources of anthropogenic GEM and their contributions were identified,
618 i.e. industrial and biomass burning (47.8%), shipping emission (19.6%), coal combustion (12.3%),
619 iron and steel production (7.6%), incineration (6.4%), and cement production (6.3%). The
620 significant contribution of shipping emission suggested that in coastal areas mercury emitted from
621 marine vessels can be significant. In addition, a considerable natural source of GEM was identified
622 by digesting temperature into the principle component analysis.

623 The formation processes of GOM and PBM based on episodic studies were also investigated.
624 The high GOM concentrations were partially attributed to strong local photochemical reactions
625 under the conditions of high O₃ and temperature. Under high PM_{2.5} concentrations, high humidity
626 and low temperature conditions, the gas-particle partitioning processess were observed at DSL,
627 which might be an important pathway for the formation of PBM.

628

629 **Author contributions.** KH, CD, and XQ conceived the study and wrote the paper. XW, YL, and
630 DW performed the measurements and collected data. All have contributed to the data analysis and
631 review of the manuscript.

632

633 **Acknowledgements**

634 This work was supported by the Natural Science Foundation of China (NSFC, Grant Nos.
635 91644105, 21777029), the National Key R&D Program of China (Grant Nos. 2018YFC0213105),
636 and Environmental Charity Project of Ministry of Environmental Protection of China (201409022).

637

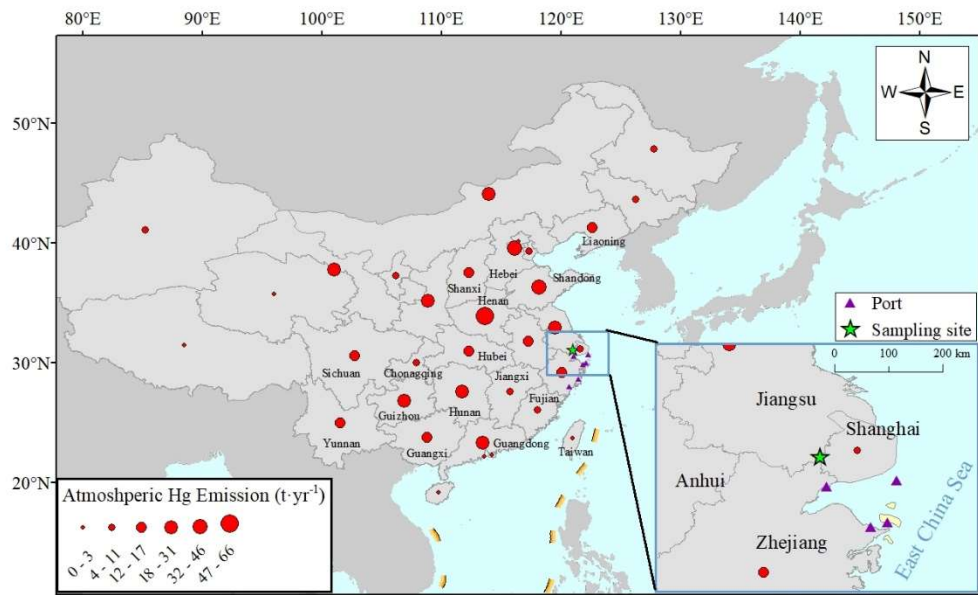
638 **References**

- 639 Amos, H. M., Jacob, D. J., Holmes, C. D., Fisher, J. A., Wang, Q., Yantosca, R. M., Corbitt, E. S., Galarneau,
640 E., Rutter, A. P., Gustin, M. S., Steffen, A., Schauer, J. J., Graydon, J. A., Louis, V. L. S., Talbot, R. W.,
641 Edgerton, E. S., Zhang, Y., and Sunderland, E. M.: Gas-particle partitioning of atmospheric Hg(II) and its
642 effect on global mercury deposition, *Atmos. Chem. Phys.*, 12, 591-603, 10.5194/acp-12-591-2012, 2012.
643 Auzmendi-Murua, I., Castillo, A., and Bozzelli, J. W.: Mercury Oxidation via Chlorine, Bromine, and Iodine
644 under Atmospheric Conditions: Thermochemistry and Kinetics, *Journal of Physical Chemistry A*, 118,
645 2959-2975, 10.1021/jp412654s, 2014.
646 Chen, L. G., Liu, M., Xu, Z. C., Fan, R. F., Tao, J., Chen, D. H., Zhang, D. Q., Xie, D. H., and Sun, J. R.: Variation
647 trends and influencing factors of total gaseous mercury in the Pearl River Delta-A highly industrialised
648 region in South China influenced by seasonal monsoons, *Atmospheric Environment*, 77, 757-766,
649 10.1016/j.atmosenv.2013.05.053, 2013.
650 Cheng, I., Zhang, L. M., Mao, H. T., Blanchard, P., Tordon, R., and Dalziel, J.: Seasonal and diurnal patterns
651 of speciated atmospheric mercury at a coastal-rural and a coastal-urban site, *Atmospheric Environment*,
652 82, 193-205, 10.1016/j.atmosenv.2013.10.016, 2014.
653 Cheng, I., Xu, X., and Zhang, L.: Overview of receptor-based source apportionment studies for speciated
654 atmospheric mercury, *Atmos. Chem. Phys.*, 15, 7877-7895, 10.5194/acp-15-7877-2015, 2015.
655 Choi, H. D., Huang, J. Y., Mondal, S., and Holsen, T. M.: Variation in concentrations of three mercury (Hg)
656 forms at a rural and a suburban site in New York State, *Sci. Total Environ.*, 448, 96-106,
657 10.1016/j.scitotenv.2012.08.052, 2013.
658 Draxler, R., and Rolph, G.: HYSPLIT - Hybrid Single Particle Lagrangian Integrated Trajectory Model, 2012.
659 Duan, J., and Tan, J.: Atmospheric heavy metals and Arsenic in China: Situation, sources and control
660 policies, *Atmospheric Environment*, 74, 93-101, 10.1016/j.atmosenv.2013.03.031, 2013.
661 Feng, X. B., Shang, L. H., Wang, S. F., Tang, S. L., and Zheng, W.: Temporal variation of total gaseous
662 mercury in the air of Guiyang, China, *J. Geophys. Res.-Atmos.*, 109, 10.1029/2003jd004159, 2004.
663 Friedli, H. R., Arellano, A. F., Geng, F., Cai, C., and Pan, L.: Measurements of atmospheric mercury in
664 Shanghai during September 2009, *Atmospheric Chemistry and Physics*, 11, 3781-3788, 10.5194/acp-11-
665 3781-2011, 2011.
666 Fu, X., Maruszczak, N., Heimbürger, L.-E., Sauvage, B., Gheusi, F., Prestbo, E. M., and Sonke, J. E.:

- 667 Atmospheric mercury speciation dynamics at the high-altitude Pic du Midi Observatory, southern
668 France, *Atmospheric Chemistry and Physics*, 16, 5623-5639, 10.5194/acp-16-5623-2016, 2016.
- 669 Fu, X. W., Feng, X. B., Qiu, G. L., Shang, L. H., and Zhang, H.: Speciated atmospheric mercury and its
670 potential source in Guiyang, China, *Atmospheric Environment*, 45, 4205-4212,
671 10.1016/j.atmosenv.2011.05.012, 2011.
- 672 Fu, X. W., Feng, X., Shang, L. H., Wang, S. F., and Zhang, H.: Two years of measurements of atmospheric
673 total gaseous mercury (TGM) at a remote site in Mt. Changbai area, Northeastern China, *Atmospheric
674 Chemistry and Physics*, 12, 4215-4226, 10.5194/acp-12-4215-2012, 2012.
- 675 Fu, X. W., Zhang, H., Yu, B., Wang, X., Lin, C. J., and Feng, X. B.: Observations of atmospheric mercury in
676 China: a critical review, *Atmospheric Chemistry and Physics*, 15, 9455-9476, 10.5194/acp-15-9455-2015,
677 2015.
- 678 Gibson, M. D., Haelssig, J., Pierce, J. R., Parrington, M., Franklin, J. E., Hopper, J. T., Li, Z., and Ward, T. J.:
679 A comparison of four receptor models used to quantify the boreal wildfire smoke contribution to surface
680 PM2.5 in Halifax, Nova Scotia during the BORTAS-B experiment, *Atmospheric Chemistry and Physics*, 15,
681 815-827, 10.5194/acp-15-815-2015, 2015.
- 682 Gratz, L. E., Keeler, G. J., Marsik, F. J., Barres, J. A., and Dvonch, J. T.: Atmospheric transport of speciated
683 mercury across southern Lake Michigan: Influence from emission sources in the Chicago/Gary urban
684 area, *The Science of the total environment*, 448, 84-95, 10.1016/j.scitotenv.2012.08.076, 2013.
- 685 Hui, M. L., Wu, Q. R., Wang, S. X., Liang, S., Zhang, L., Wang, F. Y., Lenzen, M., Wang, Y. F., Xu, L. X., Lin,
686 Z. T., Yang, H., Lin, Y., Larssen, T., Xu, M., and Hao, J. M.: Mercury Flows in China and Global Drivers,
687 *Environmental science & technology*, 51, 222-231, 10.1021/acs.est.6b04094, 2017.
- 688 Landis, M. S., and Keeler, G. J.: Atmospheric mercury deposition to Lake Michigan during the Lake
689 Michigan Mass Balance Study, *Environmental science & technology*, 36, 4518-4524, 10.1021/es011217b,
690 2002.
- 691 Liu, B., Keeler, G. J., Dvonch, J. T., Barres, J. A., Lynam, M. M., Marsik, F. J., and Morgan, J. T.: Urban-rural
692 differences in atmospheric mercury speciation, *Atmospheric Environment*, 44, 2013-2023,
693 10.1016/j.atmosenv.2010.02.012, 2010.
- 694 Liu, K., Wang, S., Wu, Q., Wang, L., Ma, Q., Zhang, L., Li, G., Tian, H., Duan, L., and Hao, J.: A Highly
695 Resolved Mercury Emission Inventory of Chinese Coal-Fired Power Plants, *Environmental science &
696 technology*, 52, 2400-2408, 10.1021/acs.est.7b06209, 2018.
- 697 Liu, M. D., Chen, L., Wang, X. J., Zhang, W., Tong, Y. D., Ou, L. B., Xie, H., Shen, H. Z., Ye, X. J., Deng, C. Y.,
698 and Wang, H. H.: Mercury Export from Mainland China to Adjacent Seas and Its Influence on the Marine
699 Mercury Balance, *Environmental science & technology*, 50, 6224-6232, 10.1021/acs.est.5b04999, 2016.
- 700 Lu, X., Hong, J., Zhang, L., Cooper, O. R., Schultz, M. G., Xu, X., Wang, T., Gao, M., Zhao, Y., and Zhang, Y.:
701 Severe Surface Ozone Pollution in China: A Global Perspective, *Environmental Science & Technology
702 Letters*, 10.1021/acs.estlett.8b00366, 2018.
- 703 Mao, H. T., Cheng, I., and Zhang, L. M.: Current understanding of the driving mechanisms for
704 spatiotemporal variations of atmospheric speciated mercury: a review, *Atmospheric Chemistry and
705 Physics*, 16, 12897-12924, 10.5194/acp-16-12897-2016, 2016.
- 706 Marsik, F. J., Keeler, G. J., and Landis, M. S.: The dry-deposition of speciated mercury to the Florida
707 Everglades: Measurements and modeling, *Atmospheric Environment*, 41, 136-149,
708 10.1016/j.atmosenv.2006.07.032, 2007.
- 709 Obrist, D., Tas, E., Peleg, M., Matveev, V., Fain, X., Asaf, D., and Luria, M.: Bromine-induced oxidation of
710 mercury in the mid-latitude atmosphere, *Nat. Geosci.*, 4, 22-26, 10.1038/ngeo1018, 2011.

- 711 Pacyna, J. M., Travnikov, O., De Simone, F., Hedgecock, I. M., Sundseth, K., Pacyna, E. G., Steenhuisen, F.,
712 Pirrone, N., Munthe, J., and Kindbom, K.: Current and future levels of mercury atmospheric pollution on
713 a global scale, *Atmos. Chem. Phys.*, 16, 12495-12511, 10.5194/acp-16-12495-2016, 2016.
- 714 Pirrone, N., Cinnirella, S., Feng, X., Finkelman, R. B., Friedli, H. R., Leaner, J., Mason, R., Mukherjee, A.
715 B., Stracher, G. B., Streets, D. G., and Telmer, K.: Global mercury emissions to the atmosphere from
716 anthropogenic and natural sources, *Atmos. Chem. Phys.*, 10, 5951-5964, 10.5194/acp-10-5951-2010,
717 2010.
- 718 Rutter, A. P., and Schauer, J. J.: The effect of temperature on the gas-particle partitioning of reactive
719 mercury in atmospheric aerosols, *Atmospheric Environment*, 41, 8647-8657,
720 10.1016/j.atmosenv.2007.07.024, 2007.
- 721 Shon, Z. H., Kim, K. H., Kim, M. Y., and Lee, M.: Modeling study of reactive gaseous mercury in the urban
722 air, *Atmospheric Environment*, 39, 749-761, 10.1016/j.atmosenv.2004.09.071, 2005.
- 723 Simoneit, B. R. T., Elias, V. O., Kobayashi, M., Kawamura, K., Rushdi, A. I., Medeiros, P. M., Rogge, W. F.,
724 and Didyk, B. M.: Sugars - Dominant water-soluble organic compounds in soils and characterization as
725 tracers in atmospheric particulate matter, *Environmental science & technology*, 38, 5939-5949,
726 10.1021/es0403099, 2004.
- 727 Tian, H. Z., Lu, L., Cheng, K., Hao, J. M., Zhao, D., Wang, Y., Jia, W. X., and Qiu, P. P.: Anthropogenic
728 atmospheric nickel emissions and its distribution characteristics in China, *Sci. Total Environ.*, 417, 148-
729 157, 10.1016/j.scitotenv.2011.11.069, 2012.
- 730 Viana, M., Amato, F., Alastuey, A., Querol, X., Moreno, T., Garcia Dos Santos, S., Dolores Herce, M., and
731 Fernandez-Patier, R.: Chemical Tracers of Particulate Emissions from Commercial Shipping,
732 *Environmental science & technology*, 43, 7472-7477, 10.1021/es901558t, 2009.
- 733 Wan, Q., Feng, X. B., Lu, J. L., Zheng, W., Song, X. J., Han, S. J., and Xu, H.: Atmospheric mercury in
734 Changbai Mountain area, northeastern China I. The seasonal distribution pattern of total gaseous
735 mercury and its potential sources, *Environmental Research*, 109, 201-206,
736 10.1016/j.envres.2008.12.001, 2009.
- 737 Wang, F., Saiz-Lopez, A., Mahajan, A. S., Martin, J. C. G., Armstrong, D., Lemes, M., Hay, T., and Prados-
738 Roman, C.: Enhanced production of oxidised mercury over the tropical Pacific Ocean: a key missing
739 oxidation pathway, *Atmospheric Chemistry and Physics*, 14, 1323-1335, 10.5194/acp-14-1323-2014,
740 2014.
- 741 Wang, X., Lin, C.-J., Yuan, W., Sommar, J., Zhu, W., and Feng, X.: Emission-dominated gas exchange of
742 elemental mercury vapor over natural
743 surfaces in China, *Atmospheric Chemistry and Physics*, 16, 11125-11143, 10.5194/acp-16-11125-2016,
744 2016.
- 745 Wu, Q. R., Wang, S. X., Li, G. L., Liang, S., Lin, C. J., Wang, Y. F., Cai, S. Y., Liu, K. Y., and Hao, J. M.: Temporal
746 Trend and Spatial Distribution of Speciated Atmospheric Mercury Emissions in China During 1978-2014,
747 *Environmental science & technology*, 50, 13428-13435, 10.1021/acs.est.6b04308, 2016.
- 748 Xiao, M., Wang, Q., Qin, X., Yu, G., and Deng, C.: Composition, Sources, and Distribution of PM2.5
749 Saccharides in a Coastal Urban Site of China, *Atmosphere*, 9, 274, 10.3390/atmos9070274, 2018.
- 750 Xu, L. L., Chen, J. S., Yang, L. M., Niu, Z. C., Tong, L., Yin, L. Q., and Chen, Y. T.: Characteristics and sources
751 of atmospheric mercury speciation in a coastal city, Xiamen, China, *Chemosphere*, 119, 530-539,
752 10.1016/j.chemosphere.2014.07.024, 2015.
- 753 Xu, X., Liao, Y., Cheng, I., and Zhang, L.: Potential sources and processes affecting speciated atmospheric
754 mercury at Kejimkujik National Park, Canada: comparison of receptor models and data treatment

- 755 methods, *Atmospheric Chemistry and Physics*, 17, 1381-1400, 10.5194/acp-17-1381-2017, 2017.
756 Ye, Z., Mao, H., Lin, C. J., and Kim, S. Y.: Investigation of processes controlling summertime gaseous
757 elemental mercury oxidation at midlatitudinal marine, coastal, and inland sites, *Atmos. Chem. Phys.*, 16,
758 8461-8478, 10.5194/acp-16-8461-2016, 2016.
759 Zhang, L., Wang, S. X., Wang, L., and Hao, J. M.: Atmospheric mercury concentration and chemical
760 speciation at a rural site in Beijing, China: implications of mercury emission sources, *Atmospheric*
761 *Chemistry and Physics*, 13, 10505-10516, 10.5194/acp-13-10505-2013, 2013.
762 Zhang, Y., Yang, X., Brown, R., Yang, L. P., Morawska, L., Ristovski, Z., Fu, Q. Y., and Huang, C.: Shipping
763 emissions and their impacts on air quality in China, *Sci. Total Environ.*, 581, 186-198,
764 10.1016/j.scitotenv.2016.12.098, 2017.
765 Zhu, J., Wang, T., Talbot, R., Mao, H., Hall, C. B., Yang, X., Fu, C., Zhuang, B., Li, S., Han, Y., and Huang, X.:
766 Characteristics of atmospheric Total Gaseous Mercury (TGM) observed in urban Nanjing, China,
767 *Atmospheric Chemistry and Physics*, 12, 12103-12118, 10.5194/acp-12-12103-2012, 2012.
768 Zhu, J., Wang, T., Talbot, R., Mao, H., Yang, X., Fu, C., Sun, J., Zhuang, B., Li, S., Han, Y., and Xie, M.:
769 Characteristics of atmospheric mercury deposition and size-fractionated particulate mercury in urban
770 Nanjing, China, *Atmospheric Chemistry and Physics*, 14, 2233-2244, 10.5194/acp-14-2233-2014, 2014.
771 Zhu, J., Wang, T., Bieser, J., and Matthias, V.: Source attribution and process analysis for atmospheric
772 mercury in eastern China simulated by CMAQ-Hg, *Atmos. Chem. Phys.*, 15, 8767-8779, 10.5194/acp-15-
773 8767-2015, 2015.
774 Zhu, W., Lin, C. J., Wang, X., Sommar, J., Fu, X., and Feng, X.: Global observations and modeling of
775 atmosphere–surface exchange of elemental mercury: a critical review, *Atmos. Chem. Phys.*, 16, 4451-
776 4480, 10.5194/acp-16-4451-2016, 2016.
777
778
779
780
781
782
783
784
785
786
787
788
789
790
791
792
793
794
795
796
797
798



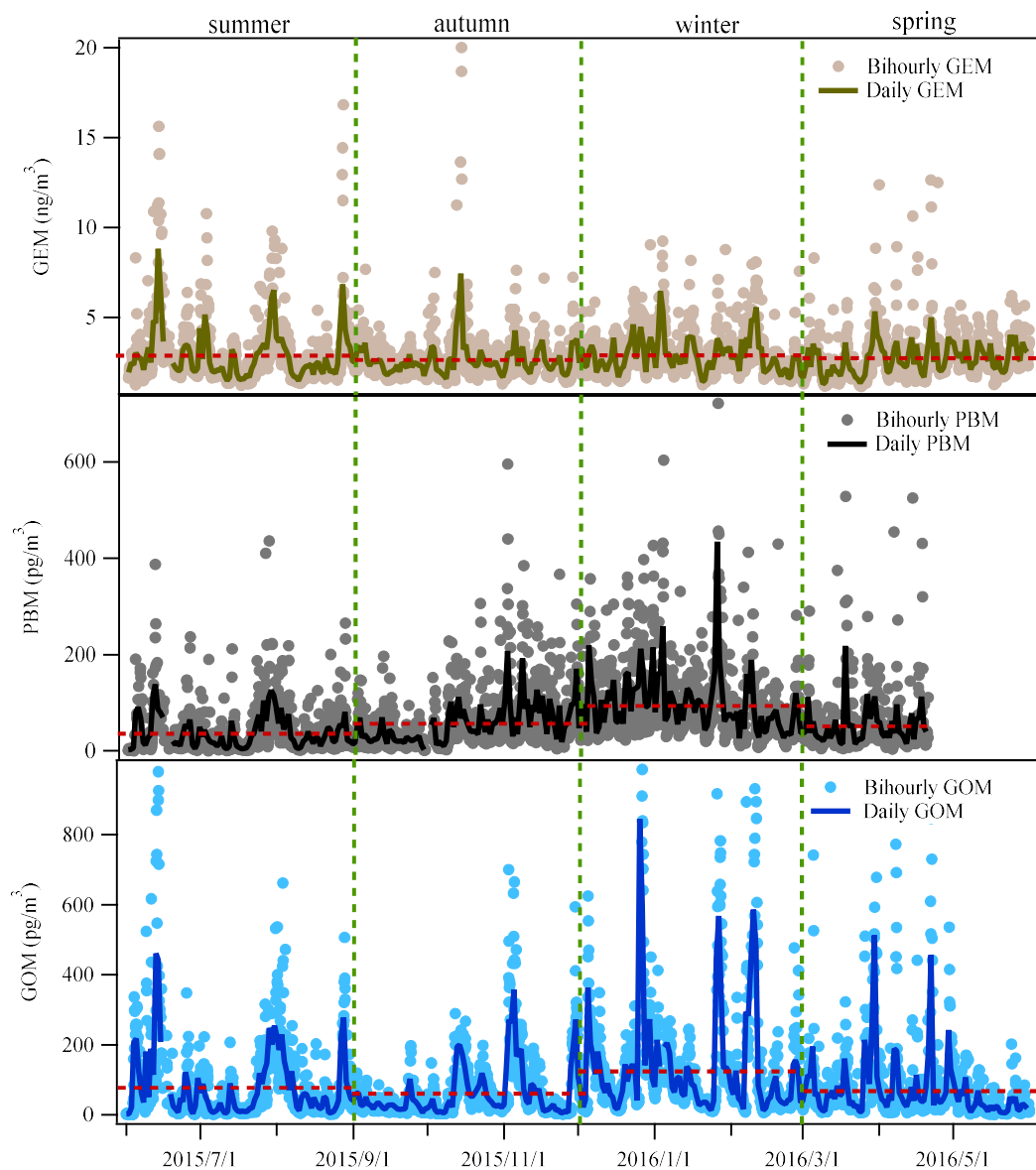
800

801

802 Figure 1. The location of the Dianshan Lake (DSL) site in Shanghai, China. The red dots in the
 803 map represent the anthropogenic atmospheric Hg emissions by each province in 2014 (Wu et al.,
 804 2016).

805

806



807

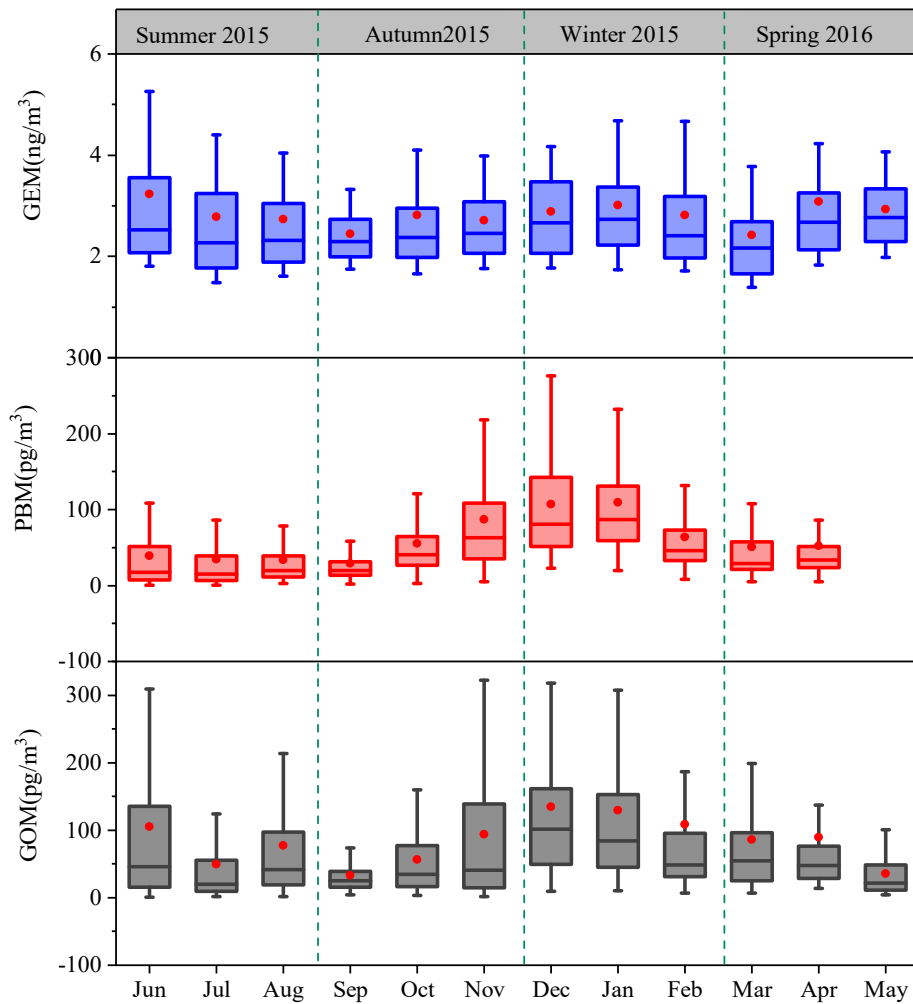
808 Figure 2. Time series of atmospheric Hg (GEM, PBM and GOM) concentrations during the whole
 809 study period at DSL. **The red-dashed lines represent the mean concentrations of Hg species in**
 810 **each season.**

811

812

813

814



815

816 Figure 3. Monthly variation of GEM, PBM, and GOM concentrations. The 10th, 25th, median, 75th
 817 and 90th percentile values are indicated in the box plots. The red dots represent the mean values.
 818

819
820
821
822

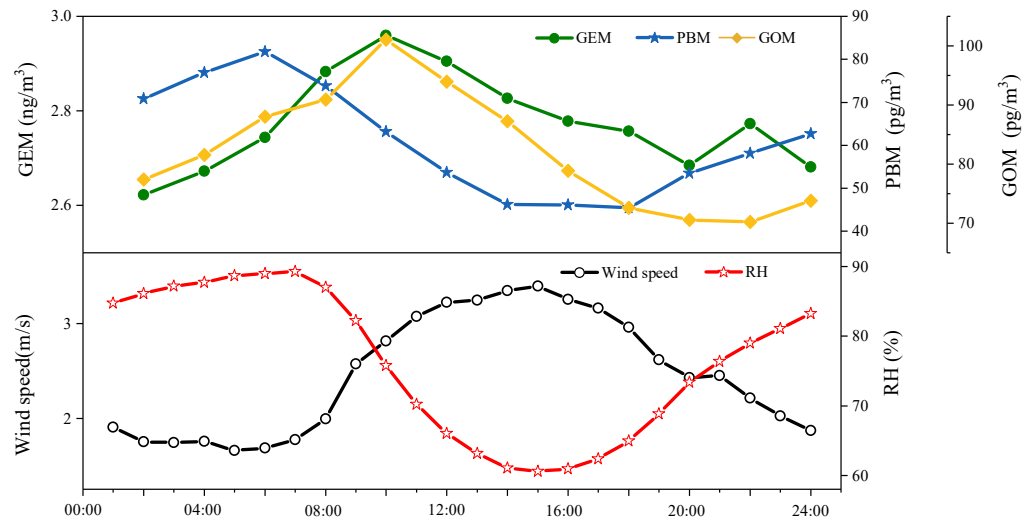
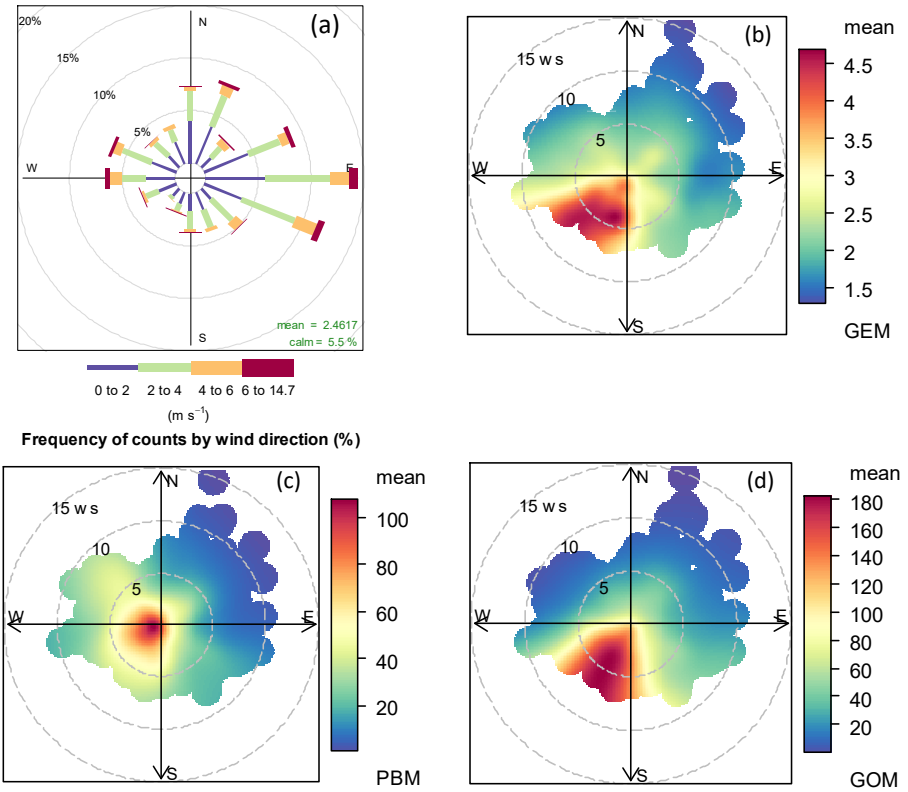
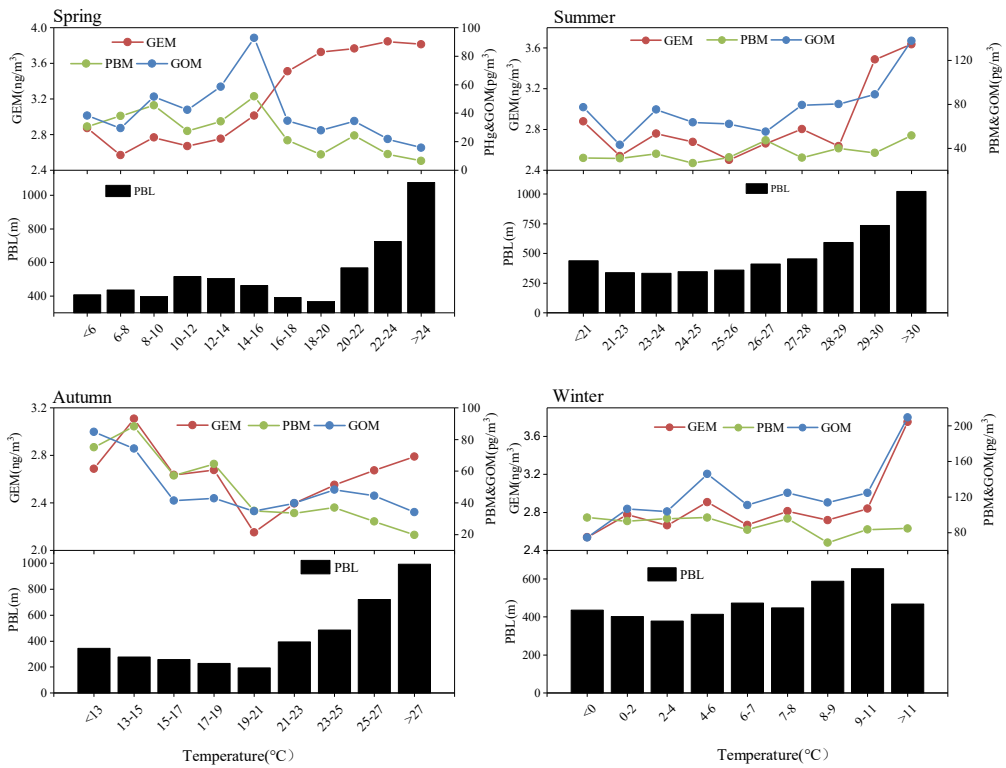


Figure 4. Annual mean diurnal variation of GEM, PBM, and GOM concentrations.



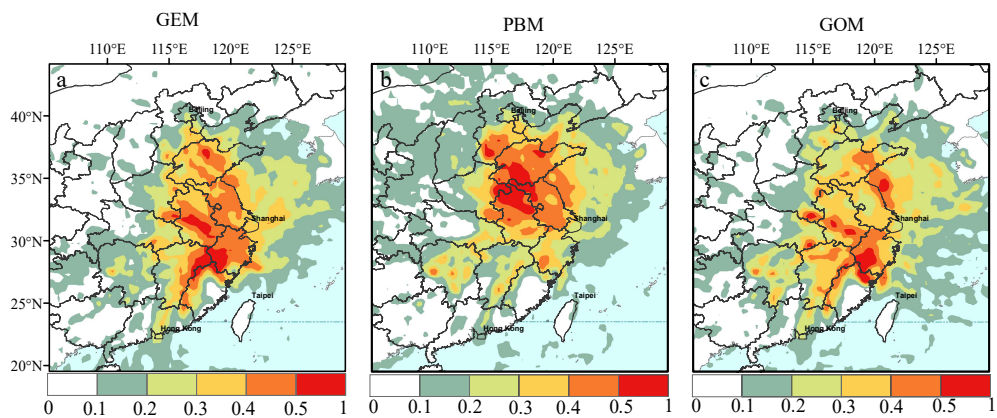
823
824

825 Figure 5. (a) Wind rose plot during the study period. Mean concentrations of (b) GEM, (c) PBM,
826 and (d) GOM as a function of wind speed and wind directions. **The radii of the circle in Figure 5 (a)**
827 **represent the frequency of wind directions and the radii of the circle in Figure 5 (b), (c), and (d)**
828 **represent the value of wind speed.**



829

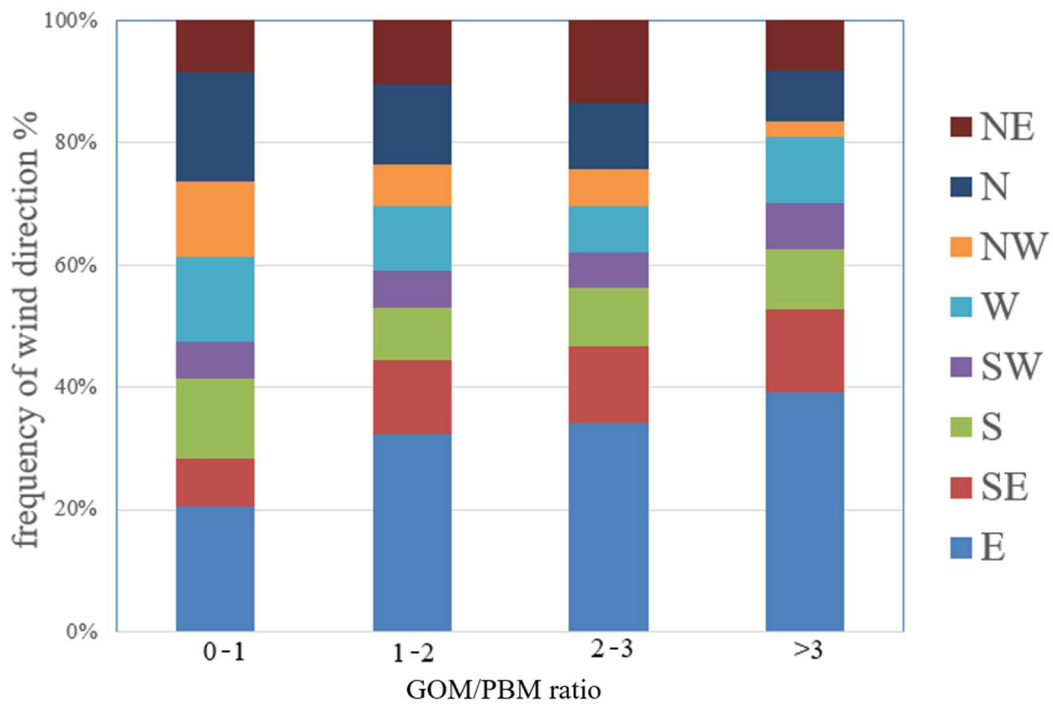
830 Figure 6. The variation of atmospheric Hg (GEM, PBM, and GOM) and PBL as a function of
 831 temperature in all four seasons.
 832



833

834 Figure 7. Potential source regions of atmospheric Hg (GEM, PBM, and GOM) at the observational
835 site according to PSCF analysis.

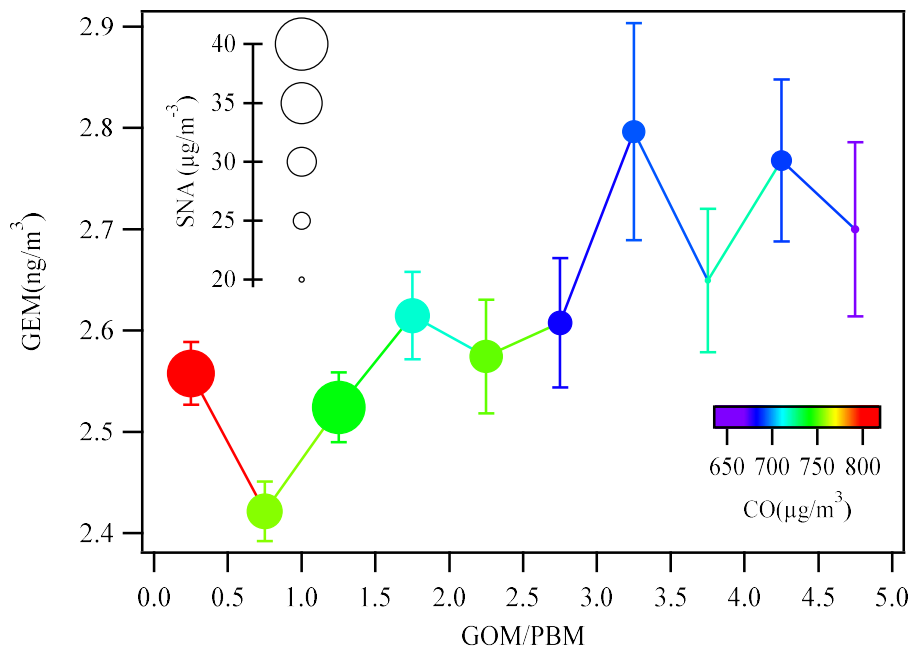
836



837

838 Figure 8. Frequency of wind directions under different ranges of GOM/PBM ratios.

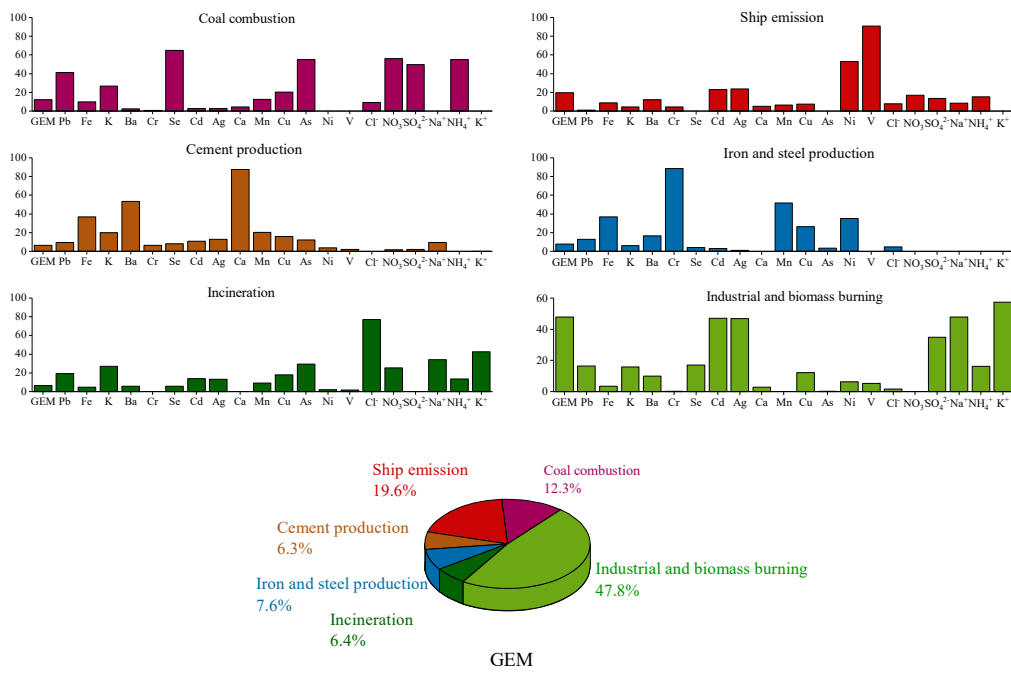
839



840

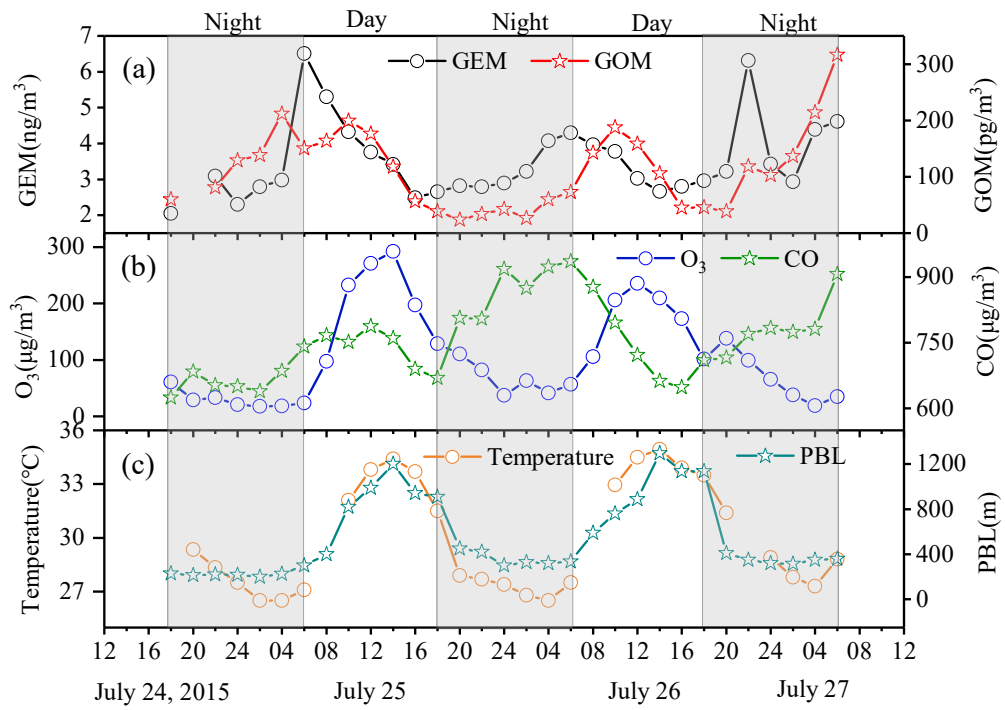
841 Figure 9. The GEM concentrations as a function of the GOM/PBM ratios in each bin of 0.5. The
 842 data points are colored by the concentrations of CO and the sizes of the dots represent the concentrations
 843 of SNA in PM_{2.5}. The bars represent one standard error of GEM concentration in each bin.

844



845

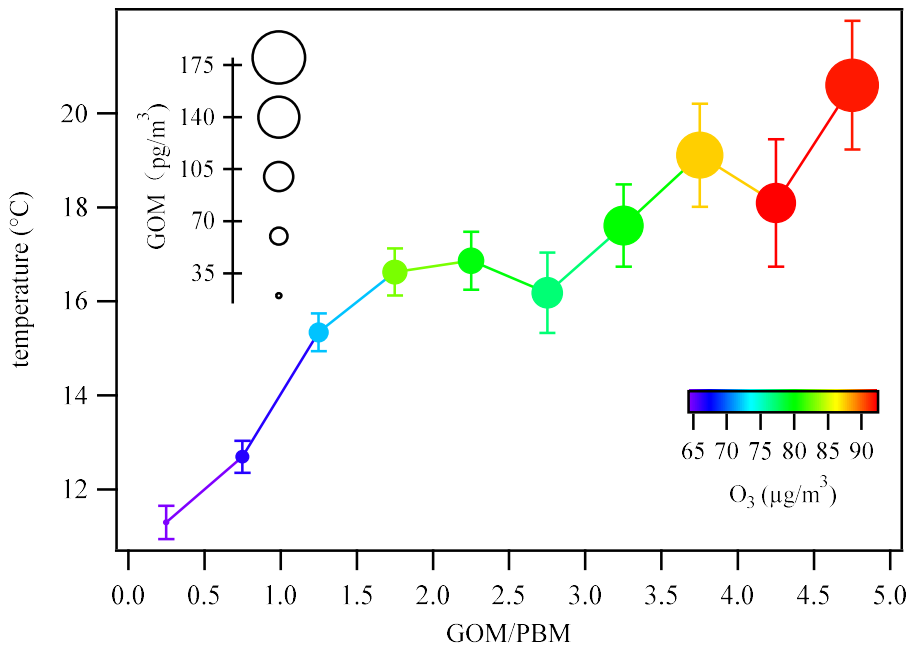
846 Figure 10. A six factor source apportionment for anthropogenic GEM based on PMF analysis.
847



848

849 Figure 11. A case study of GEM oxidation from July 24 to 27, 2015. The time-series of GEM, GOM,
850 **O₃, CO, temperature, and PBL are plotted. The shaded parts represent nighttime.**

851

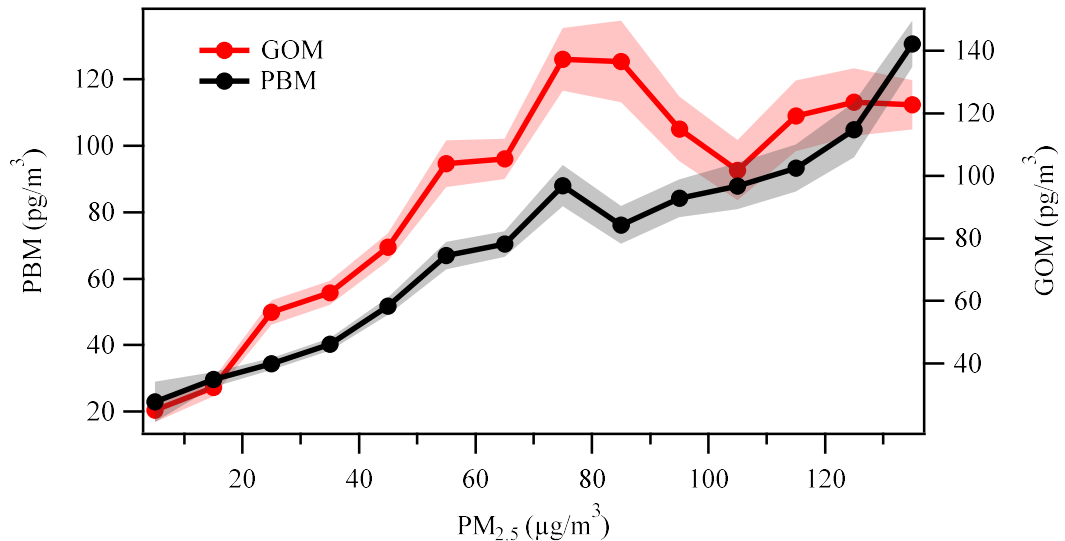


852

853 Figure 12. Temperature variations in each bin of the GOM/PBM ratios. The dots are colored by the
 854 concentrations of O₃ and the sizes of the dots represent the concentrations of GOM. The bars
 855 represent one standard error of temperature in each bin.

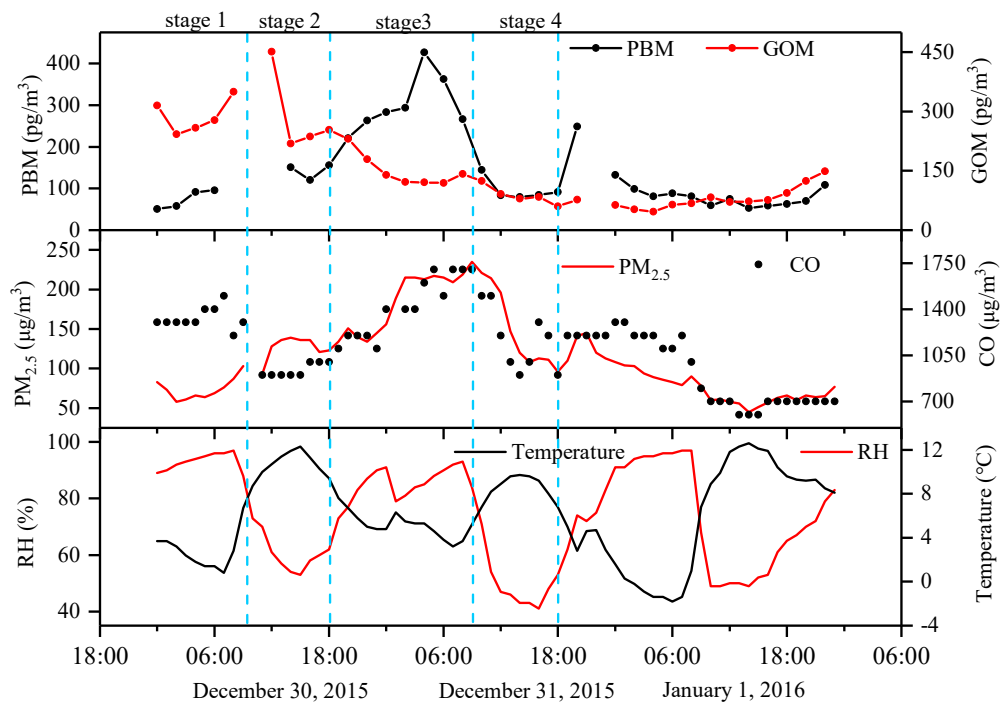
856

857



858

859 Figure 13. The variations of PBM and GOM as a function of PM_{2.5} in each bin of 10 $\mu\text{g}/\text{m}^3$. The
860 shaded areas represent one standard error of GOM and PBM concentrations.
861



862

863 Figure 14. A case study of gas-particle portioning between GOM and PBM from December 30, 2015
 864 to January 1, 2016, which was divided into different stages. The time-series of PBM, GOM, PM_{2.5},
 865 CO, temperature, and RH are plotted.

Table 1. The concentrations of speciated atmospheric mercury in this study and other sites around the world.

Location	Remarks	Year	GEM (ng/m ³)	PHg (pg/m ³)	RGM (pg/m ³)	Reference
Dianshan Lake Shanghai, China	Suburban	2015-2016	2.77±1.36	60.8±67.4	82.13±115.5	This study
Chongming Shanghai, China						
Chongming Shanghai, China	Suburban	2009-2012	2.65±1.73	21.5±25.4	8.0±8.8	Zhang et al. (2017)
Xiamen, China	Suburban	2012-2013	3.5	174.41	61.05	Xu et al. (2015)
Guiyang, China	Urban	2009	9.72±10.2	368±676	35.7±43.9	Fu et al. (2011)
Miyun, China	Rural	2008-2009	3.23	98.2	10.1	Zhang et al. (2013)
Mt. Waliguan, China	Remote	2007-2008	1.98±0.98	19.4±18.1	7.4±4.8	Wan et al. (2009)
Seoul, Korea	Urban	2005-2006	3.22±2.10	23.9±19.6	27.2±19.3	Kim et al. (2009)
Nova Scotia, Canada	Rural	2010-2011	1.38±0.2	0.4±1.0	3.5±4.5	Cheng et al. (2014)
Elora, Ontario, Canada	Rural	2006-2007	1.17	16.40	15.1	Baya and Van Heyst (2010)
Chicago, USA	Urban	2007	2.5±1.5	9±20	17±87	Gratz et al. (2013)
Reno, USA	Suburban	2007-2009	2.0±0.7	7±7	18±22	Lyman and Gustin (2009)
Rochester, NY, USA	Urban	2008-2009	1.49	6.57	4.08	Huang et al. (2010)

Table 2. PCA (Principal Component Analysis) analysis for GEM at DSL.

	Factor 1	Factor 2	Factor 3	Factor 4
GEM	0.50	0.25	0.11	0.07
SO ₂	0.69	-0.20	-0.18	0.35
NO ₂	0.38	-0.49	0.35	0.39
SO ₄ ²⁻	0.84	0.13	0.15	0.00
NH ₄ ⁺	0.88	-0.12	0.18	0.07
K ⁺	0.77	-0.25	0.04	0.39
Pb	0.80	-0.17	0.04	0.32
Se	0.87	-0.05	0.01	0.29
As	0.82	-0.23	0.06	0.33
O ₃	0.06	0.79	-0.30	0.03
NH ₃	0.03	0.73	0.36	-0.04
Temperature	-0.23	0.82	0.17	-0.03
Ni	0.24	-0.02	0.85	0.22
V	-0.03	0.11	0.90	-0.05
Fe	0.50	-0.12	0.24	0.74
Ca	0.26	0.08	0.00	0.90
Explained variance %	34.15	14.85	13.43	12.89

